

ELECTRIC PROPULSION*

by

Ernst Stuhlinger

MAY 1960



N 66-81095

FACILITY FORM 802

(ACCESSION NUMBER)

118

(PAGES)

CR-69144

(NASA CR OR TMX OR AD NUMBER)

(THRU)

None

(CODE)

(CATEGORY)

TABLE OF CONTENTS

	Page
Symbols and Units	iii
2. ELECTRIC PROPULSION SYSTEMS	
a. Introductory Remarks	1
(1) Definition of Systems	1
(2) Historical Background	2
b. Dynamics of Electric Propulsion Systems	5
(1) Characteristic Relations Applicable to Electrically Propelled Vehicles	5
(2) Variable Thrust Systems	15
c. Power Supply Systems	20
(1) Prime Sources	20
(2) Conversion Plants	22
(3) Specific Power of Thrust-Producing System	26
d. Electrostatic or Ion Propulsion Systems	27
(1) Basic Theory	27
(2) Components of an Ion Propulsion System	31
(3) Beam Formation	34
(4) Space Charge Neutralization	37
(5) Heavy Particle Systems	39

	Page
(6) Performance and Design Figures of Electrostatic Systems	42
e. Electrically Heated Systems	44
(1) Thermodynamic Considerations	44
(2) Performance Data	50
f. Magnetofluidynamic Propulsion Systems	52
(1) Principles of Operation	52
(2) Plasma Accelerators of Various Designs	55
(3) Characteristic Features of MFD Systems	59
g. Concluding Remarks	61
REFERENCES	63
TABLES I through V	72-76
ILLUSTRATIONS	

SYMBOLS AND UNITS

Note:

All equations are written in units of the cm-gram-second system, which requires that the unit of the current be 0.33×10^{-9} of one ampere, and the unit of the voltage 300 volts.

Thus:

$$1 \text{ amp} = 3 \times 10^9 \text{ c-g-s amps,}$$

$$1 \text{ volt} = 1/300 \text{ c-g-s volts.}$$

The specific charge of the cesium ion ($A = 133$) is

$$\begin{aligned} \epsilon/\mu &= 2.19 \times 10^{12} \text{ el. st. c-g-s units} \\ &= 730 \text{ amp sec g}^{-1} \end{aligned}$$

Numerical results are sometimes given in amps, volts, watts, km sec^{-1} , kg, tons, years, and G's in order to give a better feeling for the magnitudes.

Since electric propulsion systems will be useful only under reduced or vanishing gravity, these units have been avoided which contain G_0 , the gravitational force at the surface of the earth. Thus, "mass" is used instead of "weight," and "exhaust velocity" instead of "specific impulse."

a	cm sec ⁻²	acceleration
a	cm	distance
α	erg sec ⁻¹ g ⁻¹	specific power
A	—	atomic mass
b	cm	distance
β	—	ratio of densities
c	3 x 10 ¹⁰ cm sec ⁻¹	velocity of light
C	Farad	capacity
d	cm	distance
δ	—	degree of ionization
e	4.80 x 10 ¹⁰ el. st. units	charge of electron
E	erg	energy
f	dyne cm ⁻²	thrust per cm
F	dyne	thrust
φ	erg	work function
G	981 cm sec ⁻²	earth's gravity
h	6.62 x 10 ⁻²⁷ erg sec	Planck's constant
H	gauss	Magnetic field strength
ΔH	erg	enthalpy difference
i	c-g-s amp cm ⁻²	current density (see "Note")
I	c-g-s amp	current (see "Note")
j	—	$\sqrt{-1}$

k	$1.38 \times 10^{-16} \text{ erg}$ grad^{-1}	Boltzmann's constant
L	Henry	inductivity
m	g	mass
M	g	mass
\dot{m}	$\text{g sec}^{-1} \text{ cm}^{-2}$	rate of mass flow per cm^2
\dot{M}	g sec^{-1}	rate of mass flow
M_0	g	total initial mass
M_f	g	propellant mass
M_p	g	mass of thrust-producing system
M_l	g	payload
M_e	g	terminal mass
M_r	g	terminal mass
M_t	g	instantaneous mass
μ	g	mass of particle
S	c-g-s volts cm^{-1}	field strength (see "Note")
t	sec	time
T	deg Kelvin	temperature
τ	sec	time of propulsion
u	cm sec^{-1}	terminal velocity
U	c-g-s volt	voltage; potential (see "Note")
v	cm sec^{-1}	exhaust velocity
V	c-g-s volt	voltage; potential (see "Note")

2. ELECTRIC PROPULSION SYSTEMS

a. Introductory Remarks

(1) Definition of Systems

The term "electric propulsion system" is used in connection with a great variety of systems applicable to the propulsion of spacecraft. All electrical propulsion systems, in the same way as chemical, nuclear, hot water, or photon propulsion systems, are based on Newton's theorem of action and reaction. In each case, a force acts on the space vehicle according to Eq. (1)

$$F = \frac{d(Mv)}{dt} \quad (1)$$

If the exhaust velocity v is constant, and if the ejected mass is carried on the vehicle before injection, Eq. (1) leads to the well-known rocket equation first derived by Ziolkowsky:

$$u = v \ln \frac{M_e + M_f}{M_e} \quad (2)$$

where

$$M_f = \int \dot{m} dt = \text{propellant mass}$$

Electric propulsion systems are characterized by the use of electric energy for the ejection of the propellant mass. The accelerating forces may be exerted upon the propellant particles by electric fields, magnetic fields, a combination of both, the heat energy contained in an electric arc discharge, or the heat energy transferred to the propellant particles from electrically heated surfaces. Each of these systems requires a source of electric power aboard the vehicle. Besides this common feature, the various electric propulsion systems differ very decisively in a number of details. It is advisable, therefore, to differentiate between electrostatic or ion systems, magnetofluiddynamic systems, and electrically heated systems (which include arc jet systems).

(2) Historical Background

The possibility of space vehicle propulsion by means of electrically expelled particles was probably first stated by R. H. Goddard [1] in 1906. H. Oberth [2] discussed electric propulsion at some length in 1929, while, in 1946, J. Ackeret [3] provided theoretical details of rocket propulsion which apply also to electric systems. In 1947, Seifert, Mills, and Summerfield [4] mentioned the necessity of

ejecting positive and negative particles simultaneously. The first more elaborate study on electric propulsion was published by Shepherd and Cleaver [5] in 1949; they coined the term "ion rocket." More papers on electric propulsion appeared in the early '50's, notably by Spitzer [6,7,8,9]. A comprehensive study on electrically propelled space vehicles capable of manned expeditions to Mars was made by Stuhlinger [10] in 1954 and expanded in the following years. Langmuir [11], Irving [12], Bussard [13], and Boden [14] contributed very essentially to our theoretical and experimental knowledge of electric propulsion systems, beginning in 1956. A large number of papers were published during recent years, many of them describing excellent work by industrial contractors [15-20].

While the theoretical background of electrostatic propulsion systems was being developed during recent years, the possibilities of electrodynamic systems were more and more recognized. The physics of ionized plasma, often called magnetofluidynamics, one of the youngest branches of physics, became the objective of intense studies after the classical investigations by Alfven [21], Spitzer [22], Kantrowitz

[23], Landshof [24], and others [25]. High plasma flow velocities were produced in discharge tubes in which stationary or transient magnetic fields acted upon an ionized gas, in conjunction with electric fields. Studies of this kind gained considerably in importance in connection with research towards controlled thermonuclear reactions.

The arc jet propulsion system, as contrasted to electrostatic and magnetofluidynamic (MFD) systems, uses electric power to heat the propellant gas. While a high-intensity arc is burning within the arc chamber, propellant flows into the chamber and leaves it with an exhaust velocity determined by a purely thermodynamic process. The degree of ionization is low, and the exhaust velocities are roughly between those obtainable with chemical and ion or MFD systems. Even though systematic investigations of arc jet systems for propulsion began later than those of ion and MFD systems, the arc jet as an actual propulsion engine is presently much closer to technical realization than the other two systems [26 - 30].

An alternate system using the electro-thermodynamic process has been suggested in which the propellant (hydrogen) absorbs heat energy while passing over electrically heated tungsten surfaces [31]. This system would be particularly simple as far as design and operation are concerned. Exhaust velocities of the order of 6 to 10 km sec⁻¹ may be obtainable. Like the arc jet system, the electrical heater element system may find application for auxiliary propulsion units in cases where the spacecraft already carries an electric power source for other purposes.

b. Dynamics of Electric Propulsion Systems

(1) Characteristic Relations Applicable to Electrically Propelled Vehicles

Electric propulsion systems require an on-board power source of considerable magnitude (Fig. 1). The entire mass of the power-producing system, which includes the prime source, the conversion plant, the heat rejection device, and auxiliary equipment, adds to the burn-out or terminal mass of the vehicle. It is obvious that the mass of the power-producing system must be as small as possible. In fact, this mass is the predominant factor determining

the performance, and therefore the figure of merit, of an electrically propelled vehicle. The reason why an electrically propelled space vehicle may still be comparable, and even superior, to chemical rocket vehicles, is the fact that very high exhaust velocities are obtainable with electric systems. While the energy content of fuel-oxidizer combinations sets a limit to the exhaust velocities of chemical rocket motors, ion and MFD propulsion systems are not limited by these factors.

The performance of electric propulsion systems can be conveniently analyzed if the partial masses of the components of the thrust-producing system are lumped together into one term, M_p , which includes the masses of power source, power conversion system, ion source, thrust chambers, and auxiliary equipment. Since the thrust-producing system is by far the largest part of a space vehicle, it is logical to include also the masses of structural elements in this term.

The designer of a space craft is primarily interested in the transportation capability of the vehicle, as expressed by its terminal velocity,

and by the ratio of its total mass to the useful payload. Assuming that the space craft moves only through empty space without atmosphere and gravity fields, the relation between mass ratio, terminal velocity, and other pertinent parameters can be easily derived. Defining the total initial mass of the vehicle as

$$M_o = M_f + M_p + M_l$$

and the terminal mass as

$$M_e = M_p + M_l$$

we find with Eq. (2)

$$u = v \ln \frac{M_f + M_p + M_l}{M_p + M_l} \quad (3)$$

The ratio of the electric power output to the mass of the thrust-producing system, defined by

$$\alpha = \frac{P}{M_p} \quad (4)$$

characterizes the quality of powerplant and thrust chambers; α is the "specific power."

If

$$P = \frac{\dot{M} v^2}{2} = \frac{M_f v^2}{2\tau} \quad (5)$$

denotes the total power contained in the exhaust beam, and

$$F = \dot{M} v = \frac{M_f}{\tau} v \quad (6)$$

the thrust, we finally obtain the desired relation by combining Eqs. (3) to (6) [32]

$$\frac{M_o}{M_1} = \frac{e^{\frac{u}{v}}}{1 - \frac{v^2}{2\alpha\tau} (e^{\frac{u}{v}} - 1)} \quad (7)$$

Figures 2 and 3 represent this equation. The ratio M_o/M_1 is plotted versus the exhaust velocity v , with the terminal velocity u as a parameter. The product $\alpha\tau$, specific power times propulsion time, is chosen as 10^{14} and 10^{18} in Figures 2 and 3.

Equation (7) and Figures 2 and 3 show a minimum of the mass ratio M_o/M_1 for one particular exhaust velocity v , and any set of the variables u , α , and τ .

If the derivative

$$\frac{d}{dv} \left(\frac{M_o}{M_1} \right)$$

is formed of Equation (7) and equated to zero, the equation

$$\frac{v}{u} \left(e^{\frac{u}{v}} - 1 \right) - \frac{\alpha \tau}{v^2} - \frac{1}{2} = 0 \quad (8)$$

results which gives the relation between v , u , and $\alpha \tau$ for minimum (M_0/M_1) , i.e., for maximum payload. Equation (8) is plotted in Figure 4.

The designer of an electrically propelled space vehicle will first estimate the time τ of propulsion, and the available specific power α . With this $\alpha \tau$, and the desired terminal velocity u , Fig. 4 will yield that exhaust velocity v which leads to a minimum ratio M_0/M_1 . Figure 5, which was drawn from Eqs. (7) and (8), gives the minimum ratio M_0/M_1 as a function of the terminal velocity u .

In Figure 4, the shaded area covers that region in which realistic vehicle designs will be found. It is interesting to note that this region follows approximately the function

$$v = \sqrt{\alpha \tau} \quad (9)$$

which is drawn with a dashed line in Fig. 4. A simple rule of thumb follows from this fact: The optimum ex-

haust velocity of an electrical propulsion system is approximately equal to the square root of specific power times the time of operation.¹ Assuming that the specific power is a constant which reflects the state of the art of power-generating systems, the optimum exhaust velocity is simply proportional to $\sqrt{\tau}$. With a short operating time, the exhaust velocity must be low, i.e., the power supply will be small, but the propellant mass large. With a long operating time, the exhaust velocity must be high, i.e., the power supply will be large, but the propellant mass small. Short propulsion times will require a high-current, low-voltage system, whereas long propulsion times will call for a low-current, high-voltage system.

The next step in the design will be the determination of M_0 from the ratio M_0/M_1 and the payload M_1 which, along with u , α , and τ , represents the set of original design parameters. The terminal

¹ As Fig. 4 shows, this rule is only approximate. In the limiting case of $M_1 \rightarrow 0$, for example, Eq. (9) will go over into Eq. (18).

mass, M_e , follows from

$$\frac{M_o}{M_e} = e^{\frac{u}{v}} \quad (10)$$

and the mass of the thrust-producing system, M_p , from

$$M_p = M_e - M_l \quad (11)$$

The mass of the propellant, M_f , is simply

$$M_f = M_o - M_e \quad (12)$$

and the total power P

$$P = \alpha M_p \quad (13)$$

The thrust is found from

$$F = P \frac{2}{v} \quad (14)$$

and the initial acceleration from

$$a_i = \frac{F}{M_o} \quad (15)$$

The rate of propellant flow is given by

$$\dot{M} = \frac{M_f}{\tau} \quad (16)$$

Figure 5, in which the minimum ratio $(M_o/M_l)_{\min}$ is plotted versus the terminal velocity u

with the product $\alpha\tau$ as a parameter, shows that, even under optimistic assumptions, the highest terminal velocity to be expected with electrically propelled vehicles is of the order of 200 km sec^{-1} . Assuming a vanishingly small payload, this limit is determined by the duration of the propulsion period, which should not be longer than about three years, and by the specific power α , which, by 1965-1970, may be expected to be of the order of 0.3 kw kg^{-1} (dashed line in Fig. 7).

The highest terminal velocity is obtained, of course, when the payload is negligibly small. Eq. (7), for $M_1 \rightarrow 0$, transforms into

$$u = v \ln \left(\frac{2\alpha\tau}{v^2} + 1 \right) \quad (17)$$

which is plotted in Figure 6. Figure 7 shows the maximum terminal velocity, u_{max} , as a function of $\alpha\tau$.

Forming the derivative and letting

$$\frac{du}{dv} \rightarrow 0$$

leads to

$$\ln \left(\frac{2\alpha\tau}{v^2} + 1 \right) = \frac{2}{1 + \frac{v^2}{2\alpha\tau}}$$

and

$$v \approx \sqrt{\frac{\alpha \tau}{2}} \quad (18)$$

at the point where u reaches its maximum, assuming $M_1 \rightarrow 0$. Of particular interest is the ratio u/v at this maximum. Eqs. (17) and (18) yield

$$\frac{u}{v} \approx \ln 5 \approx 1.61 \quad (19)$$

The highest terminal velocity which an electrically propelled vehicle can reach with vanishingly small payload is equal to 1.61 times its exhaust velocity, or approximately

$$u_{\max} \approx 1.14 \sqrt{\alpha \tau} \quad (20)$$

Since $M_1 \rightarrow 0$, we find

$$M_e = M_p$$
$$\frac{M_o}{M_p} = e \frac{u}{v} \approx 5$$

or

$$M_p \approx \frac{1}{5} M_o$$

and

$$M_f \approx \frac{4}{5} M_o$$

(21)

The relations (19) and (21) are independent of α and τ . The amounts of v and u , however, are determined by Eqs. (18) and (20) as soon as α and τ are chosen.

Equations (9) through (21) are particularly useful for a quick estimate of the principal design and performance figures of an electrically propelled vehicle.

An important limit in the choice of τ is set by the minimum acceleration which can be accepted for a space mission. The initial acceleration of the vehicle, $a_i = F/M_0$, may be expressed in terms of the characteristic parameters of the space craft. It can be shown [32] that for vanishing payload the highest possible initial acceleration is simply given by

$$a_{ih} \approx \sqrt{\frac{\alpha}{2\tau}} \quad (22)$$

Equation (22), plotted in Figure 8, indicates that for propulsion times of the order of one year, and specific power figures of 0.2 to 0.5 kw kg⁻¹, highest initial accelerations will not be more than 2 to 3 times 10⁻⁴ G.

(2) Variable Thrust Systems

Several investigators [33,34,35,36] pointed out that the performance of an electrically propelled space vehicle improves when its thrust is varied according to a time program, at a constant level of power consumption.

Assuming gravity-free space, and assuming further that the trajectory is subject to certain initial and terminal conditions, and that total power as well as total travel time are fixed, we may derive that time program for the acceleration which leads to a maximum payload. A very interesting and exhaustive discussion of this question was given by Irving [36].

Letting

$$P = \frac{1}{2} \dot{M} v^2 = \text{const.}$$

and

$$a = \frac{F}{M} = \frac{\dot{M} v}{M}$$

we find

$$- \frac{dM}{M^2} = \frac{1}{2P} a^2 dt$$

and

$$\frac{1}{M_t} - \frac{1}{M_0} = \frac{1}{2P} \int_t a^2 dt$$

For $t = \tau$, and with Eq. (4), we obtain

$$\frac{1}{M_p + M_1} - \frac{1}{M_0} = \frac{1}{2\alpha M_p} \int_t a^2 dt \quad (23)$$

and finally

$$\frac{2 \alpha M_p M_f}{(M_p + M_1)(M_p + M_1 + M_f)} = \int_t a^2 dt \quad (24)$$

Eq. (24) shows that for any given specific power, mass of thrust-producing system, and propellant mass, the payload M_1 , and therefore the ratio M_1/M_0 , becomes a maximum when the integral $\int_t a^2 dt$ is minimized. This result marks a characteristic difference between chemical and electric rockets, i.e., between energy-limited and power-limited systems. For a chemical rocket, the trajectory is usually chosen so that the integral $\int_t a dt$ i.e., the characteristic velocity, becomes a minimum.

The assumptions stated earlier in this paragraph infer that $d^2 a/dt^2 = 0$, which means that any acceleration program will be a linear function of time. The condition that, under the same assumptions, $\int_t a^2 dt$ be a minimum is fulfilled for $da/dt = 0$.

A "constant acceleration" program is therefore an optimum program as far as payload capability is concerned. This constant acceleration is determined by $a = u/\tau$. Equation (23) thus leads to

$$\frac{M_p}{M_p + M_1} - \frac{M_p}{M_0} = \frac{u^2}{2 \alpha \tau} \quad (25)$$

Letting $dM_1/dM_p = 0$ for maximum payload M_1 , we obtain

$$\frac{M_p}{M_0} = \frac{u}{\sqrt{2 \alpha \tau}} \left(1 - \frac{u}{\sqrt{2 \alpha \tau}} \right) \quad (26)$$

$$\frac{M_1}{M_0} = \left(1 - \frac{u}{\sqrt{2 \alpha \tau}} \right)^2 \quad (27)$$

and

$$\frac{M_f}{M_0} = \frac{u}{\sqrt{2 \alpha \tau}} \quad (28)$$

The instantaneous values of mass, thrust, propellant flow, vehicle velocity, and exhaust velocity are:

$$M_t = M_0 \frac{1}{\frac{t u}{\tau (2 \alpha \tau - u)} + 1} \quad (29)$$

$$F_t = M_t \frac{u}{\tau} \quad (30)$$

$$\dot{M}_t = \frac{F_t^a}{M_0 \frac{u}{\tau} (\sqrt{2\alpha\tau} - u)} \quad (31)$$

$$u_t = a t \quad (32)$$

$$v_t = \sqrt{2\alpha\tau} + u \left(\frac{t}{\tau} - 1 \right) \quad (33)$$

at $t = 0$, we find

$$v = \sqrt{2\alpha\tau} - u \quad (34)$$

and at $t = \tau$

$$v_\tau = \sqrt{2\alpha\tau} \quad (35)$$

The expression $\sqrt{2\alpha\tau}$ was termed "characteristic velocity" by Irving.¹ He pointed out that after burn-out each particle which was ejected by the vehicle moves away from the vehicle with the velocity $\sqrt{2\alpha\tau}$.

Figure 9 shows total mass, propellant mass, rate of mass flow, exhaust velocity, and thrust as functions of time for a constant-acceleration system and a constant-thrust system. In Figure 10,

¹In this chapter, "characteristic velocity" is the terminal velocity obtained by a rocket vehicle after acceleration in gravity-free and drag-free space.

the mass ratio $(M_0/M_1)_{\min}$ is plotted versus terminal velocity again for the two systems. The diagram shows that the difference in performance is only small at low terminal velocities; it increases with increasing terminal velocity.

While a variable-thrust program leads definitely to an improvement of the payload capability of an electrically propelled vehicle, it should not be forgotten that a system with variable thrust must be built for the highest possible current and the highest possible voltage to be expected at any time during the propulsion period, and that the electric power generator must allow the required voltage-current variation. This flexibility of the thrust-producing system over a wide operating range may introduce such severe complications in the thrust control system, and such high mass penalties, that the gain in performance is more than offset by the added complexity of the propulsion system. In any case, a careful design study must be made before a decision can be reached.

c. Power Supply Systems¹

(1) Prime Sources

The power requirements of an electric propulsion system are so great that the power source is by far the largest component of an electrically propelled space vehicle. The power contained in the beam, P , and the thrust produced by the beam, F , are related by a very simple function,

$$\frac{P}{F} = \frac{1 \dot{M} v^2}{2 \dot{M} v} = \frac{v}{2}$$

independent of any other parameters. This equation implies that with increasing exhaust velocity, i.e., with decreasing propellant consumption, the power requirements increase. Figure 11 shows the power required for one kg of thrust as a function of the exhaust velocity.

Even a superficial survey of technically feasible power sources reveals that at present there are only two promising sources of energy: solar energy, and nuclear fission energy. Solar energy is of unlimited supply, but the flow of energy per second

¹ This section is kept short because power supply problems are discussed in considerable detail elsewhere in this volume.

and per cm^2 is relatively small. At the mean distance of the earth from the sun, one cm^2 receives 0.13 watt of radiative energy. At the distance of Venus, this amount is 0.24 watt, at the distance of Mars, 0.055 watt. While the space vehicle travels on the night side of a planet, no solar energy can be received.

Nuclear fission reactor technology has been developed to a state where the feasibility of space-borne reactors appears certain. The size of a power reactor for a given power output depends primarily upon the capability of the cooling system to remove the heat energy. Fast reactors with sodium coolant have been operated at 4 megawatt heat output per kg core material. Even if the power reactor were designed on a more conservative basis, its mass would be only a small fraction of the total mass of the electric powerplant. The greatest shares in the overall mass will be taken by the power conversion plant, and by the heat radiator. Representative figures of partial masses are given in Table 1.

The power reactor must be designed for an operating lifetime of one to three years, depending

upon the mission of the space vehicle. It should have a high burn-up rate for reasons of economy, but its power output and its controllability should not suffer from excessive poisoning. It appears that power reactors can be built today which meet these requirements.

Both solar and nuclear power sources are characterized by their power levels rather than by the total energy they can deliver. Propulsion systems powered by solar or nuclear sources are therefore called "power-limited" systems rather than "energy-limited" systems.

(2) Conversion Plants

Radiative energy from the sun can be converted into electric energy either directly through photovoltaic cells, thermocouples, or thermionic converters, or indirectly through a thermodynamic engine coupled with a generator. The heat energy from a nuclear reactor can be converted in thermocouples, in thermionic converters, or in a thermodynamic engine driving a generator.

Photovoltaic cells, built of doped silicon single crystals, have successfully proven their

spaceworthiness in several satellites and space probes. Guaranteed conversion efficiency is 10 to 11 percent at the present time. An increase to 15 percent appears possible within the next few years. Figure 12 shows the efficiency as a function of temperature. This figure implies that the efficiency of semiconductor photocells depends strongly on temperature; besides that, these cells are sensitive to high-energy particle radiation. Another disadvantage is their high price, and the relatively large mass of a photovoltaic converter. A representative figure for the specific mass is 45 kg kw^{-1} [37]. A silicon cell power supply providing 20 megawatts at the distance of Mars would cover an area 200×200 meters square; it would contain 200 million individual cells and weigh 900 tons. It is not likely that a photovoltaic solar energy converter of present design will become practical for large power requirements.

Thermocouple and thermionic converters, as well as turbogenerators, would use mirrors or Fresnel lenses to concentrate the solar energy. In each case, a heat rejection system is necessary, and the overall efficiency depends decisively on the

temperature difference between the hot and the cold ends of the heat cycle. One important factor in the design of the radiator is the danger of meteorite penetration. For that reason, it appears that a small high-pressure, high-temperature radiator is preferable to a large low pressure, low temperature radiator, even though it leads to a smaller temperature differential.

Thermocouples are rugged and simple in design, but their efficiencies are low. Desirable properties of the thermocouple components are high electric conductivity, low heat conductivity, high thermoelectric power, and stability at high temperatures.

Ceramics like nickel oxide, cobalt oxide, and manganese telluride make useful thermocouples at high temperatures. It is not likely that presently known thermocouples will find application for power supplies in the kilowatt or megawatt range.

Thermionic converters, particularly the gas-filled types, have been under intense study for only a short time. Although they have not yet

reached the engineering state, they promise efficiencies which theoretically go up to 30 percent and above. It is possible that thermionic converters will play a major role in future power conversion systems.

The turboelectric generator is the best-suited of all conversion systems currently developed. At the present time, an induction-type generator, driven by a turbine (Brayton or Rankine cycle) or a hot gas piston engine (Sterling cycle) is the most promising contender for the power plant of an electric propulsion system. Over-all efficiency could be of the order of 25 to 30 percent; however, optimization of the radiator design may reduce this efficiency to a lower figure.

Nuclear reactors provide heat energy at a temperature level which is limited only by the thermal properties of the materials. Thermocouples, thermionic converters, and thermodynamic engines can be heated by nuclear reactors. In general, heat production from solar energy costs more mass than heat production from nuclear energy. With a solar converter, additional mass must be invested in a heat storage device which supplies heat energy during the periods when the sun is covered by the earth, the moon, or a planet. On the other hand, a nuclear

reactor is considerably more complex than an array of solar mirrors even though the latter requires careful orientation towards the sun.

Present technologies make a turbogenerator system in connection with a fast fission reactor the most likely power source for electrically propelled space vehicles.

(3) Specific Power of Thrust-Producing System

The decisive influence of the power-generating system on the performance of an electrically propelled system becomes apparent in Eqs. (7), (8), (9), (18), and (22), where α designates the specific power of the thrust-producing system, defined by the equation

$$\alpha = \frac{P}{M_p}$$

It is convenient to refer the power consumed by the propulsion system to the total mass of power source, power conversion plant, radiator, pumps, compressors, pipes, valves, ion source, and thrust chambers. Actually, the masses of ion source and thrust chamber depend not only upon the total power of the exhaust beam, but also upon the flow density

of the beam. However, the error introduced by ignoring this fact is small if viewed against the general uncertainties of the performance and design considerations of electrically propelled space vehicles.

The numerical value of α can be estimated on the basis of presently known technologies. A number of such estimates have been made [38], [39], [40]. Figure 13 shows a representative average of several estimates of α as a function of time, referring to a system which consists of a fission reactor with turbogenerator. While at present a specific power of the order of 0.2 kw kg^{-1} appears possible, it is anticipated that around 1965 to 1970, a figure of 0.3 kw kg^{-1} may be obtainable. If the development of thermionic converters proceeds according to theoretical expectations, an even greater specific power will become feasible.

d. Electrostatic or Ion Propulsion Systems

(1) Basic Theory

The dynamics of electric propulsion systems, as described in 2(b), do not depend on the way in which the electric energy is imparted to the exhaust particles, nor on the particles' mass

or specific charge. The payload capability and the terminal velocity of an electrically propelled vehicle, as expressed by Eq. (7), are only functions of the specific power, the exhaust velocity, and the total time of propulsion. Optimum choice of the exhaust velocity leads to maximum payload for any given terminal velocity, specific power, and propulsion time, as shown in Figs. 2 and 3. Figure 4 implies that exhaust velocities of practical interest for space vehicles cover the range from about 10 km sec^{-1} to 200 km sec^{-1} . Exhaust velocities in this range can be obtained if the propellant particles are first ionized, and then exposed to the accelerating force of an electrostatic field. The velocities of particles of various atomic masses, all singly charged, are plotted in Figure 14 as a function of the potential difference through which they were accelerated. Eq. (36) gives the relation between potential difference, mass, charge, and velocity of the particles:

$$v = \sqrt{2U \frac{e}{\mu}} \quad (36)$$

An ion propulsion system must provide an ionization mechanism for the propellant particles, and an

accelerating field of the desired magnitude. The thrust developed by the beam is given by

$$F = \dot{M} v \quad (37)$$

or, since

$$P = \frac{1}{2} \dot{M} v^2$$

$$F = \sqrt{2 \dot{M} P} = \sqrt{2 \frac{M_f}{\tau} P} \quad (38)$$

Equation (38) implies that the thrust of an ion motor depends on the total electric power, the total propulsion time, and the total propellant mass, but not on the accelerating voltage, and not on the size or the specific charge of the propellant particles. The choice of the propellant material merely determines whether the ion motor is a high current, low voltage device (light particles), or a low current, high voltage device (heavy particles).

Since

$$I = \frac{\dot{M}}{\mu} \epsilon \quad (39)$$

and $IU = P$, Eq. (38) leads to

$$F = \sqrt{2 P I \frac{\mu}{\epsilon}} \quad (40)$$

and

$$F = \sqrt{2 \frac{P^2}{U} \frac{\mu}{\epsilon}} \quad (41)$$

While the particle size does not immediately influence the thrust of an ion motor, it does influence the size of the motor, and therefore its mass. The current density of the ion beam within the accelerator is determined by Child-Langmuir's law [41]

$$i = \frac{\sqrt{2}}{9\pi} \sqrt{\frac{\epsilon}{\mu}} \frac{U^{3/4}}{d^2} \quad (42)$$

Introducing Equations (36) and (37) into (42), and letting $i/I = f/F$, we obtain for the thrust per cm^2 of motor area

$$f = \frac{1}{18\pi} \frac{v^4}{d^2} \left(\frac{\mu}{\epsilon}\right)^2 \quad (43)$$

Considering in this equation v and d as constants, it is realized that the thrust per unit motor area is proportional to $(\mu/\epsilon)^2$. This is the reason why a large specific charge of the propellant particles is desirable. It should be remembered, however, that the high voltages required by large (μ/ϵ) ratios increase the danger of voltage breakdown within the

ion motor.

A space vehicle expelling electrically charged particles must necessarily expel negative and positive charges at the same rate. If only particles of one charge were ejected, the other charge would accumulate on the vehicle and would soon prevent any further expulsion of the other charge. The most direct way to keep the vehicle neutral is by emitting the electrons which are liberated in the ionization process.

Negative and positive charges must be emitted simultaneously still for another reason. The ion beam, as shown in par. d(5), must be neutralized immediately after leaving the thrust chamber, otherwise its space charge would act back into the chamber, and would suppress any further flow of ions.

(2) Components of an Ion Propulsion System

Besides a supply of electric power and a suitable propellant material, an ion propulsion system requires an ion source, a thrust chamber where the ions are accelerated, an electron emitter, and suitable arrangements to shape the ion beam, and to neutralize the positive space charge of the ions by

means of the negative electrons. Figure 15 shows the components of an ion propulsion system schematically.

The ion source should be simple and light; it must have a long operational life, an ionization efficiency better than 95 per cent, and a current density of at least 10 mA cm^{-2} . Its power consumption should be only a small fraction of the beam power.

Several sources are under investigation. Most promising appears to be the ionization of alkali atoms at hot surfaces of Pt or W, an ion source that has been studied in great detail during the past forty years [42 to 48]. Surface ionization is observed when atoms come in contact with a material whose work function is greater than the ionization energy of the striking atoms. Work functions of several surface materials are listed in Table 2; Table 3 shows ionization energies of a number of metals. The best combination seems to be cesium atoms on tungsten surfaces. Figure 16 shows the percentage of the original atoms that leave the surface as ions, plotted versus the surface temperature.

The tungsten surface may be represented by a porous plug, or by a woven structure of wires or ribbons, with cesium vapor being forced through the fine openings [49,50]. Technical details of surface contact ion sources for propulsion systems were discussed in several recent papers [51,52].

Two other ion sources have found attention in connection with ion motors: the Von Ardenne duoplasmatron source, and the bombardment-type source. In the first, a concentrated arc burns between narrowly spaced electrodes; the ion beam is extracted by an electric field and at the same time pinched to a high density by a magnetic field. Very promising results with Von Ardenne-type sources were reported recently [53]. One disadvantage of this source is the danger of electrode erosion. A Von Ardenne source is sketched in Figure 17.

In the bombardment-type source, a transverse or oblique flow of fast electrons impinges upon a beam of atoms. Ionization occurs by collision. The electrons keep oscillating at the location of the neutral atom cloud until they collide with atoms. As soon as an atom has transformed into an ion, it is

extracted by a field and forced into the accelerator gap. Bombardment-type ion sources for ion motors have been under investigation for some years with promising results [54]. Figure 18 shows a schematic of an ion source with adjacent accelerator gap.

(3) Beam Formation

The formation of the beam is achieved by ion-optical means. The Pierce gun design, widely used for high-power electron beams, can be applied to ion beams [55] if the ions are generated at a well-defined surface with negligible velocity spread. Interception of the electrodes by ions must be avoided as far as possible in order to reduce surface erosion; a representative figure of permissible interception is 0.01 per cent.

The length of the acceleration gap between ion source and accelerating electrode cannot be chosen at will. The current density of the ion beam is a function of the specific charge of the ions, of the accelerating voltage, and of the gap length as determined by Child-Langmuir's law (Eq. 42). Figure 19 shows the current density as a function of the voltage for cesium ions, with the gap length as parameter.

Designating the cross section of the beam with $A = \pi r^2$ and combining Eqs. (41) and (42), a relation is found between thrust, voltage, and the "aspect ratio" ($2r/d$) of an ion motor, provided that the beam is space charge limited:

$$F = \frac{1}{18} U^2 \left(\frac{2r}{d} \right)^2 \quad (44)$$

Equation (44) implies that the thrust of an ion motor is determined by the voltage and the aspect ratio of the accelerating chamber, independent of (ϵ/μ) . The aspect ratio of a useful ion engine should be as large as possible.

Since Eq. (44) is rigorously valid only for plane parallel electrodes, it is useful to derive an expression which is a measure for the aspect ratio, but depends only on measurable electric quantities. Substituting $i = I/A$ in Eq. (42), we find

$$\frac{I}{U^{3/2}} = \frac{\sqrt{2}}{36} \sqrt{\frac{\epsilon}{\mu}} \left(\frac{2r}{d} \right)^2 \quad (45)$$

The term $(I/U^{3/2})$ is called "perveance." An ion motor should have a perveance as high as possible. While the optimization of the exhaust velocity (see Fig. 4)

may require a relatively low accelerating voltage of 2000 or 3000 volts, the desire for a high current density in the ion beam makes an accelerating voltage of the order of 20,000 to 30,000 volts necessary. Both requirements can be met by an "accel-decel" system in which an accelerating and a subsequent decelerating field are applied (Figure 20). The current density of the ensuing beam is determined by the accelerating voltage, but the exhaust velocity, and the total power, correspond only to the potential difference between ion source and final electrode. A more detailed analysis of the situation [56,32,58] shows that the full ion current arriving at the accelerating electrode is transmitted to the plane of the decelerating electrode under certain conditions. This is illustrated by Figure 21 where d/a is the ratio of the decelerating to the accelerating gap width, and U_d/U_a the ratio of the decelerating to the accelerating potential. Within the region underneath the curve, any combination between d/a and U_d/U_a leads to full current transmission through the decelerating gap. If $U_d = U_a$, i.e., if the decelerating gap is field free, full transmission persists even up to

$d_0 = 2.82 a$, provided that the width d_0 is reached by increasing the gap from $d < d_0$. If $d > d_0$, part of the ions turn around in the space charge field and return. If $d = \infty$, all of the ions return. If d is decreased again, less and less ions return, until the full current is transmitted at $d = 2.0 a$, as shown in Figure 21.

(4) Space Charge Neutralization

As mentioned above, a space charge limited ion current can travel from the accelerating electrode up to 2.82 times the accelerating gap width through a field-free space without being reduced by space charges. However, the exhaust beam of a space rocket must be capable of traveling infinitely deep into field-free space. The beam of an ion rocket therefore must be neutralized shortly after leaving the accelerating electrode.

Neutralization can be achieved by mixing electrons into the ion beam. In spite of considerable effort, the problem of neutralization of an ion beam has not been completely solved [32,58,59]. One reason why the formation of a neutral plasma is difficult to accomplish is the considerable velocity with

which the electrons enter the ion beam because of electrostatic attraction. Another reason is the low particle density within the beam which precludes energy-dissipating collisions. If only one pencil-shaped beam had to be neutralized, the neutralization problem would be greatly relieved by the lateral spreading of the beam. However, an ion motor for practical use must contain several thousand closely packaged pencil-sized beams, an arrangement which does not leave much room for lateral beam spreading. Figure 22 shows schematically how ion beams and electron emitters may be arranged, and how electrons and ions would mix.

The distance from the rear electrode at which neutralization must be accomplished is of the order of a few centimeters, or even less. This distance depends upon the (μ/ϵ) - ratio of the particles. At a given thrust per cm^2 and a given exhaust velocity, the distance at which neutralization must be achieved is proportional to (μ/ϵ) , as implied by Eq. (43). This is another reason why a large (μ/ϵ) of the propellant particles is desirable.

Negative ions instead of electrons for beam neutralization have been considered. The velocity

of negative ions could be easily matched to the velocity of the positive ions, and the formation of a neutral plasma would be no particular problem. Difficulties arise with the efficient, but simple production of negative ions; all sources of negative ions which are known so far have a relatively poor efficiency. Also, it seems to be difficult to arrange positive and negative ion sources in such a way that the ions mix within the required short distance from the accelerating electrodes. A schematic of a propulsion system emitting negative and positive ions is shown in Fig. 23. The efficient neutralization of the exhaust beam is probably the most acute single problem presently existing in the field of electrostatic propulsion systems.

(5) Heavy Particle Systems

The thrust of an ion motor is determined by the total electric power, the total propellant mass, and the operating time (Eq. 38). The specific charge of the propellant particles does not appear in this relation. However, it is advantageous to use a propellant with a large μ/ϵ ratio for two reasons: first, the larger the μ/ϵ , the smaller is the motor area required for a given thrust at a given exhaust velocity; and second, the larger the μ/ϵ , the longer is the

section of the beam which is available for beam neutralization. Both these relations are apparent in Eq. (43).

Heavier particles require a larger accelerating potential in order to reach a given velocity. In spite of the excellent insulation properties of a high vacuum, the voltages which can be handled safely by a propulsion system are limited by the danger of spontaneous breakdown between electrodes. It seems that a field strength of about 50,000 volt cm^{-1} represents an upper limit. It is difficult to estimate the maximum voltage for which a propulsion system can be safely designed, but this maximum voltage will probably be not higher than 10^6 volt. Optimization of the electric power generator may set an even lower limit to the maximum voltage.

Figure 24, based on the equation

$$v = \sqrt{2 U e/\mu}$$

shows the exhaust velocity of the propellant particles as a function of their mass-to-charge ratio for various accelerating voltages. The region of practical interest is shaded. Heavy particles lead to a high-voltage, low-current system, whereas lighter particles

lead to a low-voltage, high-current system.

Figure 24 implies that particles up to an μ/ϵ of about one-hundred times that of Cs are desirable. Several methods of producing spherical particles of sub-micron size are known. Charging the particles would be accomplished by having them contact a charged surface whose potential U they assume. Their charge ϵ will then be

$$\epsilon = U C$$

where the capacity C is equal to the radius r of the particles.

The upper limit of their charge will be set by the critical field strength S which leads either to a break-up of the particles, or to a spontaneous discharge. This critical field strength depends on the material; it is of the order of 10^8 volt cm^{-1} . Since the mass of one particle is

$$\mu = \frac{4}{3} \pi r^3 \rho$$

and since

$$\frac{\mu}{\epsilon} \approx 100 \left(\frac{\mu}{\epsilon} \right)_{Cs} ,$$

we obtain

$$r = \frac{75S}{\pi\rho} \left(\frac{\mu}{\epsilon} \right) Cs$$

or

$$\begin{aligned} r &\approx 1.8 \times 10^{-6} \text{ cm} \\ &\approx 1.8 \times 10^{-2} \text{ microns} \end{aligned}$$

Particles of this size must be charged to 180 volts in order to achieve a μ/ϵ one-hundred times greater than that of Cs. While particles of this size can be produced, it seems that severe problems arise in the propellant feed system, and in the charging of the particles at a sufficiently high and continuous rate. Mere "electrostatic spraying" of a liquid, a process which has been known for a long time, appears to be impractical because sizes and charges of the particles vary over too wide a range.

Heavy molecules, like UF_6 , offer a possibility of increasing the μ/ϵ substantially beyond that of Cs. However, no ionization method is developed yet which would be efficient enough to make a UF_6 system superior to a Cs system.

(6) Performance and Design Figures of Electrostatic Systems

Based on reasonable assumptions regarding the specific power and the efficiency obtainable

from ion propulsion systems, the performance, capabilities, and the major design parameters, of space vehicles propelled by ion motors may be derived from the equations presented in this chapter. At first, decisions will be made regarding the desired payload, the required characteristic or terminal velocity, the anticipated travel time, and the available specific power. With these figures, Eq. (8) and Figure 4 yield the exhaust velocity v ; the minimum ratio M_0/M_1 is found from Eq. (7). It provides M_0 and, through Eq. (10), the terminal mass M_e , which in turn allows the determination of M_p and M_f . The power P results from Eqs. (4) or (5), the thrust F from Eq. (6). As soon as the propellant is chosen, Eq. (36) will provide the voltage, and Eq. (39) the current. The initial acceleration is given by $a = F/M_0$.

Table 4 lists a number of space vehicles and their more important design and performance parameters. These figures are based on cesium as propellant, and on a specific power of $\alpha = 0.3 \text{ kw kg}^{-1}$.

The limited efficiency of the power conversion system is, of course, taken into consideration in these figures. The efficiency of the conversion

of electric energy into kinetic energy of the beam, however, was assumed to be 100 per cent. This assumption is certainly not realistic; there will be losses within the ion source, and losses caused by the heat radiation of the ion source, and by the beam spreading. The best total conversion efficiency of an ionic thrust chamber obtained so far is about 65 per cent. It is probable that efficiencies of 85 to 90 per cent, or even more, will be reached ultimately.

e. Electrically Heated Systems

(1) Thermodynamic Considerations

The performance of rocket propulsion systems in which the propellant gas is heated by electric energy is determined by the same equations (1 - 35) which describe electrostatic or electromagnetic systems. Electrically heated systems differ in the way the electric energy is converted into kinetic beam energy. Generally speaking, the propellant is fed in gaseous, liquid, or solid form into the chamber where it is heated by an arc or by a hot surface. The heated gas leaves the chamber through a conventional nozzle. A schematic of an arc-heated rocket motor is shown in Figure 25. A number of research groups have carried out investigations of arc-heated systems during the past few years [61].

The velocity of the exhaust particles is determined by the flow rate of the propellant, the

electric power input, the nature and thermodynamic properties of the exhaust gas, and the geometric form of the nozzle. Exhaust velocities up to 16 km sec^{-1} and arc temperatures of 40,000 °K were obtained by proper cooling techniques [62].

The upper limit of the exhaust velocity of arc-heated systems is presently considered to be of the order of 25 km sec^{-1} . This exhaust velocity would be reached with arc temperatures between 50,000 and 100 000 °K; about one-half of the original energy would be absorbed by the film cooling medium, the other half would be converted into kinetic beam energy. At temperatures in the 50 000° to 100 000 °K range, where the conductivity of a plasma is better than that of copper, the electric circuitry will limit the power input into the arc.

If heating is achieved by an electric arc, the immediate region of the burning arc contains a considerable number of ions. However, at the average energy densities which can be maintained within the chamber, the degree of ionization at some distance from the arc is so small that the working fluid, even in the throat area, can be considered as a "hot gas," and not a plasma. Normal thermodynamic laws apply.

The exhaust velocity is given by St. Venant-Wentzel's equation

$$v = \sqrt{2 G \frac{RT}{\mu} \frac{\gamma}{\gamma-1} \left[1 - \left(\frac{P_e}{P_c} \right)^{\frac{\gamma-1}{\gamma}} \right]} \quad (46)$$

or, in a more general form, by

$$v = \sqrt{\frac{2E}{M}} \quad (47)$$

where E/M designates that part of the energy content of the gas per unit mass which transforms into kinetic energy of the exhaust beam. The energy per gram which is available for this conversion is the "free energy" or enthalpy of the gas. If H_c is the enthalpy within the chamber, and H_e the enthalpy at the end of the expansion nozzle, and if η_n designates the nozzle efficiency (approximately 95 per cent), we find:

$$v = c_0 \sqrt{\eta_n (H_c - H_e)} \quad (48)$$

This equation shows that the exhaust velocity is determined in essence by the enthalpy of the gas. It is the problem of the engine designer to select a propellant which has sufficiently high enthalpy at a

bearable temperature.

Table 5 lists a number of chemical rocket propellants and their enthalpies [63].

The maximum temperature which can be withstood by a rocket chamber and nozzle is primarily determined by the wall material and the cooling methods. While a temperature of the order of 3000 °K was considered an upper limit several years ago, modern rocket chambers can be built to allow chamber temperatures which are much higher. As long as the temperature of a propellant is below the limit imposed by the chamber walls, the exhaust velocity is determined by the enthalpy of the reaction according to Eq. (48). When the temperature within the chamber approaches the permissible limit before full use has been made of the available enthalpy, the temperature becomes the factor governing the exhaust velocity, according to Eq. (46). In this case, a propellant of low atomic weight is desirable. This situation is represented by a rocket chamber heated by a nuclear reactor. While the supply of energy is almost unlimited, a temperature limit is set by the wall materials through which the heat energy must be conducted. This limit, with present

technologies, is below 3000°K. In that case, hydrogen with its low atomic weight is by far the best propellant.

If the propellant is heated by an electric arc, the heat energy need not be transferred through any walls, and arc temperatures up to about 40 000°K have been handled by proper design and cooling of chamber and nozzle. In this higher temperature region, the enthalpy of a real gas is no longer a function of only the temperature and the atomic mass, but also of dissociation and ionization, and of pressure. When propellants are compared, a careful analysis must be made of the enthalpy as a function of temperature. Even the permissible temperature within the chamber is not independent of the propellant; it is influenced by the heat transfer properties, and by the pressure of the propellant gas. These complex relationships are the reason why hydrogen is not necessarily the best propellant for an arc-heated system. In fact, helium, lithium, nitrogen, argon and even water, are strong contenders.

Figures 26 and 27 show the enthalpies of hydrogen and water as functions of temperature. Hydrogen, for example, (Figure 26) has a fast

increase of enthalpy between 3000° and 5000°K, and another one beyond 10 000°K. The first rapid increase is caused by dissociation, the second by ionization. The physical meaning of this enthalpy increase is the following: when the chamber temperature increases beyond about 3000°K, more and more of the input energy is used to dissociate the hydrogen molecules. However, part of this dissociation energy is recovered in the nozzle during expansion; some of the atoms re-associate under release of energy, and part of this energy, in the form of enthalpy, represents itself as increase of the kinetic beam energy.

The study of the enthalpy helps greatly to understand the processes within chamber and nozzle. However, it does not yet give the desired relations between input power P , mass flow rate \dot{M} , and exhaust velocity v , which are necessary for a performance estimate of the arc-heated propulsion system. Generally, the following equation holds:

$$\frac{P}{\dot{M}} = \frac{E}{M} = \Delta H + H_p \quad (49)$$

where

$$\frac{E}{M} = \text{energy input per gram propellant}$$
$$\Delta H = \text{enthalpy transformed into kinetic beam energy}$$
$$H_b = \text{enthalpy carried away by the beam, including non-recovered dissociation energy per gram, non-recovered ionization energy per gram, and heat and radiation losses per gram.}$$

The magnitudes of these components depend on the properties of the propellant, on temperature, and on pressure. It is obvious that the function $v = f(P, \dot{M})$ can be determined for each propellant only by a very careful and complex analysis of theoretical and experimental data. Figure 28 shows the exhaust velocity of hydrogen as a function of temperature and pressure for an expansion ratio of 1:40. Figure 29 [64] gives an example of how dissociation and ionization of a gas depend on temperature; it shows the abundance of N_2 , N , N^+ , N^{++} , and N^{+++} within a nitrogen plasma in the temperature region from 5000°K to $40\,000^\circ\text{K}$. Temperatures of this magnitude can be reached within high-intensity arcs.

(2) Performance Data

An example of a rocket motor with lithium as propellant may illustrate the characteristic features

of the arc-heated system [63]:

Propellant	lithium
Molecular weight	6.94
Chamber pressure	1 mm Hg
Expansion ratio of nozzle	1:40
Enthalpy of lithium	71 600 cal/g
Chamber temperature	5000°K
Exhaust velocity	19 500 m sec ⁻¹
Propellant flow	0.484 g sec ⁻¹
Beam power	92 kw
Power conversion factor	0.63
Total power input	145 kw
Thrust	0.96 kg

Chamber and nozzle of this motor must be cooled.

If a combination of regenerative and film cooling is applied about 5% of the total input power is transferred to the coolant in the cooling jacket, while 10% will be absorbed by the film. The mass of the propellant injected as film coolant must be added to the amount of "propellant flow" shown in the above list.

An arc-heated motor of this type appears to be within present-day technology. The formation of

a "hot spot" on electrodes by the impinging arc can be avoided by magnetically rotating the arc in such a way that the point of impact moves continuously over a large electrode area.

Promising applications for arc-heated systems may be found by first using Eq. (9) which implies that a system with an exhaust velocity of the order of 1.5×10^6 cm sec⁻¹ has an optimum operating time of the order of a few weeks, depending on the specific power α . Propulsion times of this order are required by correction systems for precision satellites, by orbital transfer systems, and by lunar ferry systems. It is anticipated that arc-heated propulsion engines will find application in such systems within a few years.

f. Magnetofluidynamics Propulsion Systems

(1) Principles of Operation

As soon as a gas is sufficiently ionized to conduct an appreciable current, magnetic forces can be exerted upon the gas. If the magnetic forces are strong enough, the gas will be accelerated to velocities of the order of 200 km sec⁻¹, or even more.

Ionization of a gas produces a plasma containing ions, electrons, and neutral particles. If a gas is ionized by heating, its conductivity is a direct function of the temperature. Figure 33 shows the conductivity of air versus the air temperature. As a whole,

the plasma remains electrically neutral, and therefore is not subject to space charge effects. A plasma propulsion system, like an arc-heated system, can therefore produce an area density of the jet which is many times greater than that of an ion system. For that reason, plasma motors will always have a much smaller size than ion motors of the same thrust. However, the basic relations between power, thrust, exhaust velocity, specific power, and terminal velocity, as derived earlier in this chapter, are applicable to plasma systems in the same way in which they were applied to ion and arc heated systems in the previous paragraphs.

The physics of MFD systems is much more complicated, and much less understood than that of ion systems and arc-heated systems. Besides the theory of electricity and thermodynamics, MFD incorporates the theory of fluid flow under unusual conditions [66, 67, 68]. Thermodynamic equilibrium is not reached, and temperatures are extremely high, at least locally. As a rule, an MFD propulsion system represents a most complex entity which is difficult to analyze theoretically. Only a brief description will be given in this chapter.

If a particle of mass μ and charge ϵ is exposed to a combined electric and magnetic field, a force f_e is exerted upon it of the form

$$\vec{f}_e = \mu \frac{d\vec{v}}{dt} = \epsilon (\vec{S} + \vec{v} \times \vec{H}) \quad (52)$$

Negatively and positively charged particles move in opposite directions in a given electric field, and the magnetic forces therefore accelerate the particles in the same direction.

A particularly simple form of Eq. (52) results when it is applied to an electric arc which burns between two parallel rails, while a magnetic field exists perpendicular to the plane of the rails and the arc (Fig. 31). In this case, the total force per unit length, f_a , acting on the arc in a direction normal to H and I is simply

$$f_a = I H \quad (53)$$

This force accelerates the mass of the plasma which constitutes the arc, and by Newton's First Theorem, the same force is exercised in opposite direction upon the system that carries the plasma motor. Even though the mass contained in an arc plasma is only of

the order of 10^{-5} g in practical cases, the force, according to Eq. (53), may be of the order of kilograms; it produces plasma accelerations close to 10^9 G's.

The plasma velocity resulting from the accelerating force (Eq. 53) will always be limited because of the counter-voltage induced by the external field within the moving arc, very similar to the situation encountered in shunt-wound motors. The maximum or "idling" speed, neglecting all possible losses, is given by

$$\vec{v}_m = \frac{\vec{S} \times \vec{H}}{H^2} \quad (54)$$

Besides this relatively simple "rail" type MFD system, a number of other systems have been investigated theoretically and by experiment. They will be discussed below.

(2) Plasma Accelerators of Various Design

The plasma button source, developed by Bostick [69,70], is shown schematically in Figure 32. Closing of a switch initiates an arc discharge between the electrodes from a condenser bank. The plasma within the arc is driven away from the electrodes by

its own magnetic field and obtains high velocities within discharge times of microseconds. Thrust forces of several pounds at exhaust velocities up to many km per second have been measured. The requirements placed upon the condensers are severe because of the very short discharge times. Plasma button sources appear to be inferior to rail type systems as far as energy utilization is concerned.

The rail type system (Fig. 31), as mentioned above, lends itself more easily to theoretical analysis than any other MFD system. The rails may be two parallel wires, two flat plates, or two concentric cylinders. The arc discharge may be initiated through an ionized gas, or by an exploding wire. A particular switching device is unnecessary since each cycle starts with the establishment of the primary arc and terminates when the plasma leaves the rail system. If no external magnetic field is applied, the plasma moves only under the influence of its own magnetic field which tends to increase the current loop; the system is then analagous to a series-type electric motor. With an external magnetic d-c field, it resembles a series-shunt type motor.

Rail systems provide a longer discharge

time than button systems, and hence have a better energy transfer efficiency. Condenser requirements are less stringent. However, a considerable amount of energy is wasted for heating and erosion of the rail electrodes. Plasma velocities of 10 km sec^{-1} , in some instances even up to 40 km sec^{-1} , have been obtained [72,73].

An interesting modification, called "Backstrap System," has been investigated by Kolb [74]. The discharge current from the condenser is conducted along the rear of a T-shaped discharge tube (Figure 33) where it produces a strong magnetic field that drives the plasma out through a nozzle. Exhaust velocities up to 40 km sec^{-1} were measured at an efficiency of 39 per cent. This system, too, requires condensers of extremely short time constants.

Previous extensive work on electromagnetic shock tubes [66,79] provided experimental and theoretical data for the pulsed discharge system [67, 68,71,72,75,76,77,78]. As illustrated in Fig. 34, a discharge is initiated through a gas between two concentric cylinders. The current flows out through the inner cylinder, then radially through the gas

towards the outer cylinder, and then back through the outer cylinder. This current flow around the toroidal body of gas produces a strong ring-shaped magnetic field through the toroid. The combined electric and magnetic fields produce a force on the plasma in the forward direction. A field coil around the system generates a relatively weak d-c field parallel to the axis; representing a magnetic bottle, it prevents an immediate contact of the hot plasma with the cylinder walls. Approximately one-half of the electric energy transferred to the plasma is converted into kinetic energy, the other half into heat. An expansion nozzle may be used to recover part of the heat energy.

Exhaust velocities up to 200 km sec^{-1} , and even 800 km sec^{-1} , have been reported; efficiencies are still relatively low. Pulsed discharge systems of this type may lend themselves to variation of the exhaust velocity over a wide range, possible from 10 to 1000 km sec^{-1} .

A very intriguing modification of the MFD propulsion system is the traveling wave accelerator (Fig. 35). It resembles an induction-type single phase

or polyphase motor inasmuch as a traveling magnetic field pulls a conductor along. A "slip speed" must exist between the traveling field and the conductor; otherwise, no energy would be transferred from the field to the conducting plasma. The traveling magnetic field acts at the same time as a magnetic "mirror" which keeps the hot plasma from the walls and stabilizes the plasma toroid. High accelerating forces are desirable for better efficiency and stability. Lithium and nitrogen have been used successfully as propellants [71], and exhaust velocities up to 250 km sec^{-1} were obtained at energy transfer efficiencies up to 85 per cent [67]. The propellant feed system, and the striking of the initial arc at the desired pulse rate, seem to offer some difficulties. Auxiliary equipment needed to produce the high-power traveling wave and the high rate of condenser discharges is relatively heavy.

(3) Characteristic Features of MFD Systems

Although MFD propulsion systems comprise a wide variety of plasma accelerators, there are a number of features which are common to all of them. MFD motors allow a high area density of the propellant flow; the ratio of thrust over area of an MFD

engine is therefore large. Exhaust velocities range from about 10 to 1000 km sec⁻¹ in the various systems. High exhaust velocities are desirable for better discharge stability, and for more efficient conversion of electromagnetic energy into kinetic energy of the beam. The higher the rate of change of the magnetic field, the thinner is the layer of plasma in which currents are induced, and the smaller are the eddy current losses within the plasma. As an approximate average rule, about one-half of the electromagnetic energy absorbed by the plasma is converted into kinetic energy, and one-half into heat energy.

MFD systems require relatively complex auxiliary equipment such as condensers with low time constant, and for high voltages; magnetic d-c or a-c field coils; high-rate switching devices; and propellant feed systems adapted to special pulsing and pressure requirements. At the present time, over-all efficiencies are still of the order of only 15 to 40 per cent, while long lifetimes are hard to achieve. Total masses of the propulsion systems are high. Most likely, MFD systems will require more research and development time before immediate applications can be visualized.

g. Concluding Remarks

Electric propulsion systems depend on light-weight, efficient, and reliable sources of electric power. Arc-heated systems become attractive when electric power sources of the SNAP VIII-type, and larger units, are available. They will find application for satellite correction, satellite orbit transfer, and lunar ferry systems. Ion and MFD systems will be useful when electric power supplies with power-to-mass ratios of 0.1 kw kg^{-1} or more become available. Missions for ion and MFD systems will be flights to the moon, to the planets, and to interplanetary space, both unmanned and manned. At the present state of development, it appears that ion systems are closer to technical realization than MFD systems. A very considerable improvement of MFD systems would be gained if some of their operating power were delivered by a nuclear fusion reaction within the plasma.

A great many industrial companies, universities, and government laboratories are presently engaged in theoretical and experimental studies of electric propulsion systems. The National Aeronautics and Space Administration, and the Armed Forces, have been sponsoring

a considerable number of study projects under government contracts. Besides, theoretical and experimental work is underway at several NASA Field Centers.

REFERENCES

1. Goddard, R.H. (1959). R. H. Goddard, An Autobiography-Robert H. Goddard Notebook dated Sep 6, 1906. Astronautics 4, 4, 24.
2. Oberth, H. (1929). "Wege zur Raumschiffahrt." R. Oldenbourg, München-Berlin.
3. Ackeret, J. (1946). Helvet. Physica Acta 19, 103.
4. Seifert, H.S., Mills, M.W., & Summerfield, M. (1947). "Physics of Rockets." Amer. Journ. of Phys. 15, 255.
5. Shepherd, L.R. & Cleaver, A.V. (1948-1949). J. Brit. Interplan. Soc. 7, 185, 234; J.B.I.S. 8, 23, 59.
6. Forbes, G.F. (1950). "The Trajectory of a Powered Rocket in Space." J. Brit. Interplan. Soc. 9, 75.
7. Lawden, D. F. (1950). "Note on a Paper by G. F. Forbes." J. Brit. Interplan. Soc. 9, 230.
8. Spitzer, Jr., L. (1952). "Interplanetary Travel Between Satellite Orbits." Amer. Rocket Soc. Journ. 22, 92.
9. Preston-Thomas, H. (1952) J. Brit. Interplan. Soc. 11, 173.
10. Stuhlinger, E. (1954). "Possibilities of Electrical Space Ship Propulsion." V. Internat'l Astron. Cong., Innsbruck, p. 100.
 Stuhlinger, E. (1955). "Electrical Propulsion Systems for Space Ships with Nuclear Power Source." J. Astronautics, Vol 2, p. 149; Vol 3, p. 11, 33.
 Stuhlinger, E. (1957). "Design and Performance Data of Space Ships with Ionic Propulsion Systems." VIII Int'l Astron Cong., Barcelona. Springer, Verlag, Vienna, Austria, p. 403.

- Stuhlinger, E. (1958). "Advanced Propulsion Systems for Space Vehicles." IXth International Astron. Cong., Amsterdam, 1958. Springer Verlag, Vienna, Austria.
- Stuhlinger, E., & Seitz, R.N. (1959). "Some Problems in Ionic Propulsion Systems." I.R.E. Trans. Military Electronics MIL-3, 27.
- Stuhlinger, E. (1959). "Lunar Ferry with Electric Propulsion System." Paper presented at Annual Meeting of the Japanese Rocket Society, Tokyo, Japan (May).
11. Langmuir, D.B. (1956). "Optimization of Rockets in which Fuel is not used as propellant." Ramo-Wooldridge Corp. Rpt. ERL 101, (Sep).
 12. Irving, J.H. (1958). Space Technology Course, UCLA.
 13. Bussard, R.W. (1956). "A Nuclear-Electric Propulsion System." Journ. Brit. Interplan. Soc. 15, 297.
 14. Boden, R.H. (1957). "The Ion Rocket Engine." Rocketdyne Rpt. R-645P.
 15. Eilenberg, S.L. "Accelerator Design Techniques for Ion Thrust Devices." Rocketdyne Rpt R-1430, 1959.
 16. Speiser, R.C., Dulgeroff, C.R., & Forrester, A.T., "Experimental Studies with Small Scale Ion Motors." ARS Preprint 926, 1959. ARS Meeting, Washington, D.C., 1959.
- Dillaway, R.B., "Typical Propulsion Systems for Space Flight." Space Propulsion Session, IAS 26th Ann Mtg, New York, Jan 27-30, 58.
17. Giannini, G.M., "The Plasma Jet and its Application." TN 57-520, Office of Sci. Research, 1957.

- Waniek, R.W., "Problems of Magnetic Propulsion of Plasma," Second Symposium on Advanced Propulsion Concepts, AVCO, Boston, Mass., Oct. 1959.
18. Fox, R.H., "Study of Electric Propulsion Systems for Space Travel." UCRL 5478, Lawrence Radiation Laboratory, Feb 6, 1959.
- Krulikovski, B.K., "An Alkali Metal Ion Source." IPU 59-08, Naukovi Povidomlemia Fizyka, Kiev U. No. 1, 1956, pp. 11 - 12.
- Stavisskii, Y.Y., Bondarenko, I.I., Krotov, V.I., Lebedev, S. Y., Pupko, V.Y., and Stumbur, E.A., "Experiment to Obtain Reaction Thrust In a Laboratory Model of an Ion Engine." Soviet Physics & Tech. V. 4, #8.
19. Langmuir, D.B., "Low Thrust Flight: Constant Exhaust Velocity in Field-free Space." Space Technology, ed by H. Seifert, John Wiley & Sons, 9-01, 1959.
- Kaufmann, H.R., "One-Dimensional Analysis of Ion Rockets." NASA Rpt TN D-261.
20. Ghai, M. L., "Plasma Propulsion for Space Applications." ARDC-OSR Contractor's Conference, Oct 1, 1958.
- Edwards, R.N. & Kuskevics, G., "Cesium-Ion Rocket Research Studies." Paper No. 59-AV-32, 1959, ASME.
- Childs, J.H., "Design of Ion Rockets and Test Facilities." IAS Nat'l Summer Meeting, Los Angeles, Calif., June 1959.
21. Alfven, H., "On the Existence of Electromagnetic-hydrodynamic Waves," Arkiv for Matematik Astronomi och Fysik, vol. 29B, no. 2, 1943; see also Nature, vol. 150, 1942, pp. 405-406.

22. Spitzer, L, Jr., "Physics of Fully Ionized Gases," Interscience Publishers, Inc., New York, 1956.
23. Kantrowitz, A., Resler, E.L. and Lin, S.C., "Electrical Conductivity of Highly Ionized Argon Produced by Shock Waves," J. Appl. Phys., vol. 26, Jan. 1955, pp. 95-100.
24. Landshoff, R.K.M. (Editor), "Magnetohydrodynamics," A Symposium; Stanford University Press, 1957.
"The Plasma in a Magnetic Field," Stanford University Press, 1958.
25. Alfven, H., "Cosmical Electrodynamics," Clarendon Press, 1953.
Sears, W.R., "Magnetohydrodynamic Effects in Aerodynamic Flows," ARS Journal, Vol. 29, pg. 397, 1959.
26. Finkelburg, W., "The High Current Carbon Arc and its Mechanism." J. Appl. Phys. 20, 468, 1949.
27. Maecker, H. & Peters, T., "Messung der Plasmaleitfähigkeit im Hochleistungsbogen," Zeitschrift für Physikalische Chemie, vol. 198, No. 5/6, 1951, pp. 319-328.
28. Cann, Gordon, Adriano Ducati, and Vernon Blackmon, "Experimental Studies on the Thrust from a Continuous Plasma Jet," Paper presented at Advanced Propulsion Systems Symposium, Rocketdyne, AFOSR, Los Angeles, California, 1957.
29. Malin, M.E., et al., "Application of Electric-Arc Plasma Generators to Propulsion," Paper presented at Ninth International Astronautical Federation, Amsterdam, 1958.
30. Heller, G. (1959). "The Plasma Jet as an Electric Propulsion System for Space Application," ARS 1040-59, November 1959.

31. Moeckel, W.E., Private Communication, Lewis Flight Propulsion Laboratory, NASA, March 1960.
32. Stuhlinger, E & Seitz, R.N. (1960). "Electrostatic Propulsion Systems for Space Vehicles," chapter to be included in the 1960 Edition of "Advances in Space Science," edited by F. I. Ordway, III, Academic Press, New York.
33. Michielsen, H. (1957). Astronaut. Acta 3, 130.
34. Fox, R. (1959). "Optimum Exhaust Velocity Programming and Propulsion Efficiency," Amer. Astron. Soc., Inc., Vol. VI, No. 1.
35. Blum, E.K., "Optimal Rocket Trajectories," Unpublished Report, Ramo-Wooldridge Corp., 1957.
36. Irving, J.H. (1956). "Optimum Program for Single Stage Rockets in which Expellant is not the Source of Power." Ramo-Wooldridge Corp. report.
37. Huth, J.H., "Space Vehicle Power Plants", The Rand Corporation, p-1861, 1959.
38. "Advanced Energy Sources & Conversion Techniques," Seminar sponsored by the U. S. Dept. of Defense, ASTIA No. AD 209301, Pasadena, 1958.
39. Zwick, E.B., & Zimmermann, R.L., "Space Vehicle Power Systems," ARS Journal, Vol. 29, No. 8, 553, 1959.
40. Zarem, A.M., "Power Systems," Astronautics, November 1959, p. 44.
41. Child, E.D. (1911). "Discharge from Hot CaO." Phys. Rev. 32, 492.
Langmuir, I. (1913). The Effect of Space Charge and Residual Gases on Thermionic Current in High Vacuum." Phys. Rev. 2, 450.

42. Richardson, O.W. (1921). "The Emission of Electricity from Hot Bodies," Longmans, Green & Co., London & New York.
43. Ives, H.E. (1923). "Positive Rays in Alkali Metal Vapor Thermionic Tubes." Phys. Rev. 21, 385.
44. Saha, M.N. (1921). "Versuch einer Theorie der Physikalischen Erscheinungen bei Hohen Temperaturen mit Anwendungen auf die Astrophysik," Zs. Physik 6, 40.
45. Thomson, J.J. (1921). "Rays of Positive Electricity ." Longmans, Green & Co., New York.
46. Aston, F.W. (1921). "The Mass Spectra of the Alkali Metals." Phil. Mag. Ser. 6.42, 436-441.
47. Langmuir, I. & Kingdon, K.H. (1923). "Thermionic Phenomena due to Alkali Vapors." Phys. Rev. 21, 380-381.
48. Taylor, J. B. & Langmuir, I. (1933). Phys. Rev. 44, 423.
49. Shelton, H., Wuerker, R.F., & Sellen, J.M. (1959). "Generation and Neutralization of Ions for Electrostatic Propulsion," ARS paper 882-59.
50. Kuskevics, G. (1959). "Ion Rocket Efficiency Studies," 10th Congress of the International Astronautical Federation, London
51. Baldwin, G.C., Downing, R., Edgar, R.F., Goodale, E.E., Sawyer, J.F., & Stauffer, L.H. (1958). "Experimental Investigation Pertinent to an Ionic Propulsion Concept," G.E. General Engr. Lab Rpt. No., 58GL355.
52. Forrester, A.T. & Speiser, R.C. (1959). "Cesium Ion Propulsion", Astronautics, Vol. 4, No. 10, 34.

53. Von Ardenne, M., "New Developments in Applied Ion and Nuclear Physics," Lib. Trans. 758, AERE, Harwell (Berkshire, 1957.
Also: Private Communication, Dr. J. Gale, Goodrich-High Voltage Engineering Corp., March 1960.
54. Meyerand, R.^G & Brown, S.C., "High Current Ion Source," Review of Scientific Instruments 30, 110, 1959.
55. Raether, M.J. & Seitz, R.N. (1959). "A Pierce Gun Design for an Accelerate-Decelerate Ionic Thrust Device," ARS paper 884-59.
56. Fay, C.E., Samuel, A.L. & Shockley, W. (1938). "On the Theory of Space Charge Between Parallel Plane Electrodes," Bell Systems Tech. Journal, 17, 49.
58. Langmuir, D.B. "Problems of Thrust Production by Electrostatic Fields." Vistas in Astronautics, Vol II. Pergamon Press, 191, 1959.
59. Eilenberg, S.L. & Huebner, A.L.C. (1959). "Engineering & Scientific Problems of Ion Propulsion," ARS Meeting, San Diego, California.
61. Giannini, G.M., "The Plasma Jet", Scient. American, Vol. 196, p. 80 1957.
Boden, R.H., "Electrical Space Propulsion," Rocketdyne Rpt, 1959.
62. Ducati, A.C. & Cann, G.L., "Plasma Propulsion," Paper presented at the 14th Annual ARS-Meeting, 1959.
63. Heller, G. (1959). "Propulsion for Space Vehicles by the Thermodynamic Process," Army Ballistic Missile Agency Rpt No. DV-TM-3-59, 12 Feb 1959.

64. Finkelburg, W., "The High Current Carbon Arc and its Mechanism." Journ. Appl. Phys. 20, 468, 1949.
65. Bussard, R.W., "Nuclear Rocket Propulsion Possibilities," Space Technology, ed. by H. Seifert, John Wiley & Sons, 17-01, 1959.
66. Kash, S.W., "Magnetically Driven Shock Waves," Experiments at Lockheed Missile Systems Division, Magnetohydrodynamics, Stanford Press (1957).
67. Camac, M., Kantrowitz, A., Petschek, H.E., "Plasma Propulsion Devices for Space Flight," IRE Transactions on Military Electronics, Vol. MIL-3, No. 2, p. 34 (1959).
68. Post, R.F., "Controlled Fusion Research - An Application of the Physics of High Temperature Plasmas," Rev. Mod. Phys., 28, No. 3, p. 338 (1957).
Kruskal, M., & Schwarzschild, M., "Some Instabilities of a Completely Ionized Plasma," Proc. Roy. Soc., A, 223, p. 348, (1954).
69. Bostick, W., "Plasma Motors," Advances in Astronautical Sciences, Vol. 2, 2-1, (1957).
70. Rayle, W., "Plasma Propulsion Possibilities," IRE Transactions on Military Electronics, Vol. Mil-3, No. 2, p. 42 (1959).
71. Gauger, T., Vali, V., & Turner, T.E., "Laboratory Experiments in Hydrodynamic Propulsion," Advances in Astronautical Sciences, Vol. 3., 7-1, (1958).
72. Patrick, R.M., "A Description of a Propulsion Device which Employs a Magnetic Field as the Driving Force," Second Annual AFOSR Astron. Symp., Denver, Col. (1958).

73. Janes, G.S., & Patrick, R.M., "The Production of High Temperature Gas by Magnetic Acceleration," Avco Res. Rpt 27 (1958).
74. Kolb, A.C., "Production of High-Energy Plasmas by Magnetically-Driven Shock Waves." Phys. Rev. 107, 345, 1957.
75. Post, R.F., "Acceleration of a Plasma by Time-Varying Magnetic Fields." UCRL-4407, Livermore Site, 1954.
76. Bostick, W., "Experimental Studies of Plasmoids." Phys. Rev. 106, April-June, 1957.
77. Cowling, T.G., "Magnetohydrodynamics," Interscience Publishers No. 4, 1957.
78. Resler, E.L., Jr., & Sears, W.R., "The Prospects for Magneto-Aerodynamics," Journ. Aero/Space Sciences, Vol. 24, No. 4, 1958,
79. Clauser, M.U., "Magnetohydrodynamics," Chapter 18 of "Space Technology," Ed. by H. Seifert, John Wiley & Sons, 1959.
Sears, W.R., "Magnetohydrodynamic Effects in Aerodynamic Flows," ARS Journal, Vol. 29, p. 397, 1959.

TABLE I¹Component Masses of Turbo-electric
Power Plant (20 MWe)

Reactor (20% conversion efficiency)	1500 kg
Heat Exchanger with Working Fluid	2500 kg
Turbine and Compressor	10000 kg
Radiation Cooler	16000 kg
Generator	20000 kg
Shield	20000 kg
TOTAL	<u>70000 kg</u>

$$\alpha = \frac{20000}{70000} \approx 0.3 \text{ kw kg}^{-1}$$

¹Ref. 32

TABLE II¹

Work Function ϕ and Melting Temperature
 T_m of Various Metals

Metal	Work Function ϕ (photoelectric) in eV	Melting Temp- erature T_m °C
Ag	4.7	960
C	4.81	3550
Cr	4.37	1890
Ir	4.9	2454
Mo	4.3	2620
Os	4.5	2700
Pt	5.2	1773
Re	5.1	3167
Ta	4.1	3027
W	4.5	3370

¹Ref. 32

TABLE III¹

Ionization Energies Q
of Various Elements

<u>Element</u>	<u>Atomic No.</u>	<u>Q (e⁻-volts)</u>
H	1	13.5
He	2	24.5
Li	3	5.36
C	6	11.2
Na	11	5.12
K	19	4.32
Kr	36	13.9
Rb	37	4.16
Cs	55	3.87
Hg	80	10.39

¹Ref. 32

TABLE IV¹

CHARACTERISTIC DATA OF ION PROPULSION SYSTEMS
FOR VARIOUS MISSIONS

	Time of pre- pulsion τ	Payload M _L tons	Total mass M ₀ tons	Terminal velocity u km s ⁻¹	Exhaust velocity v km s ⁻¹	End mass M _e tons	Propellant mass M _p tons	Mass of propul- sion system M _p tons	Thrust F kg	Power L kw	Initial accel- eration		Current I amp	Voltage U volt
											a _i G	G		
SUSTAINER	1	4	5	15	141	4.5	0.5	0.5	0.227	159	4.45x10 ⁸	11.6	13600	
SATELLITE CORRECTION	0.03	~5	5	0.46	38	~5	0.006	—	0.027	5	5.4x10 ⁶	5	1000	
SATELLITE TRANSFER	0.08	50	72.2	6.0	60	65.5	6.7	15.5	16.9	4650	2.29x10 ⁴	2000	2325	
LUNAR FERRY	0.17	100	136	10.4	60	119	17.0	19.0	19.7	5700	1.45x10 ⁴	2360	2420	
MARS	1.6	150	435	72	120	243	192	93	46.8	27900	1.06x10 ⁴	2800	9950	
JUPITER	1.5	1	5.3	90	120	2.5	2.8	1.5	0.75	450	1.38x10 ⁴	44.5	10100	
SATURN	2.5	1	10.9	140	180	5.0	5.9	4.0	1.36	1200	1.22x10 ⁴	54	22200	
DEEP SPACE	3	1	16	160	200	7.2	8.8	6.2	1.9	1900	1.16x10 ⁴	68	28000	

¹ Ref. 32

TABLE V¹

Enthalpies of Gases from Various Reactions

Chemical energy, monopropellant, solid or liquid:		
Hydrazine		545 cal gm ⁻¹
Nitroglycerine		1615 cal gm ⁻¹
B ₁₀ H ₄ + NH ₄ ClO ₄		1800 cal gm ⁻¹
Chemical energy, liquid propellant:		
Hydrocarbon + oxygen		2280 cal gm ⁻¹
Hydrogen + oxygen		3000 cal gm ⁻¹
Hydrogen + fluorine		3070 cal gm ⁻¹
Hydrogen + ozone		3880 cal gm ⁻¹
Lithium + oxygen		4720 cal gm ⁻¹
Beryllium + oxygen		5730 cal gm ⁻¹
Free Radicals:		
CH ₃		2770 cal gm ⁻¹
NH		3750 cal gm ⁻¹
N		8000 cal gm ⁻¹
Ne*		18800 cal gm ⁻¹
He*H		100000 cal gm ⁻¹
Nuclear Energy:		
Fission		2 x 10 ¹⁰ cal gm ⁻¹
Fusion		2 to 8 x 10 ¹⁰ cal gm ⁻¹
Electric Energy (arc heated):		
Hydrogen	2000°K	7 x 10 ³ cal gm ⁻¹
	4000°K	7 x 10 ⁴ cal gm ⁻¹
	7000°K	8 x 10 ⁴ cal gm ⁻¹
	10000°K	13 x 10 ⁴ cal gm ⁻¹

(P_c = 0.1 atm)

¹ Ref. 63

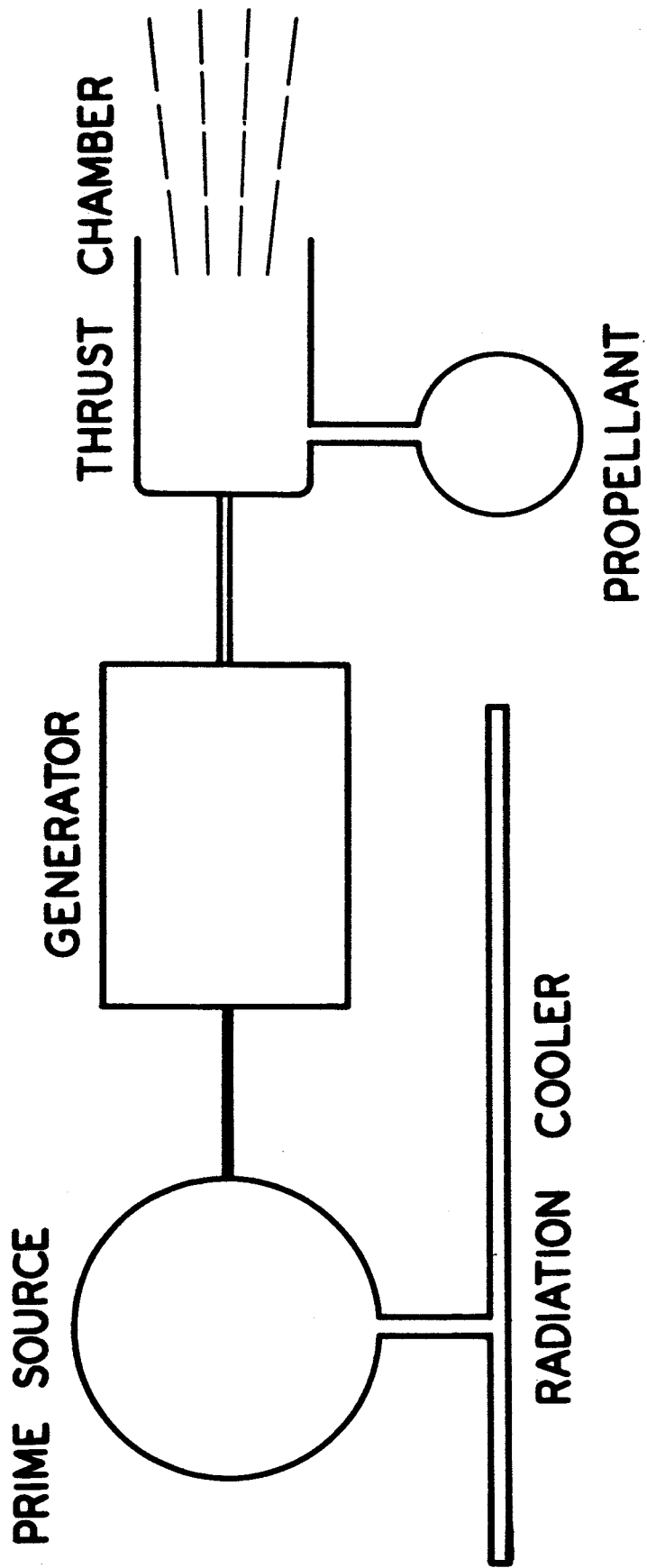


FIG. 1 - BASIC COMPONENTS OF ELECTRIC PROPULSION SYSTEM

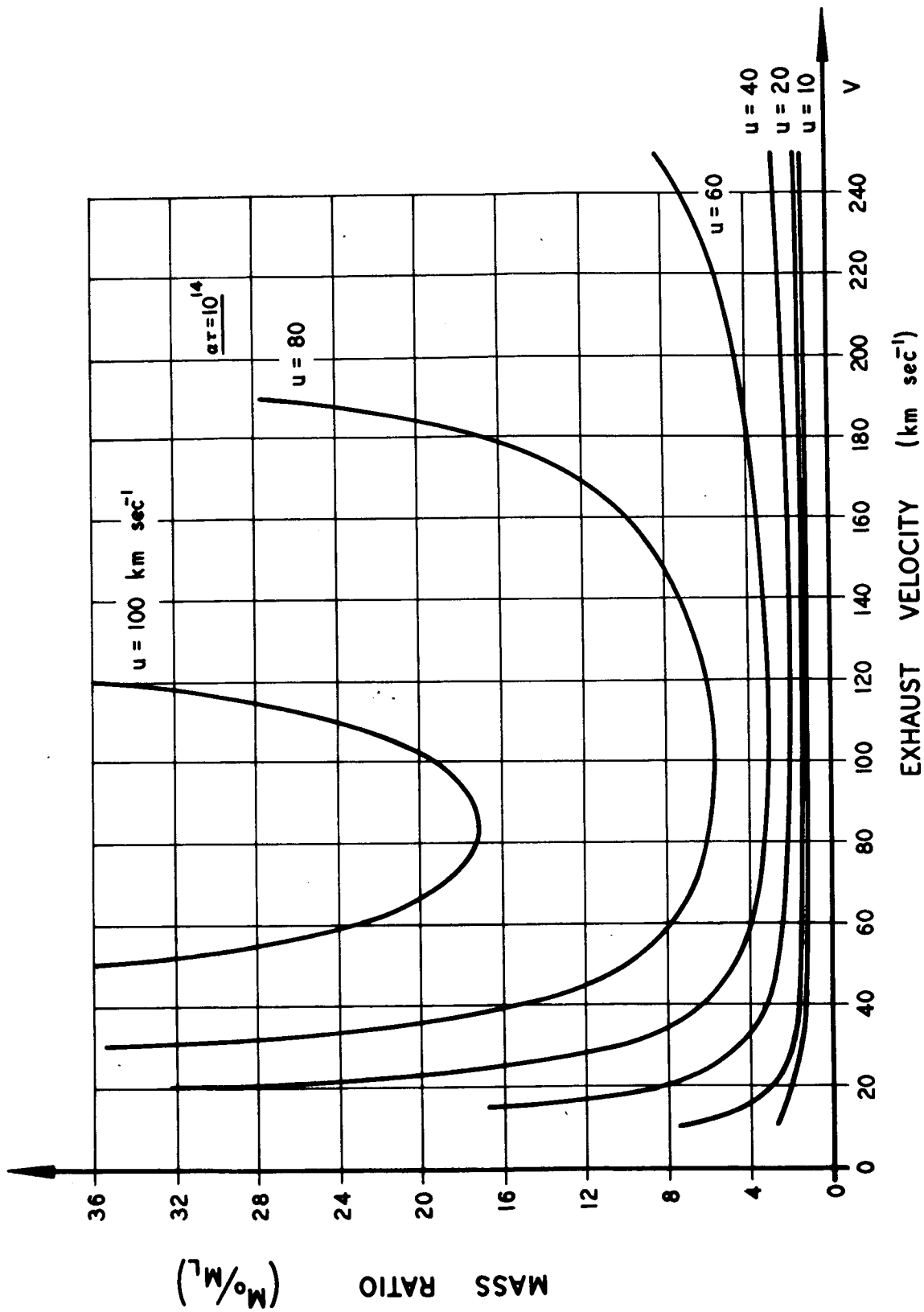


FIG. 2 - Mass ratio M_0/M_1 as a function of exhaust velocity with terminal velocity, specific power, and propulsion time as parameters.

$$\alpha\tau = 10^4 \text{ erg g}^{-1}$$

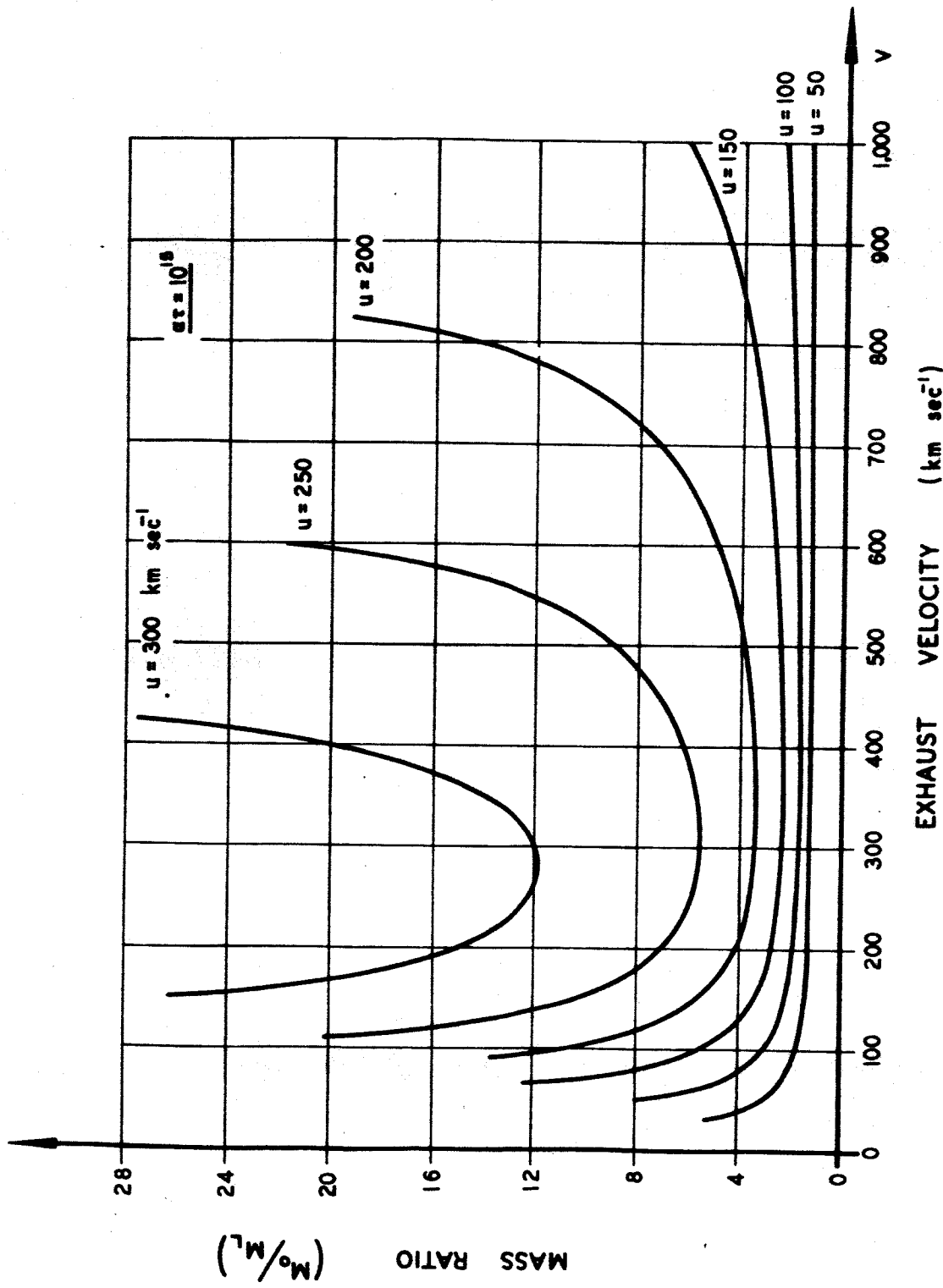


FIG. 3 - Mass ratio M_0/M_1 as a function of exhaust velocity with terminal velocity, specific power, and propulsion time as parameters.

$$\alpha\tau = 10^{18} \text{ erg g}^{-1}$$

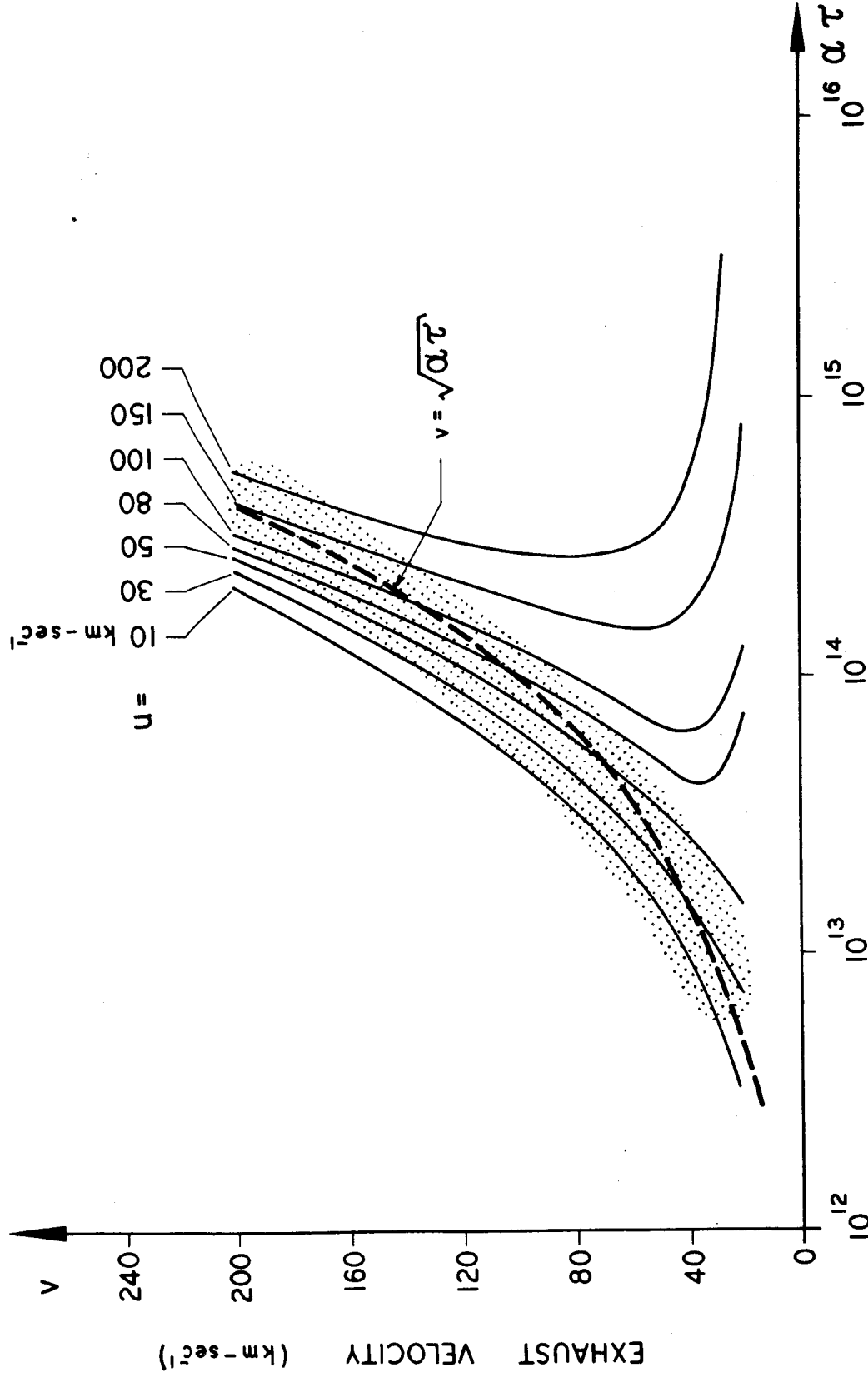


FIG. 4 - Optimum exhaust velocity v as a function of $\alpha\tau$ with terminal velocity u as a parameter (payload is maximized).

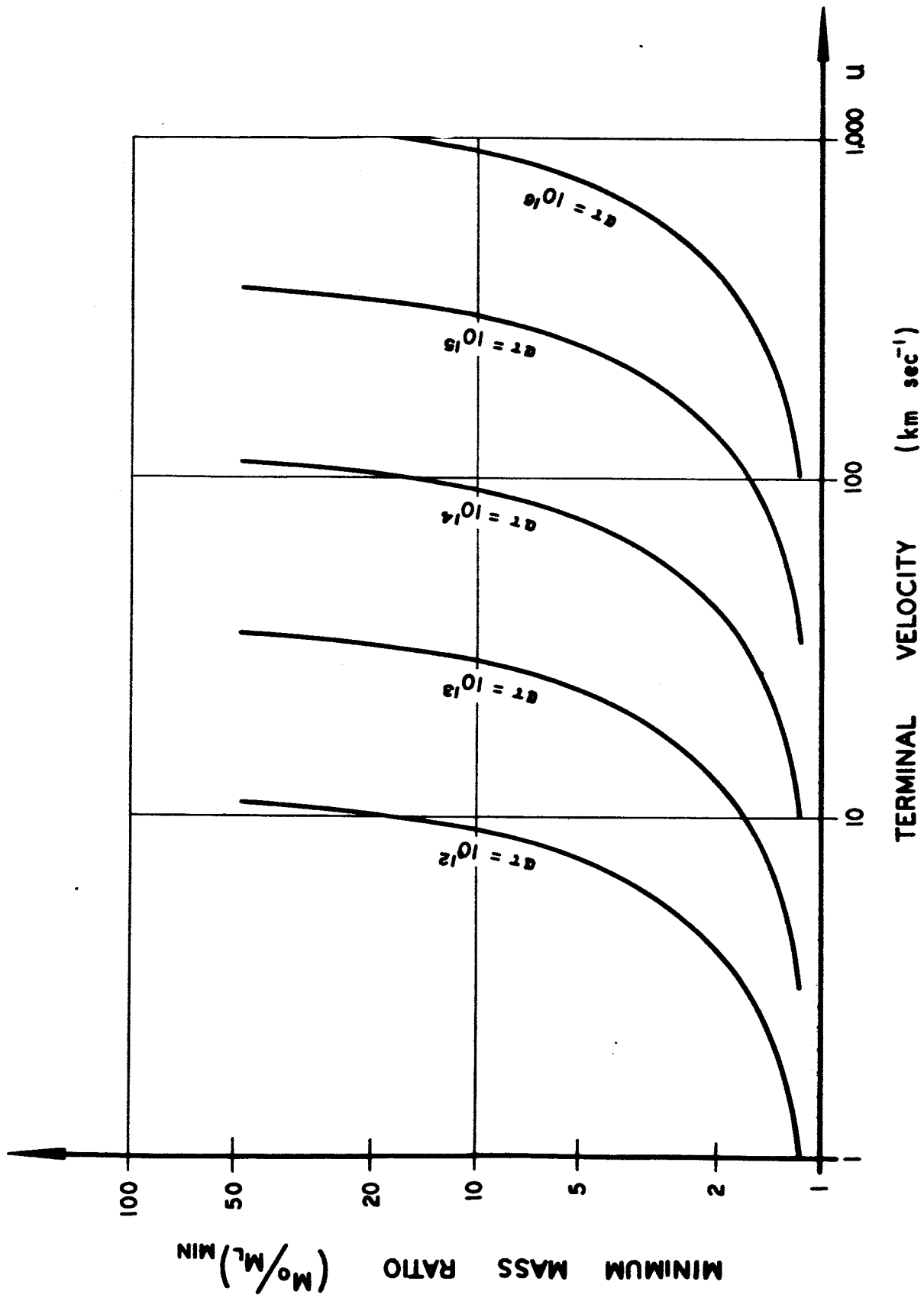


FIG. 5 - Minimum mass ratio $(M_0/M_1)_{\min}$ as a function of terminal velocity with $\alpha\tau$ as parameter.

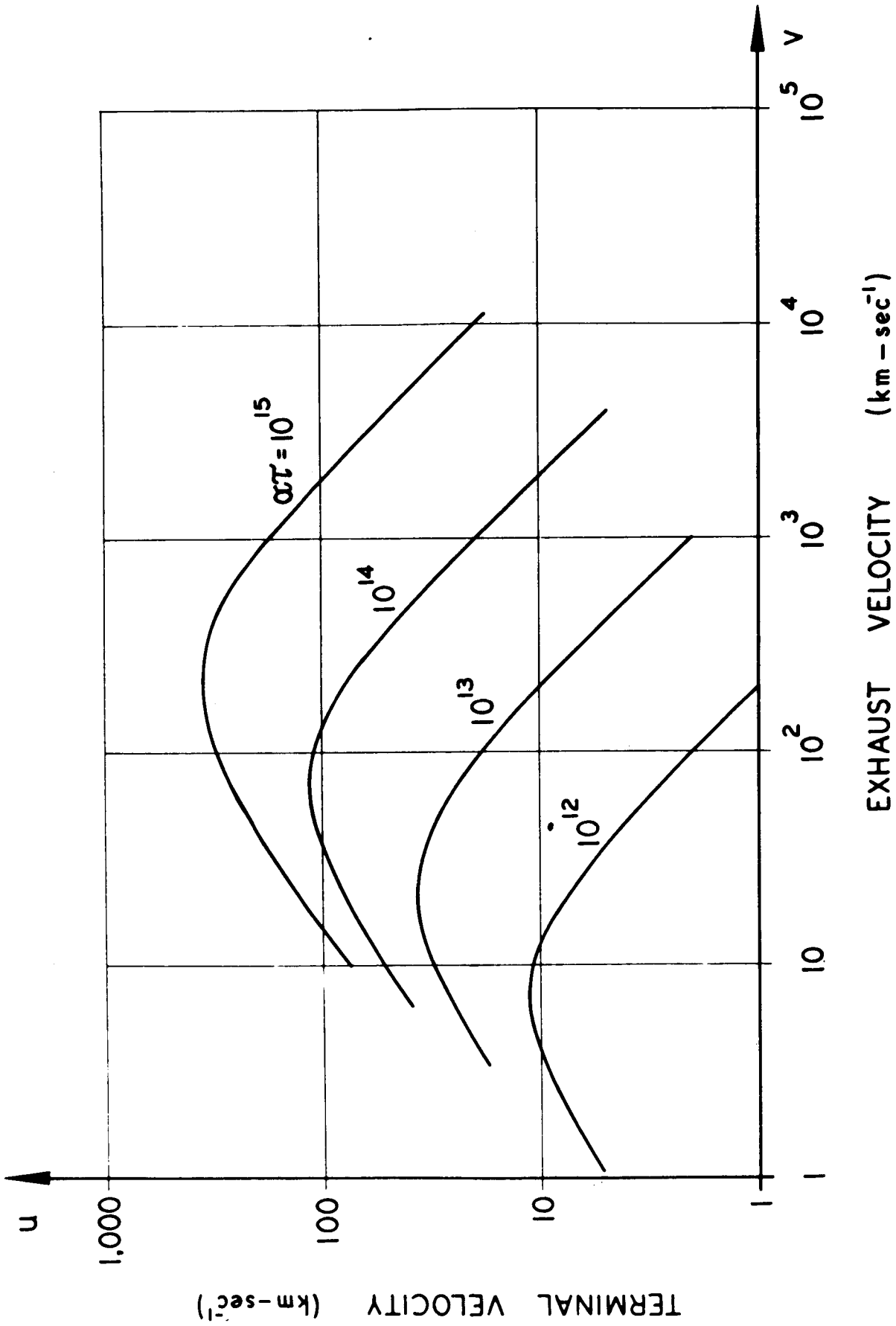


FIG. 6 - Terminal velocity u as a function of exhaust velocity v for vanishing payload.

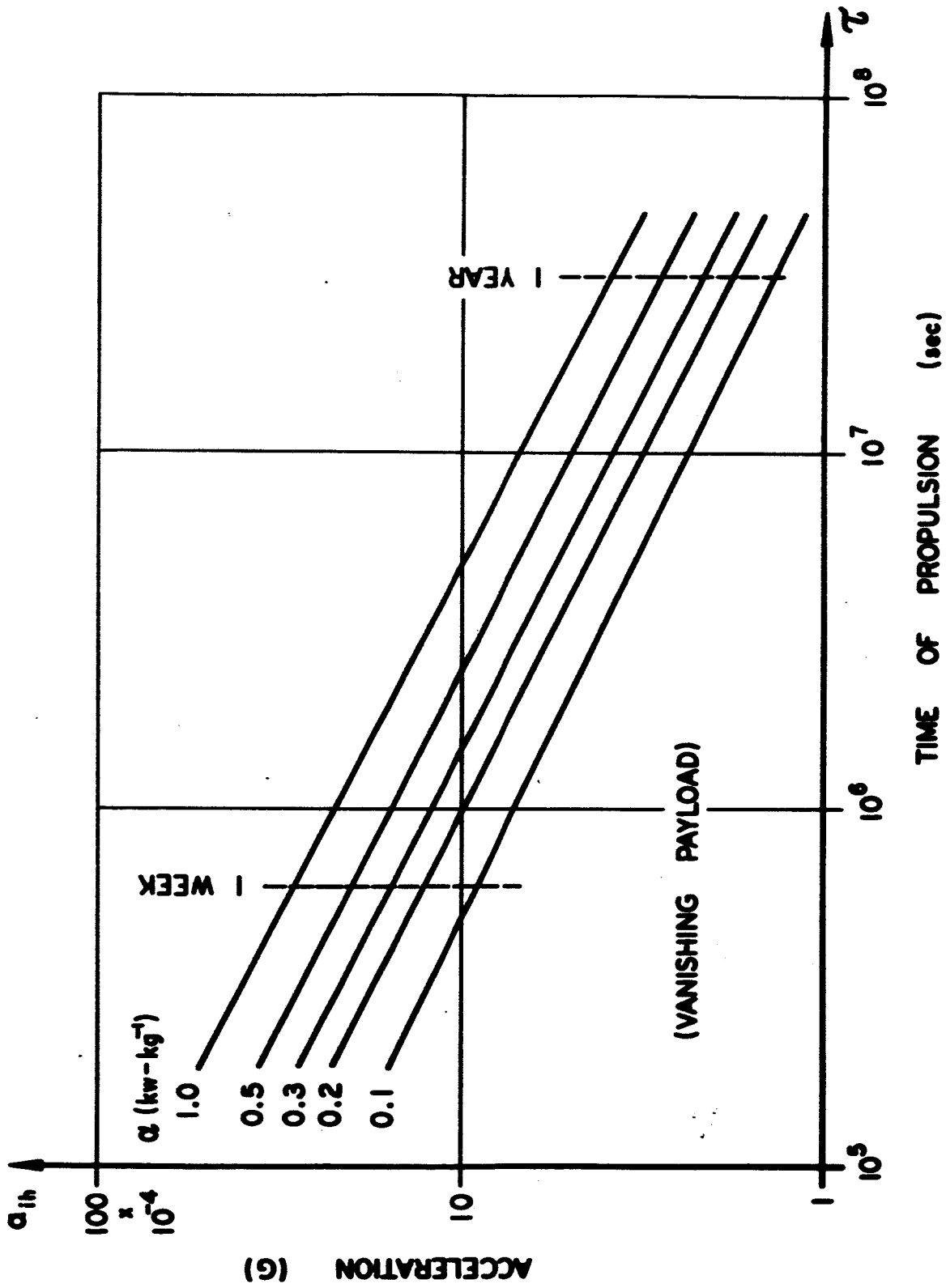
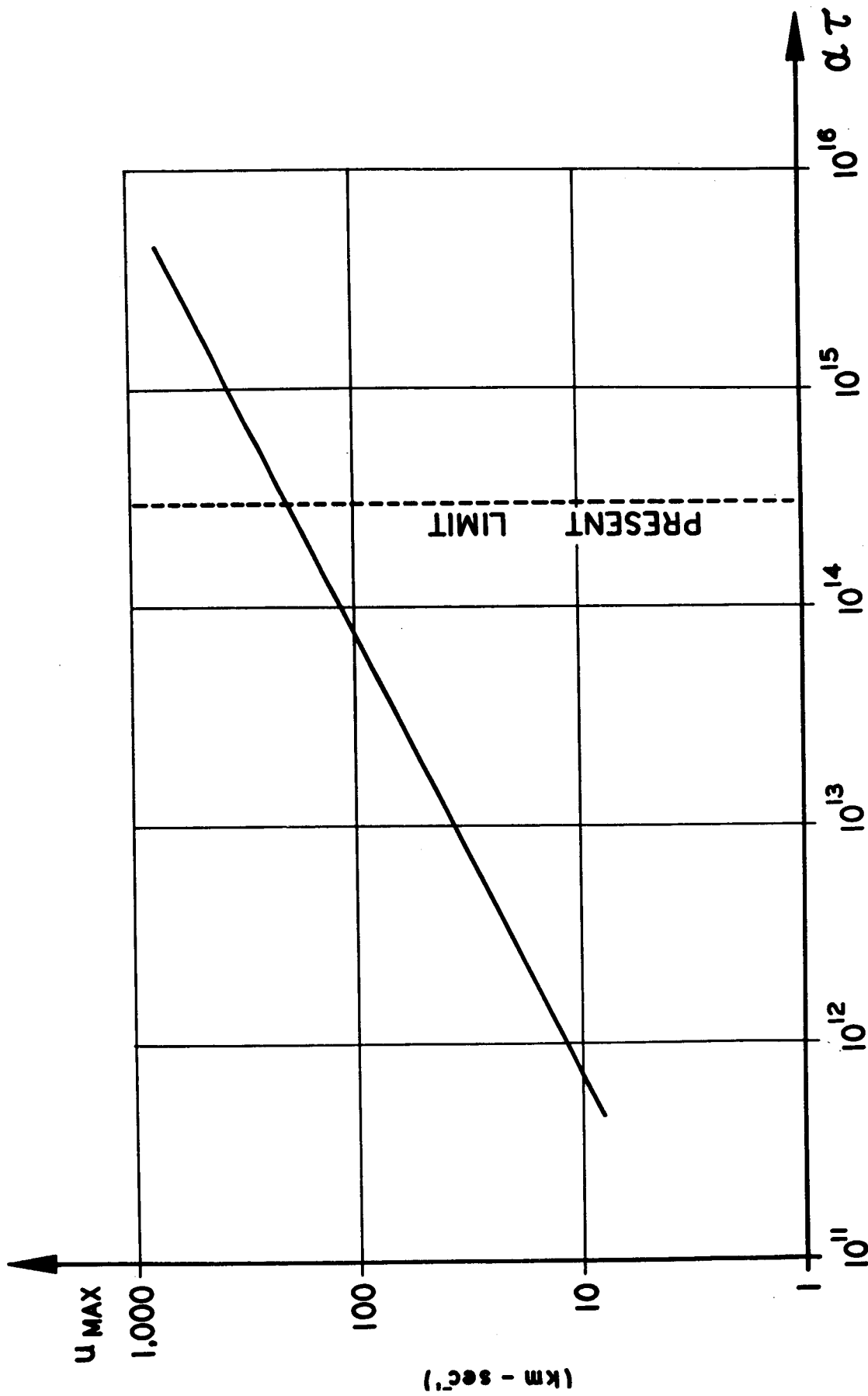


FIG. 7 - Maximum terminal velocity u as a function of α .



SPECIFIC POWER X OPERATING TIME (erg - g⁻¹)

FIG. 8 - Highest initial acceleration as a function of α and τ for vanishing payload.

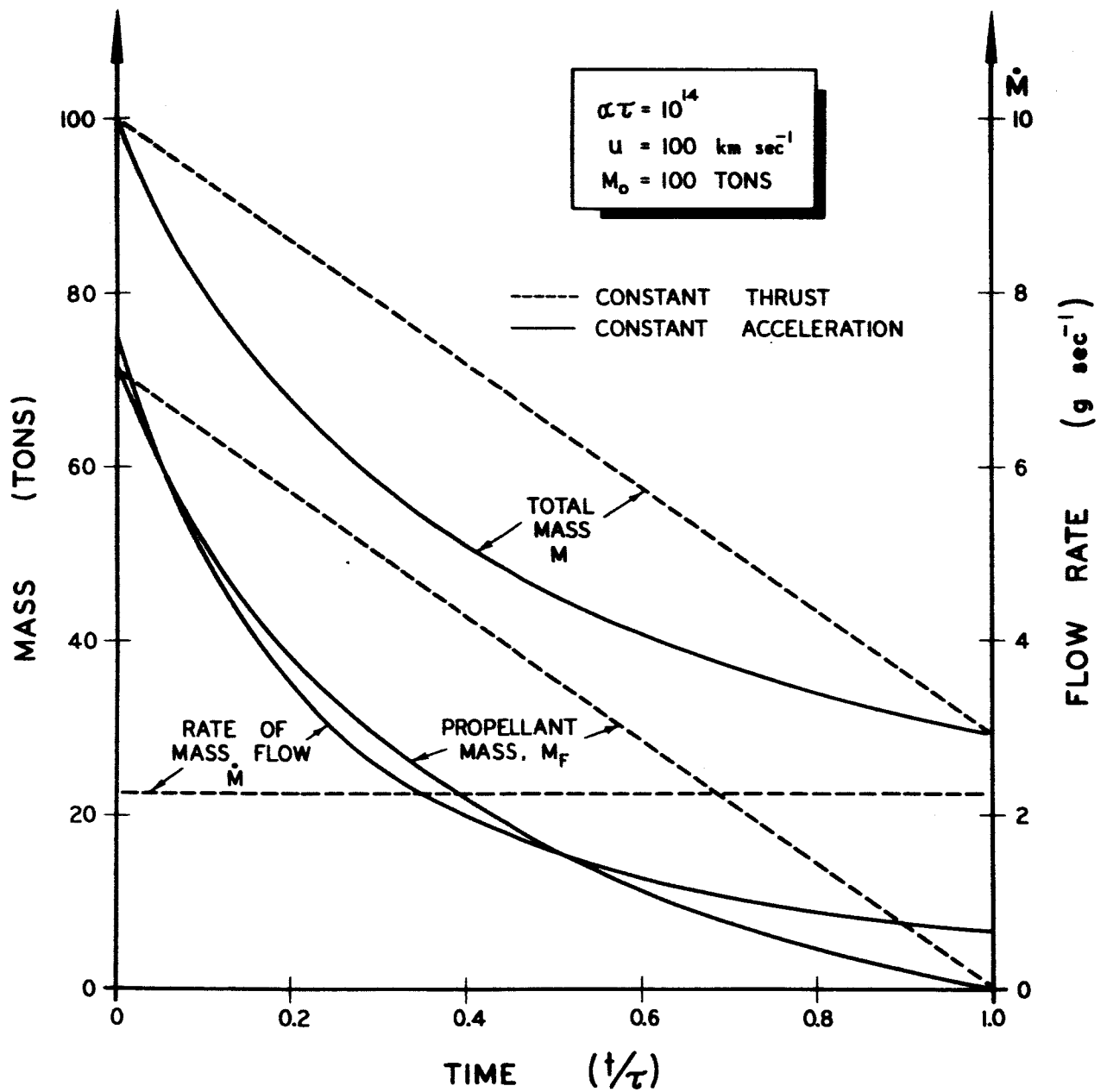


FIG. 9a - Total mass, propellant mass, and rate of mass flow as functions of time for constant thrust and constant acceleration systems.

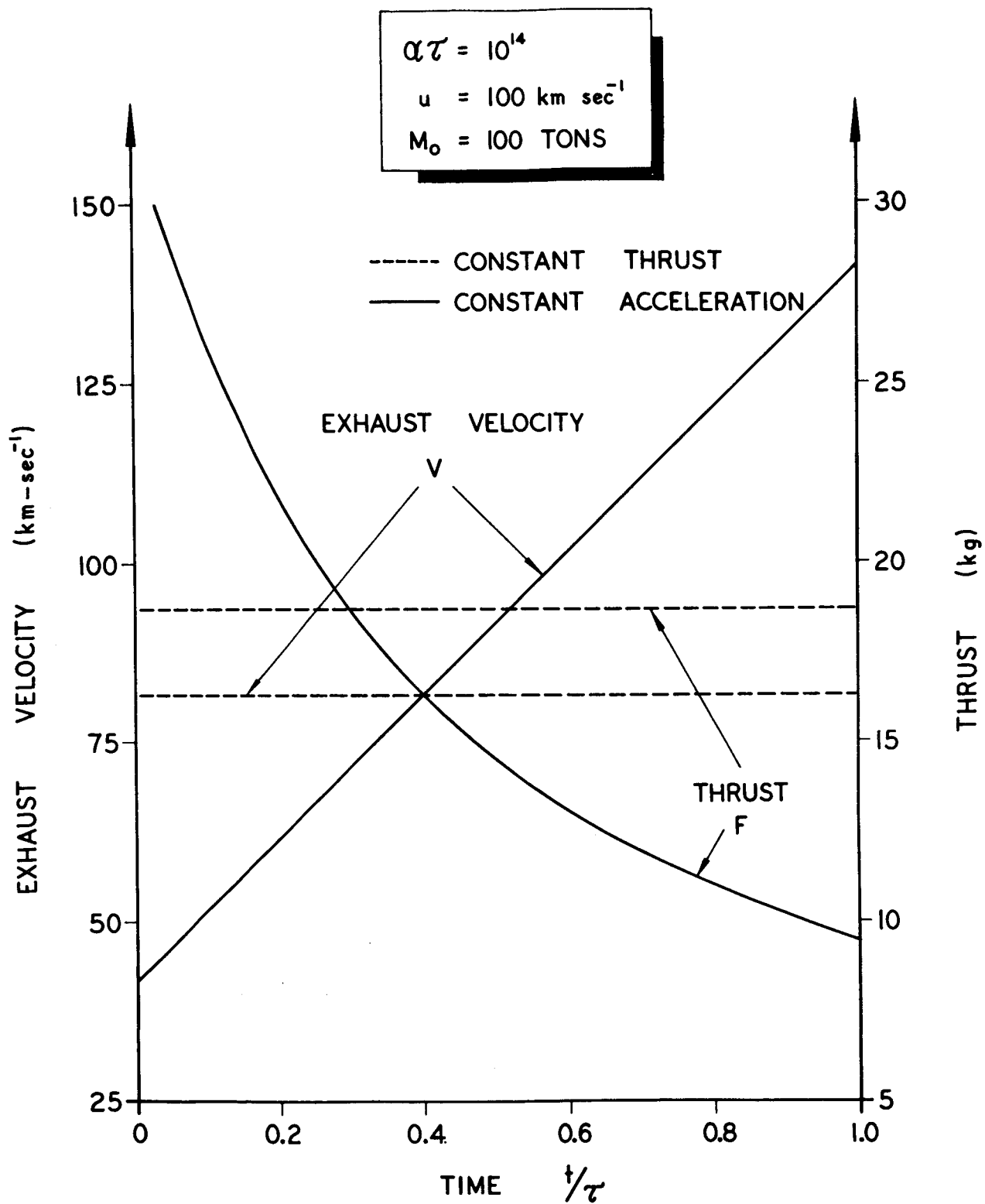


FIG. 9b - Exhaust velocity v and thrust F as functions of time for constant thrust and constant acceleration systems.

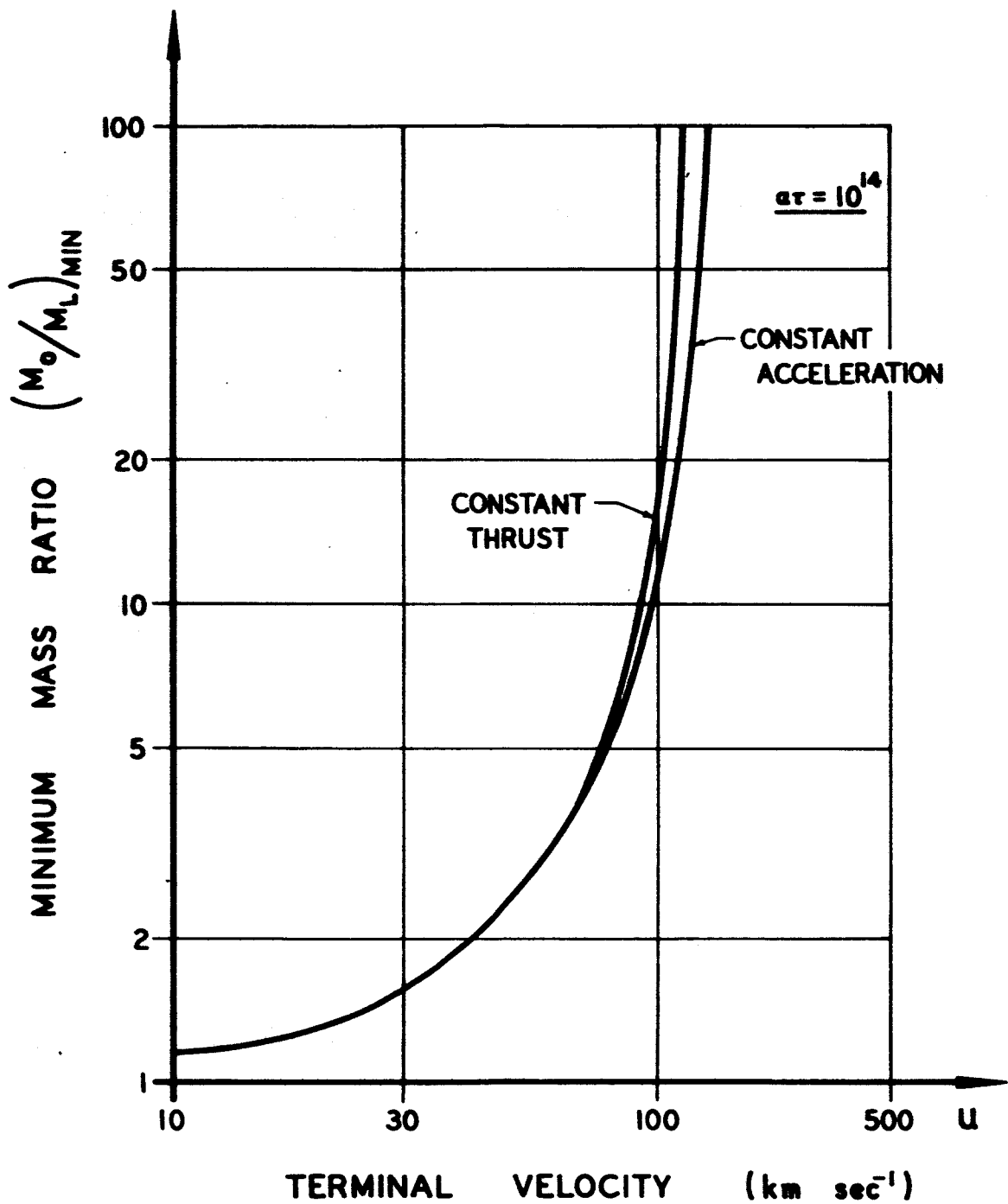


FIG. 10 - Minimum mass ratio $(M_0/M_1)_{\min}$ of constant thrust and constant acceleration vehicles as function of time.

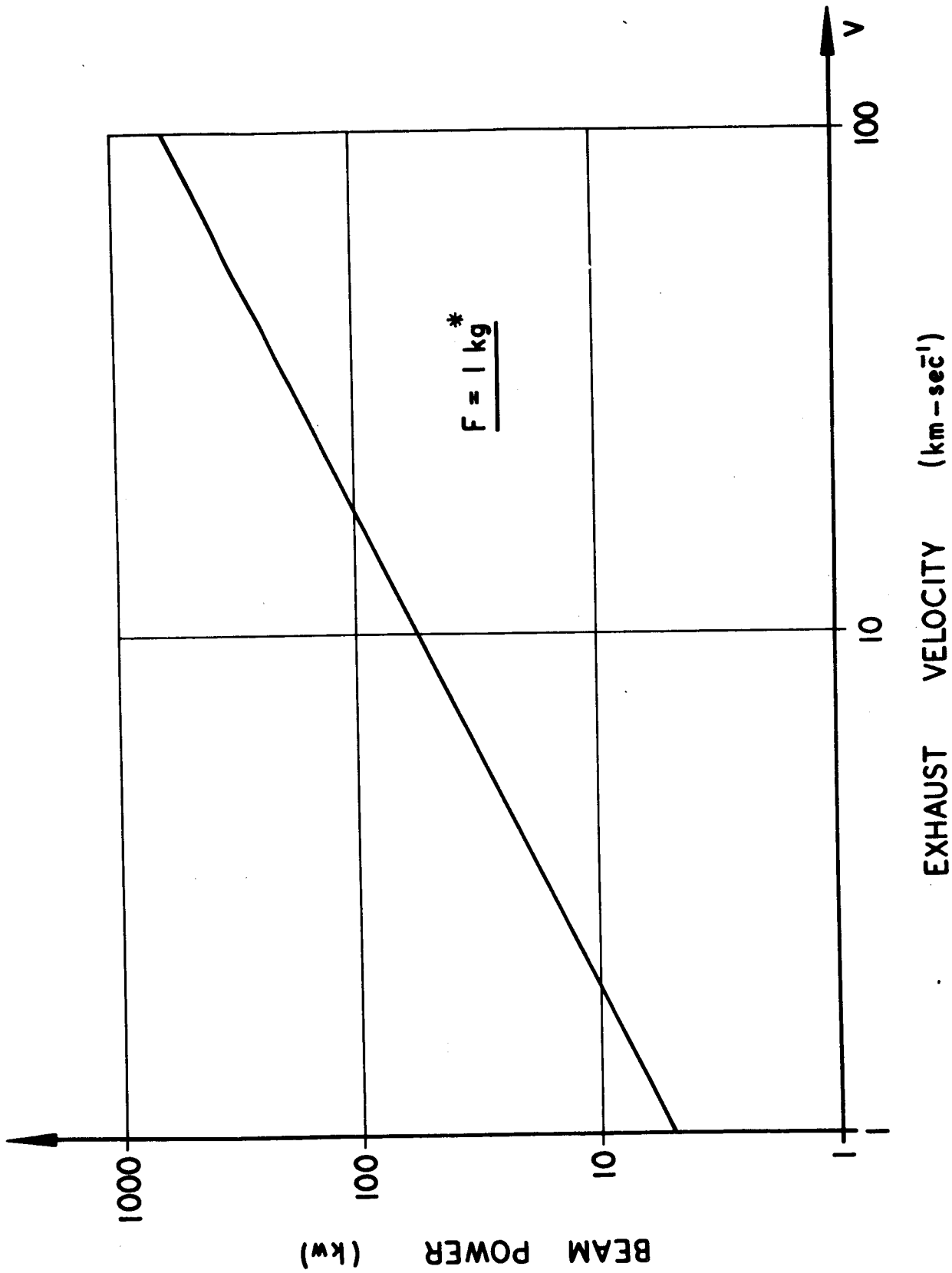
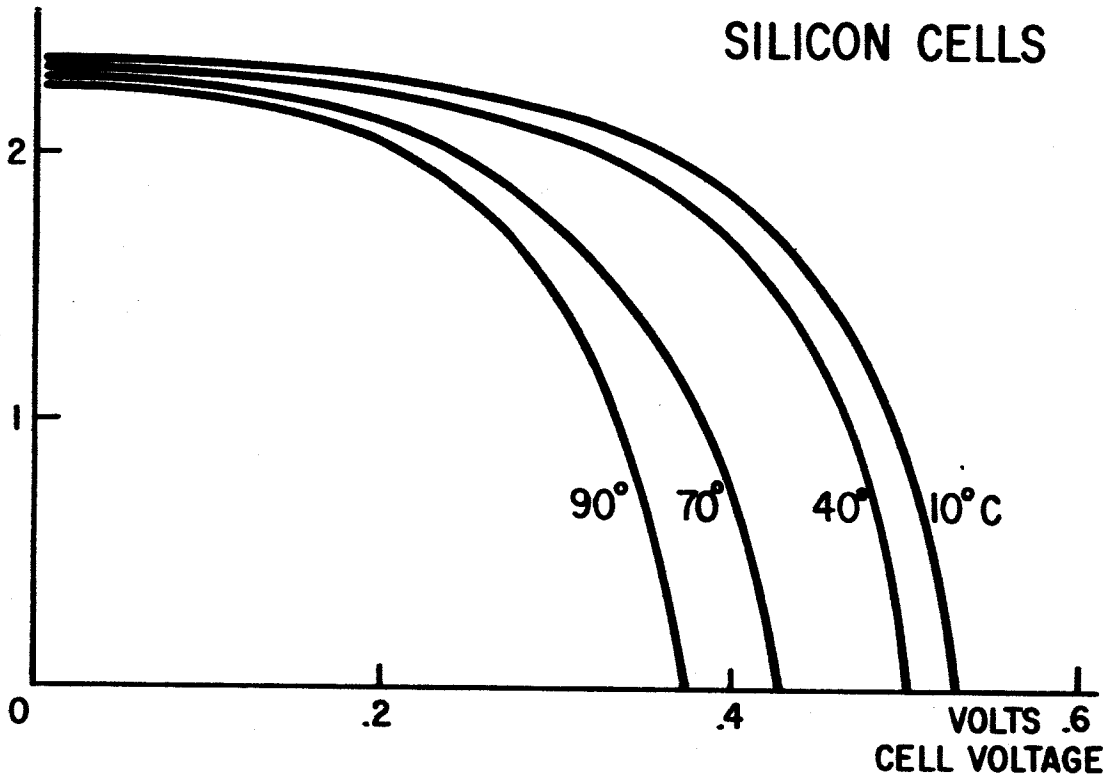


FIG. 11 - Power required for 1 kg of thrust as a function of exhaust velocity.

RELATIVE
CURRENT

SILICON CELLS



RELATIVE
POWER

SILICON CELLS

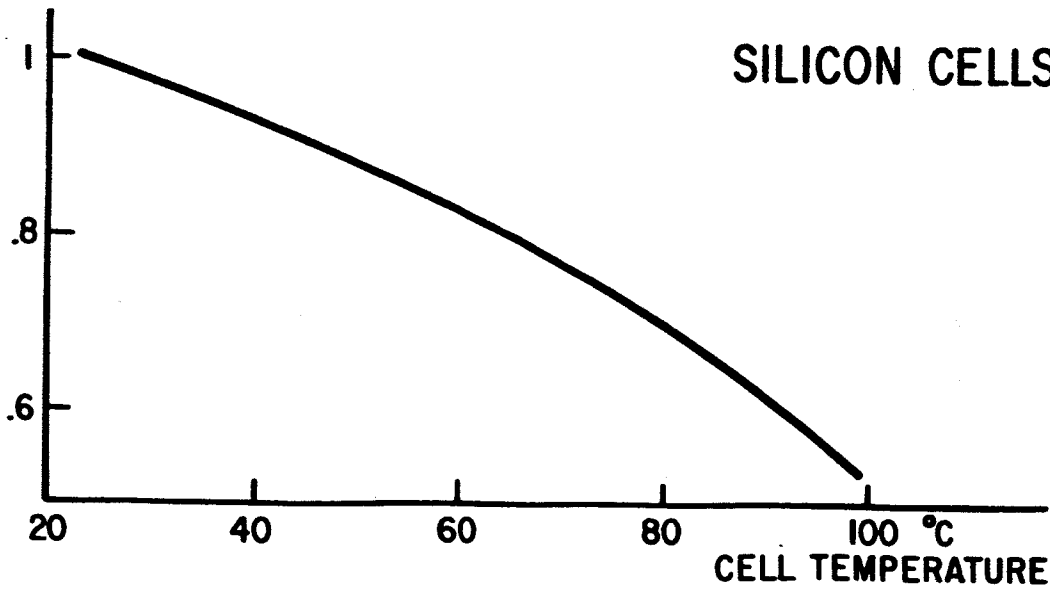


FIG. 12 - Current and power of silicon solar cells as a function of temperature

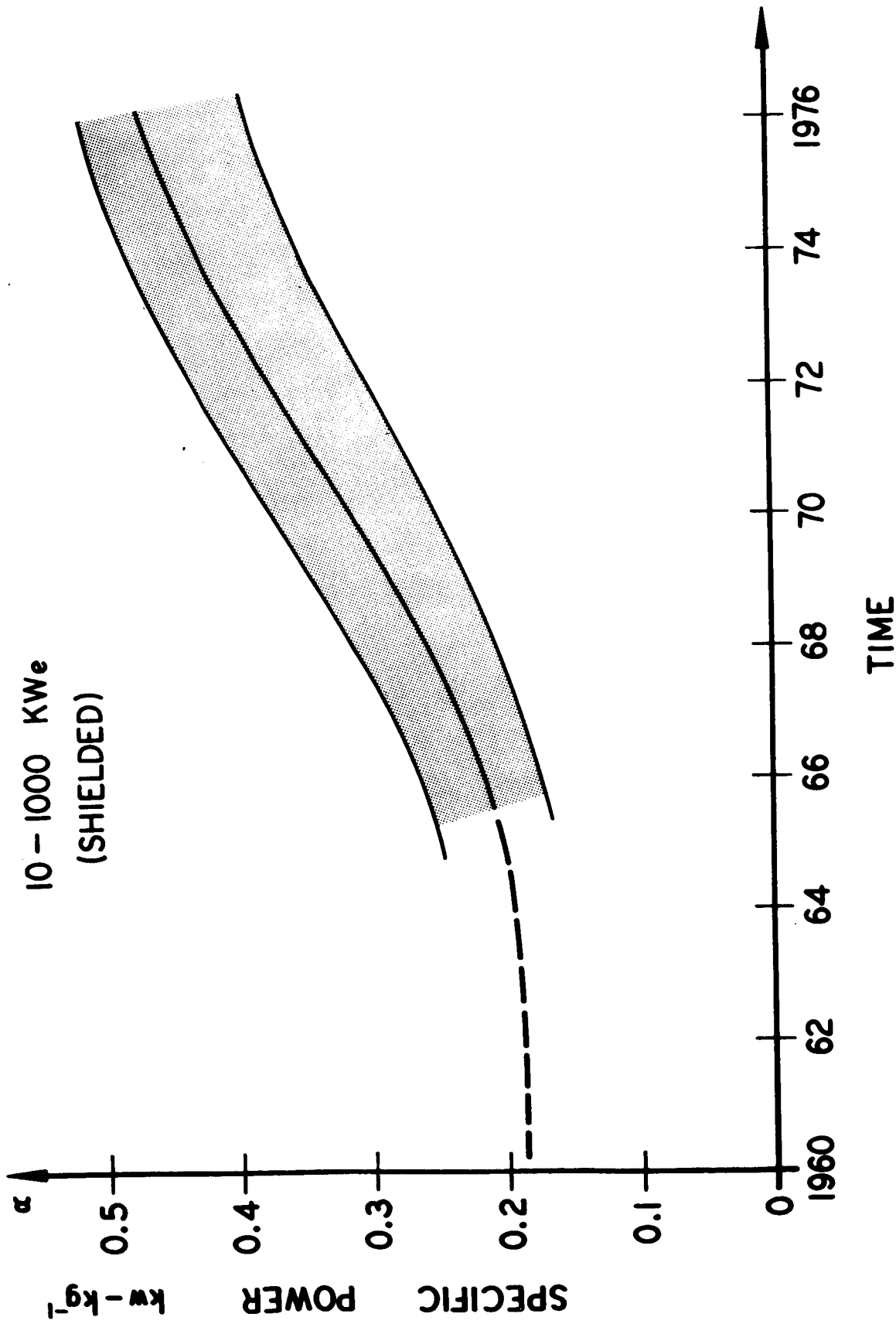


FIG. 13 - Estimated specific power of power supplies available in the 1965-1970 period.

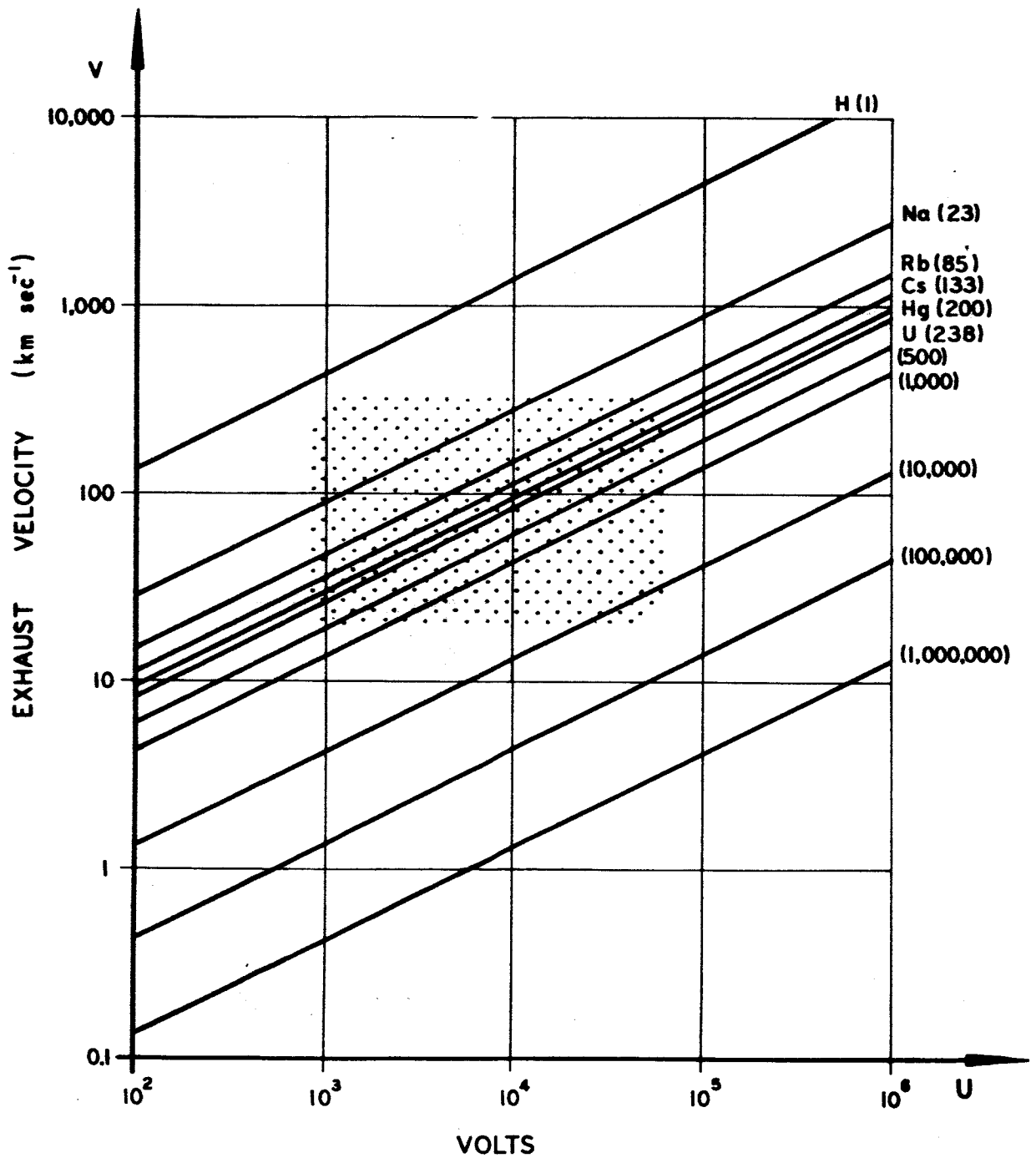


FIG. 14 - Exhaust velocity as a function of accelerating voltage and particle mass (Each particle carries one electron charge.).

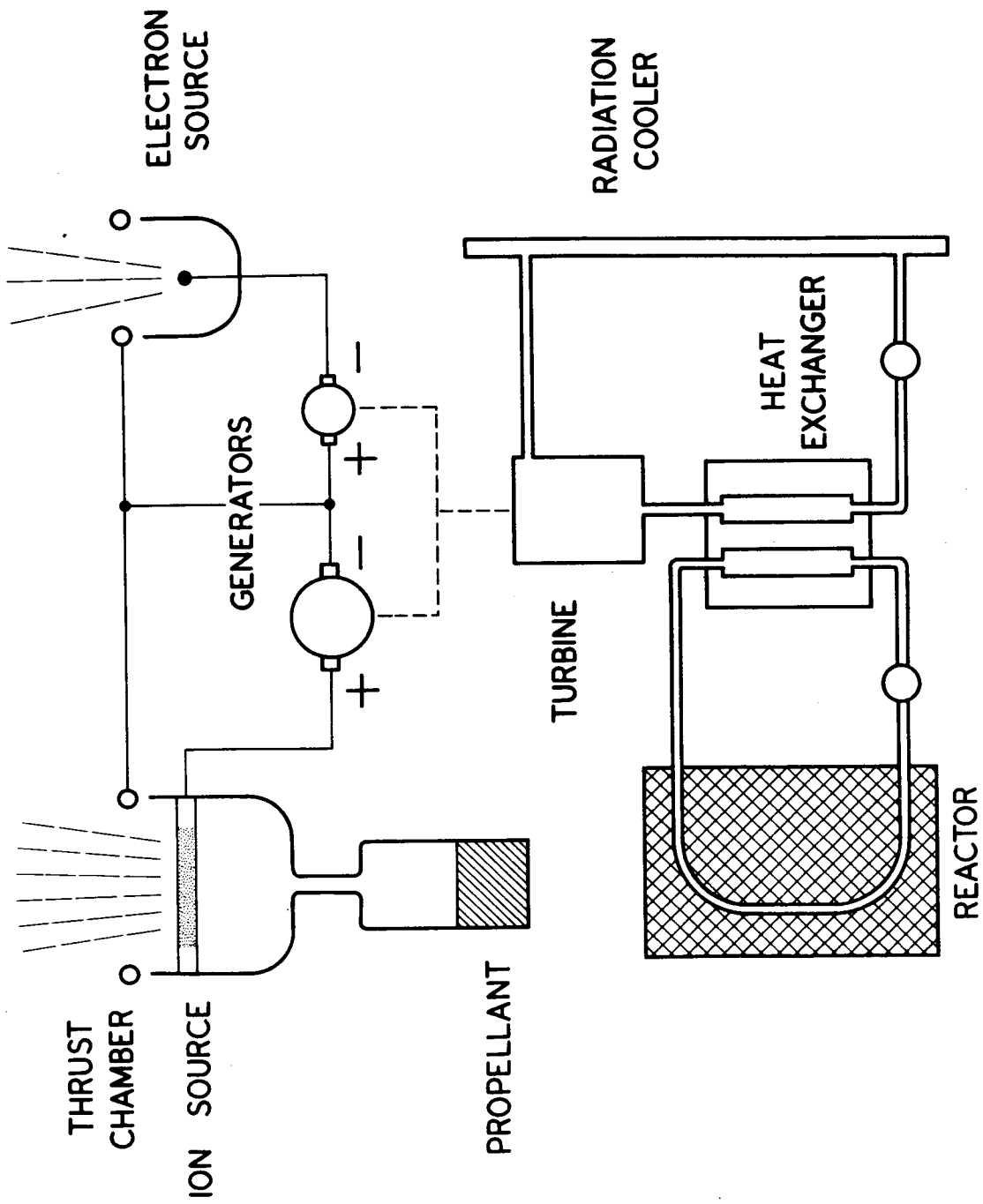


FIG. 15 - Schematic of ion propulsion system

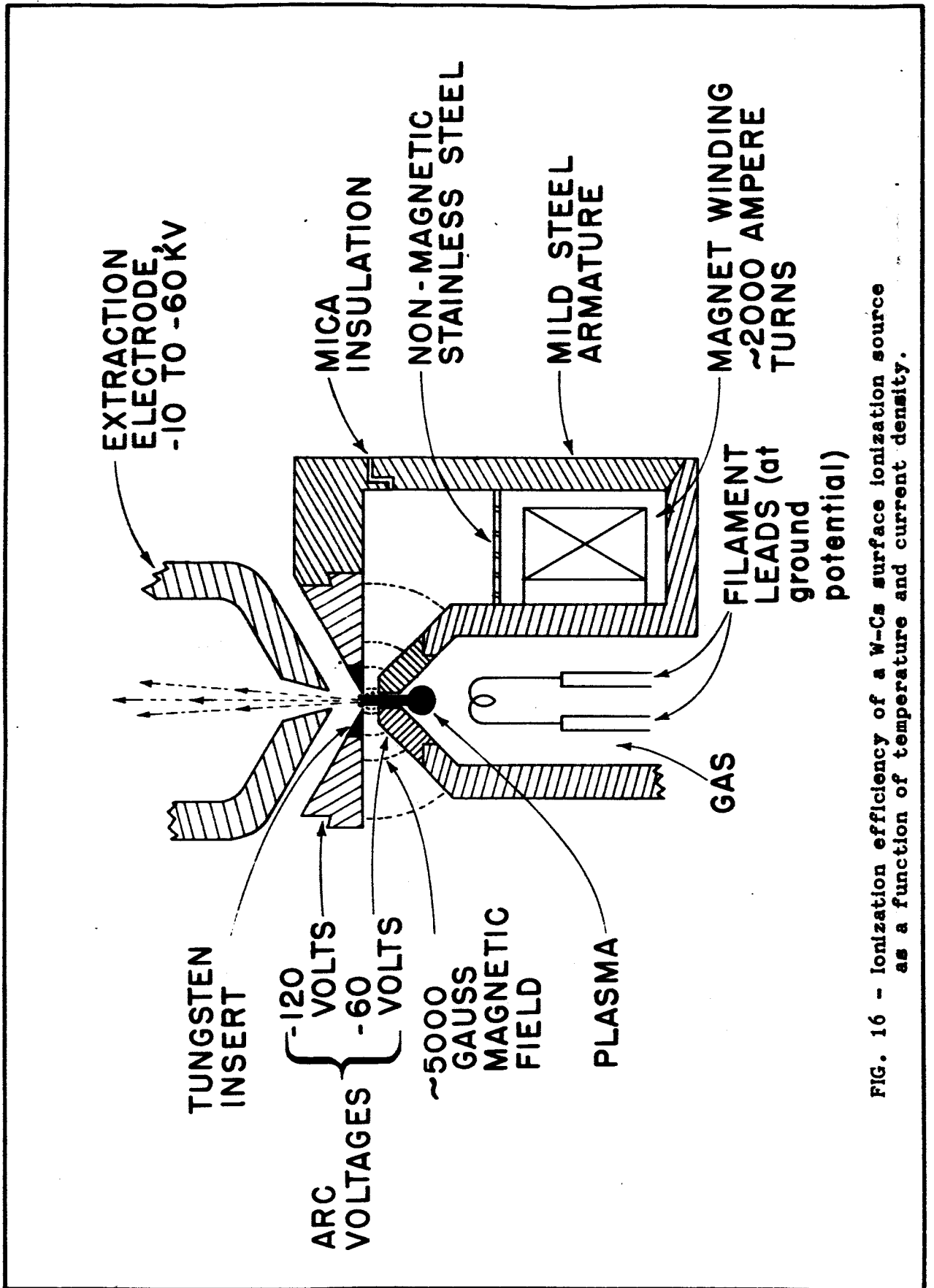


FIG. 16 - Ionization efficiency of a W-Cs surface ionization source as a function of temperature and current density.

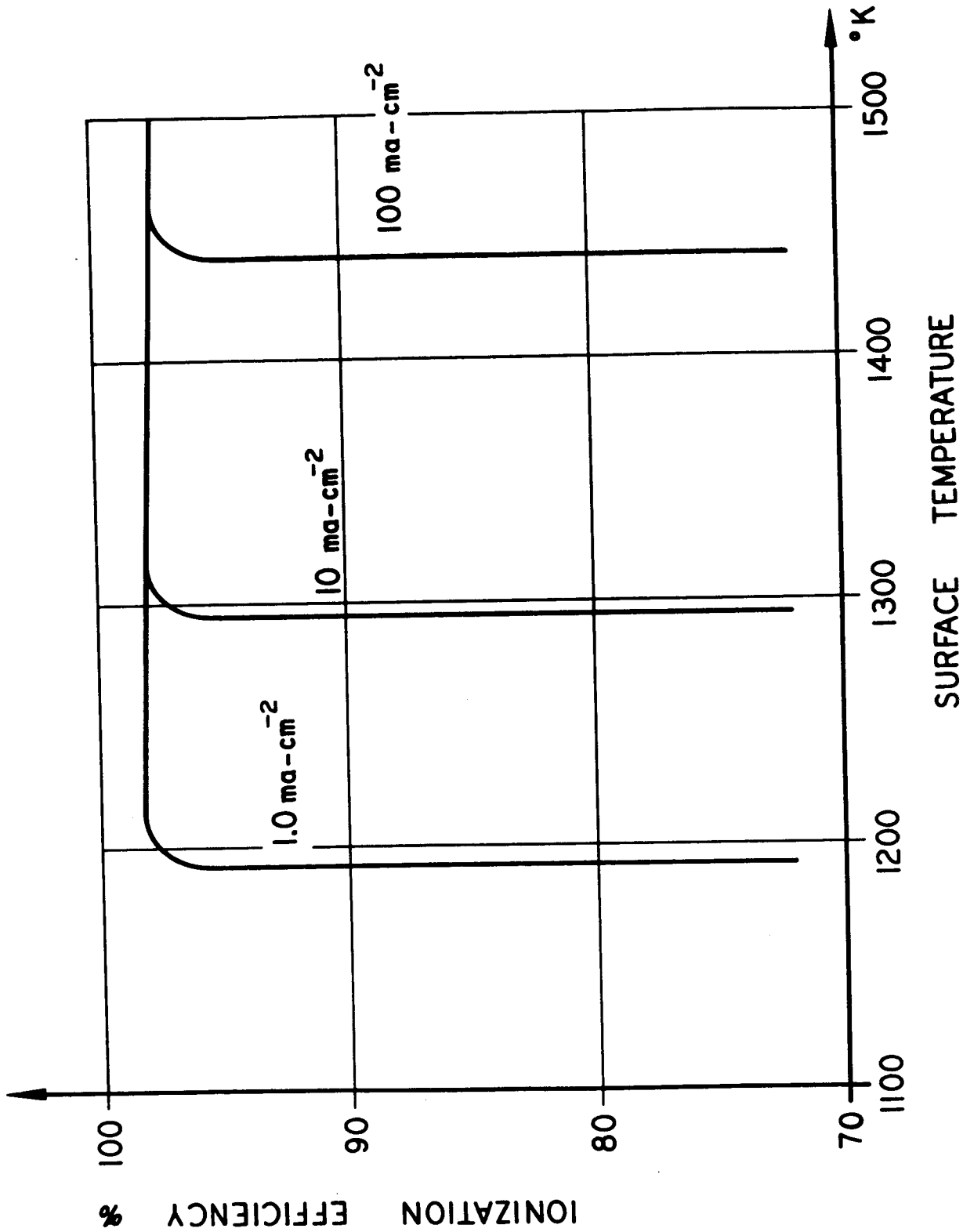


FIG. 17 - Schematic of Von Ardenne duoplasmatron ion source.

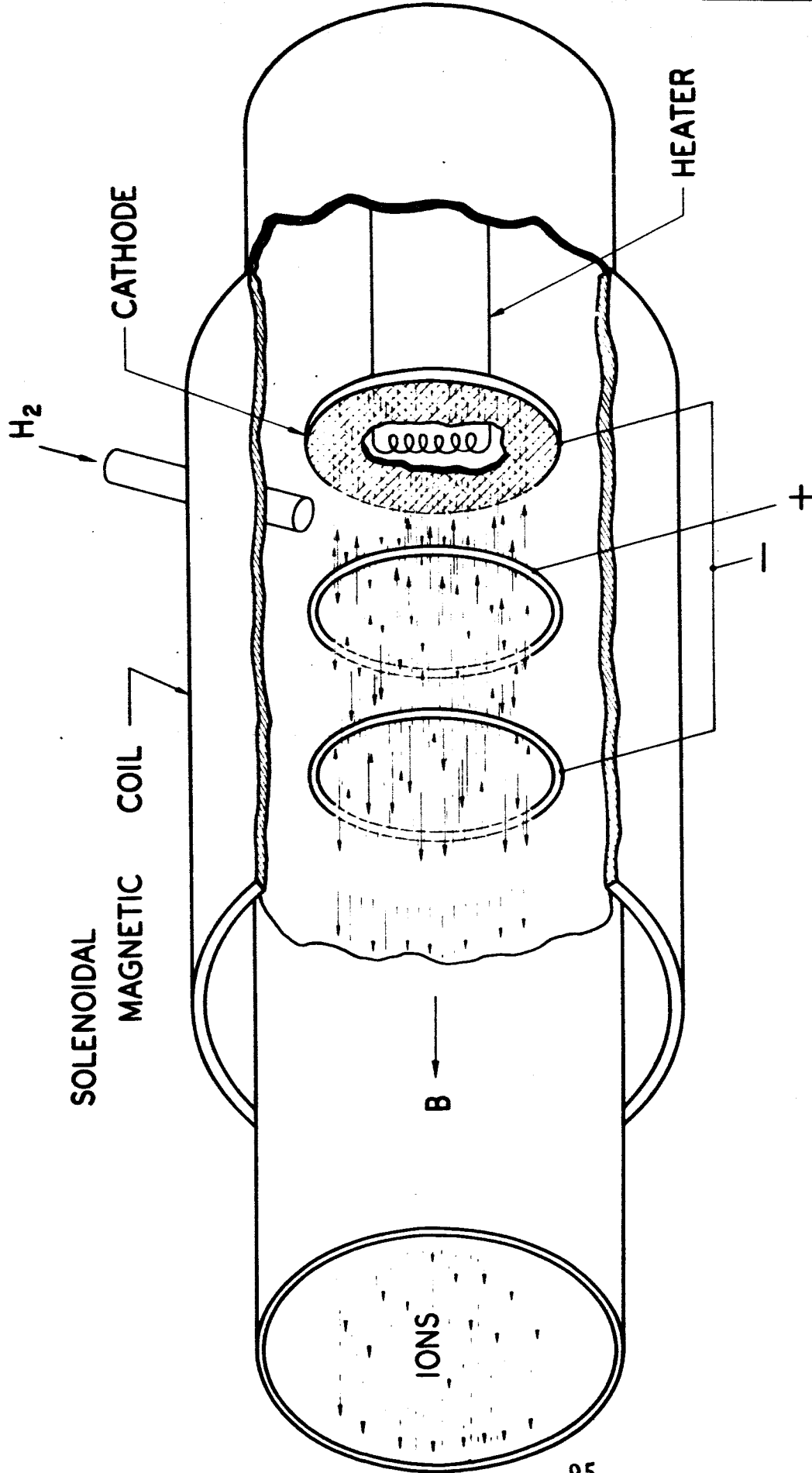


FIG. 18 - Schematic of a bombardment type ion source

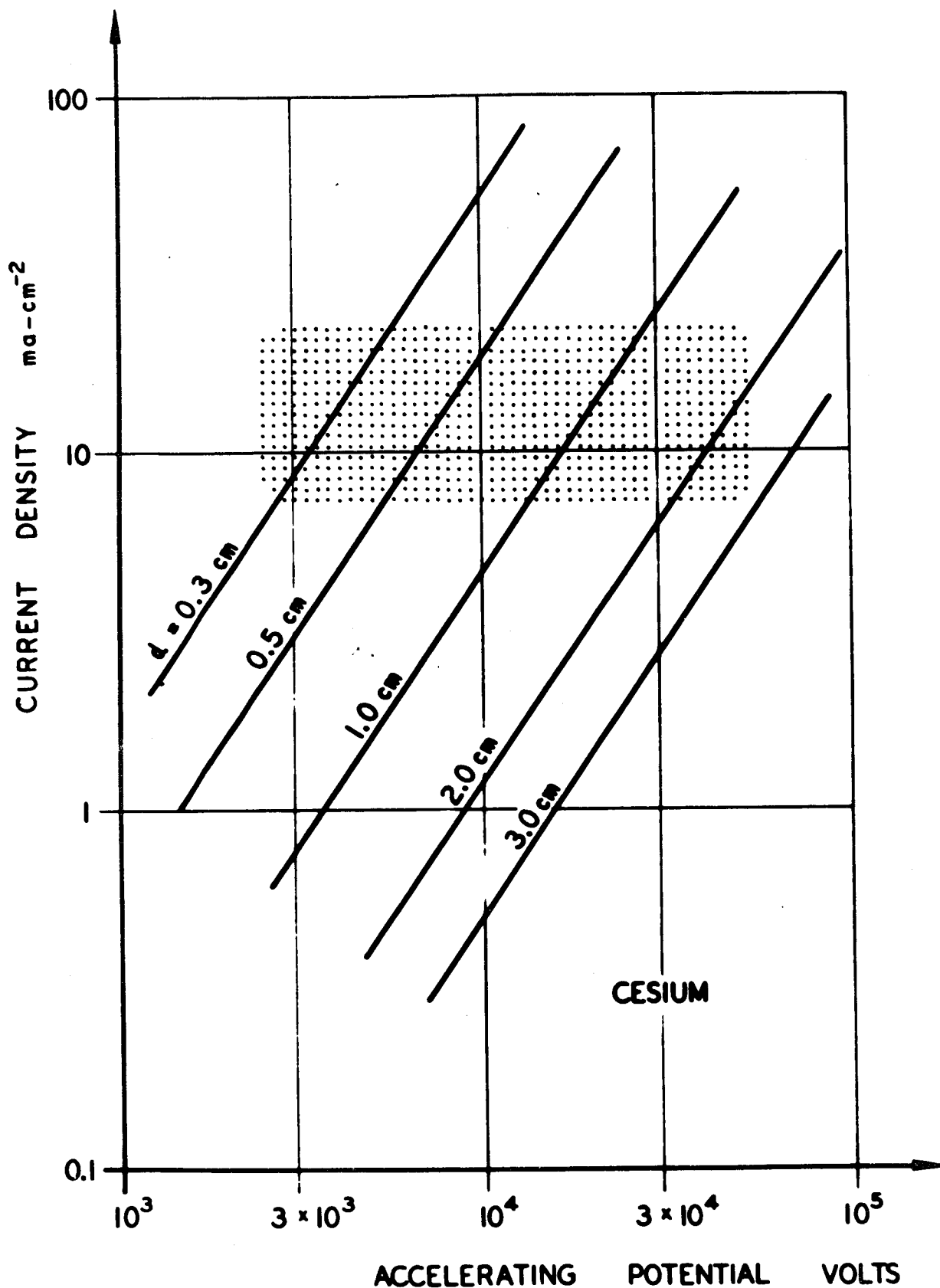


FIG. 19 - Current density of a space charge limited current flow (Child-Langmuir law)

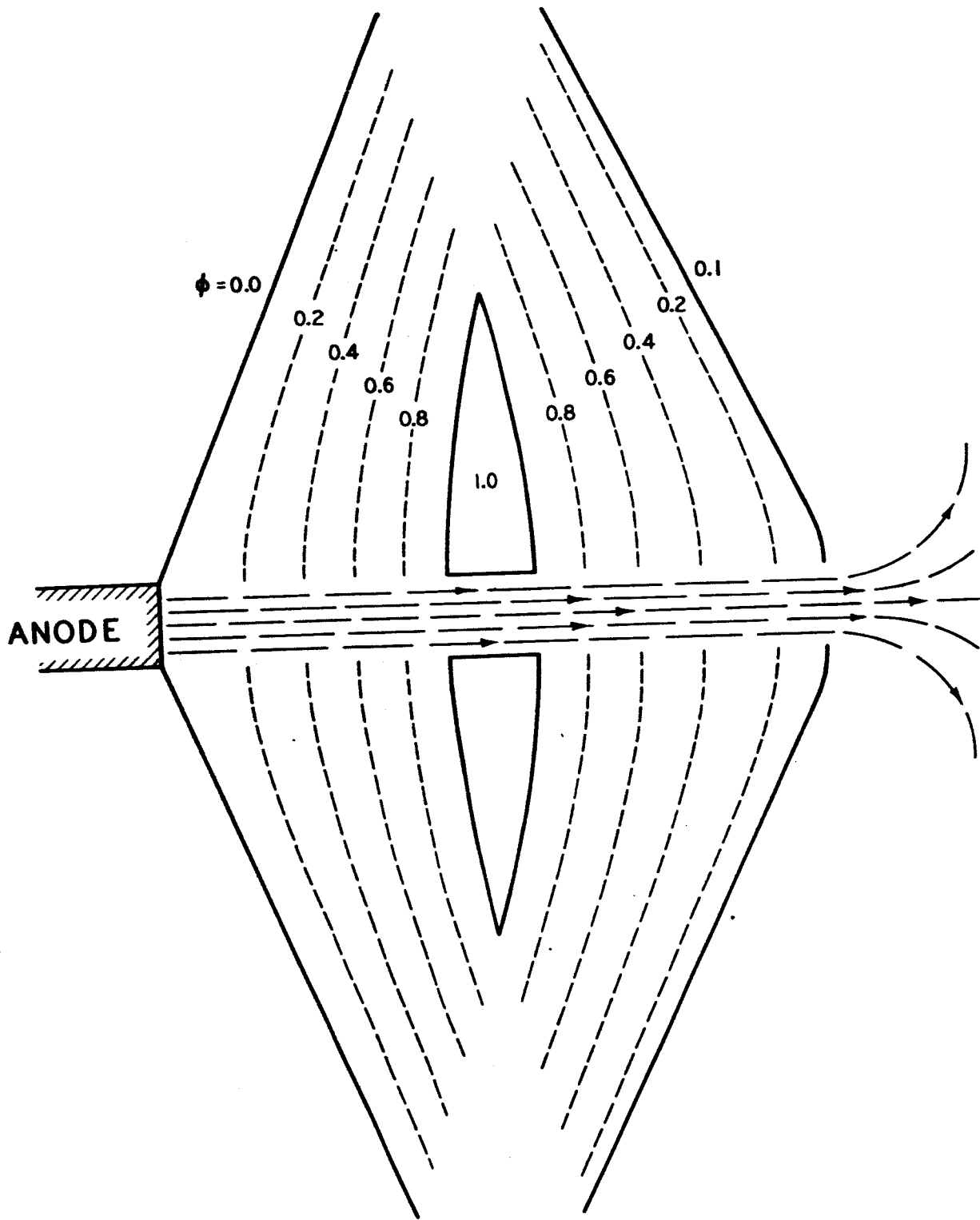


FIG. 20 - Pierce gun design with accel-decel system

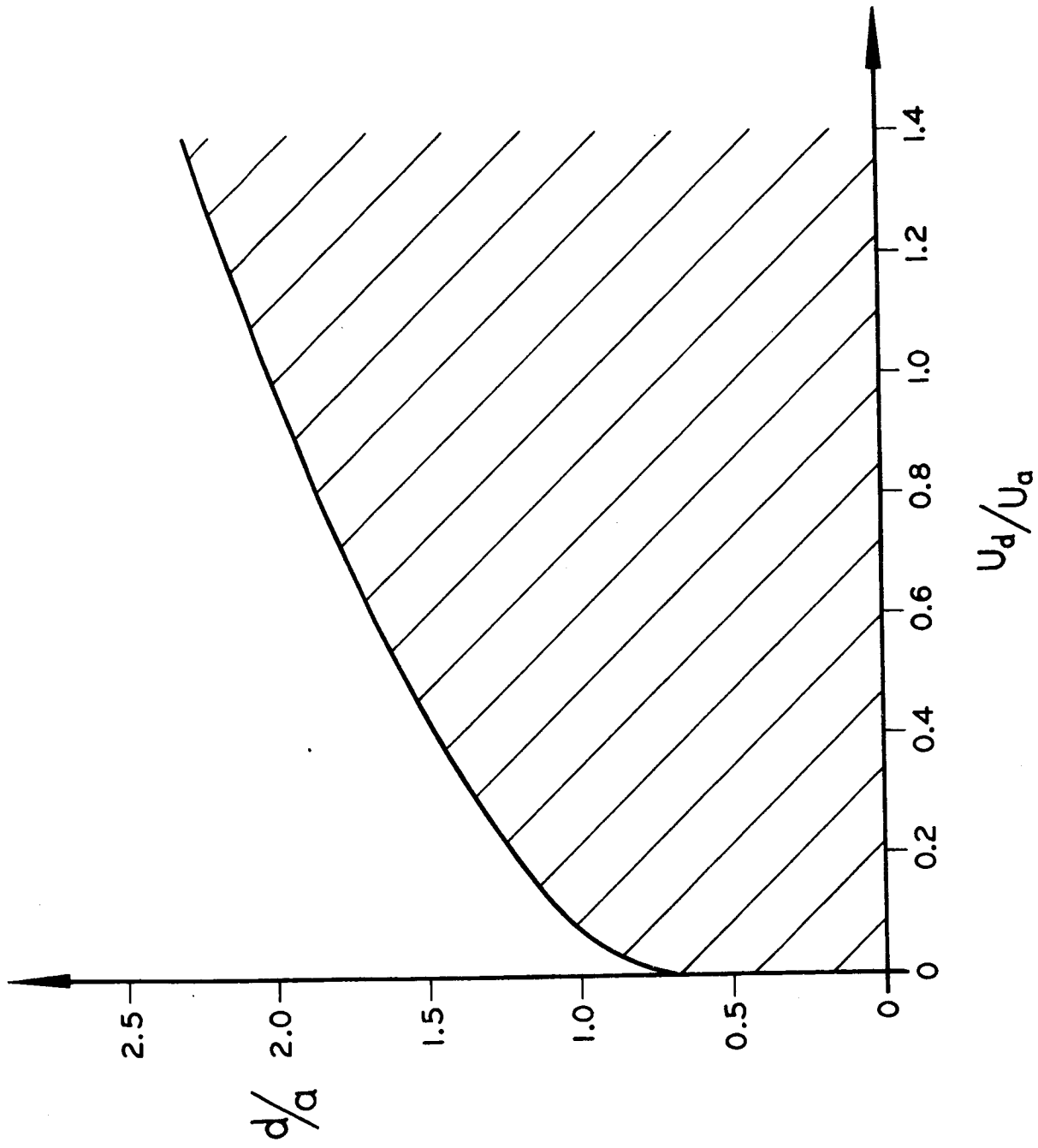


FIG. 21 - Operating region of an accel-decel thrust system

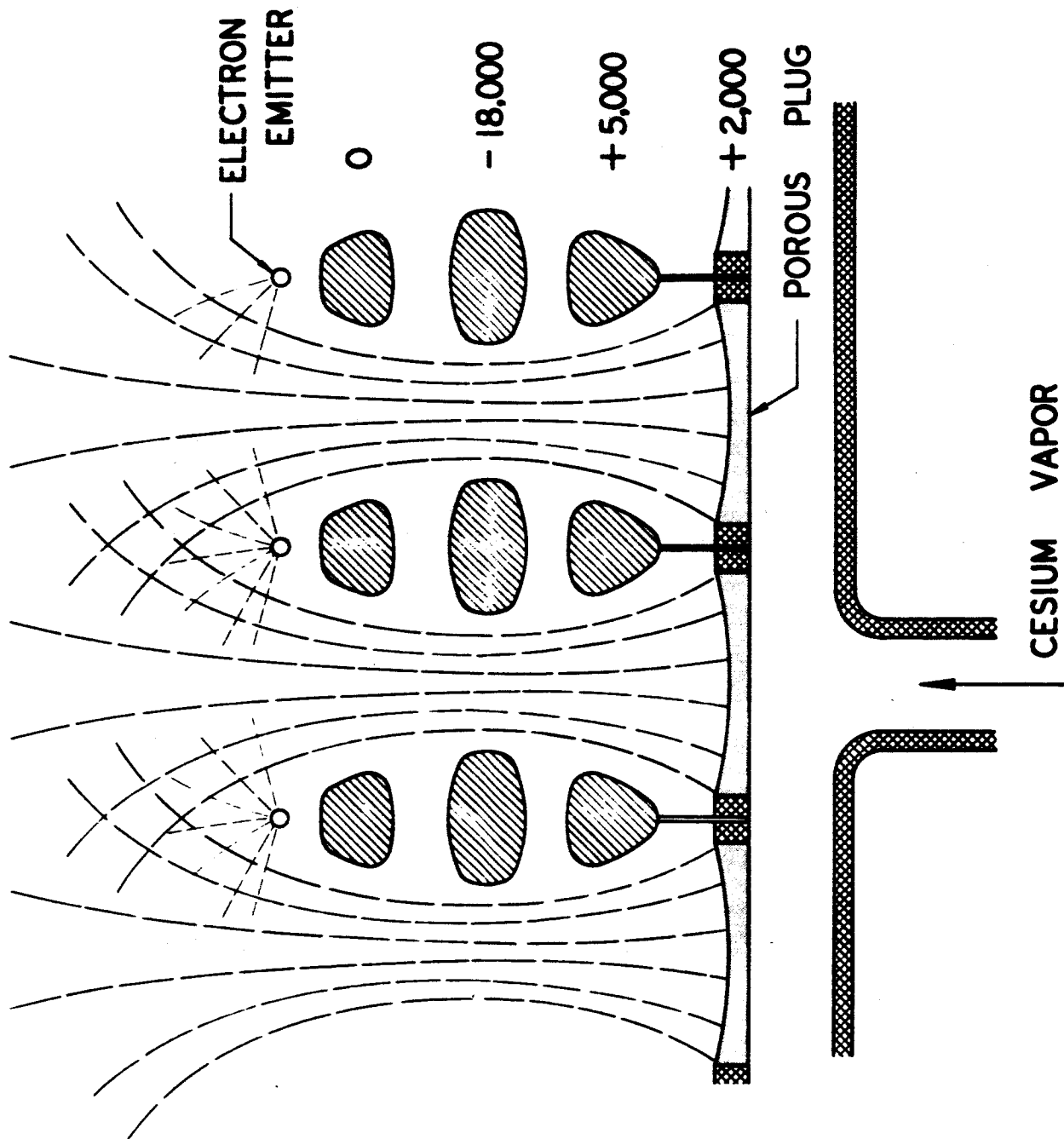


FIG. 22 - Schematic of ion beams and electron emitters

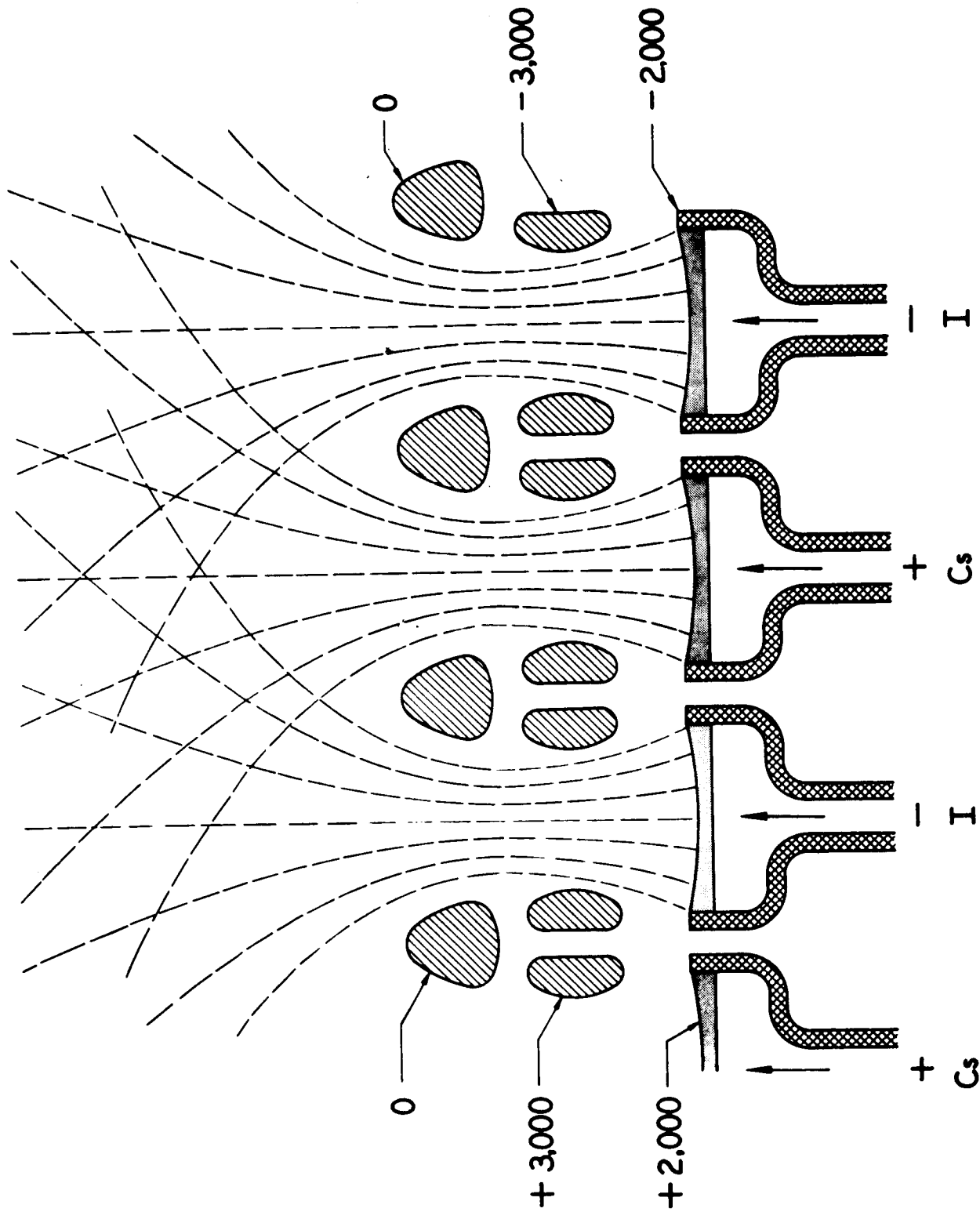


FIG. 23 - Schematic of positive and negative ion sources

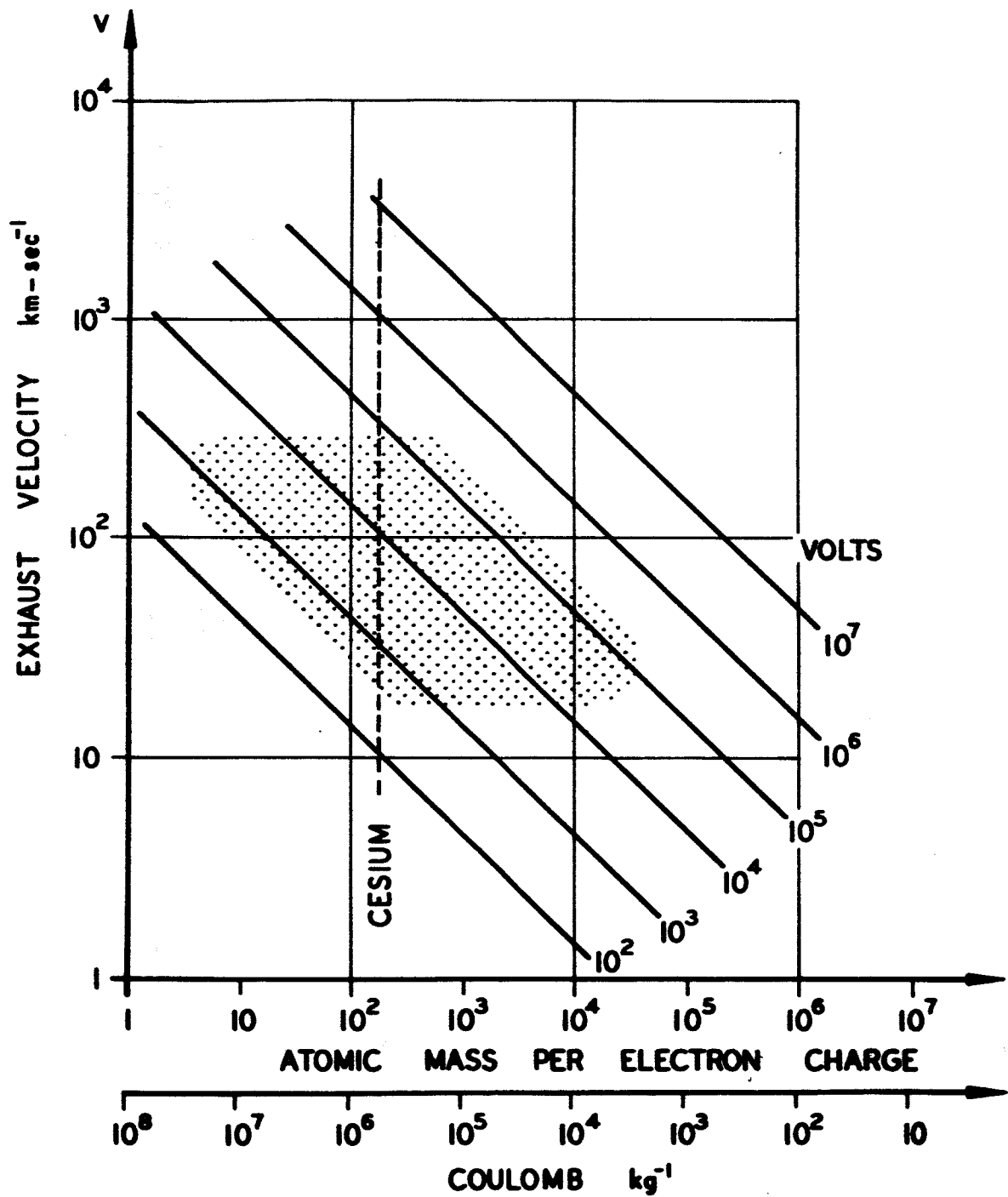


FIG. 24 - Exhaust velocity as a function of particle mass (each particle carries one electron charge).

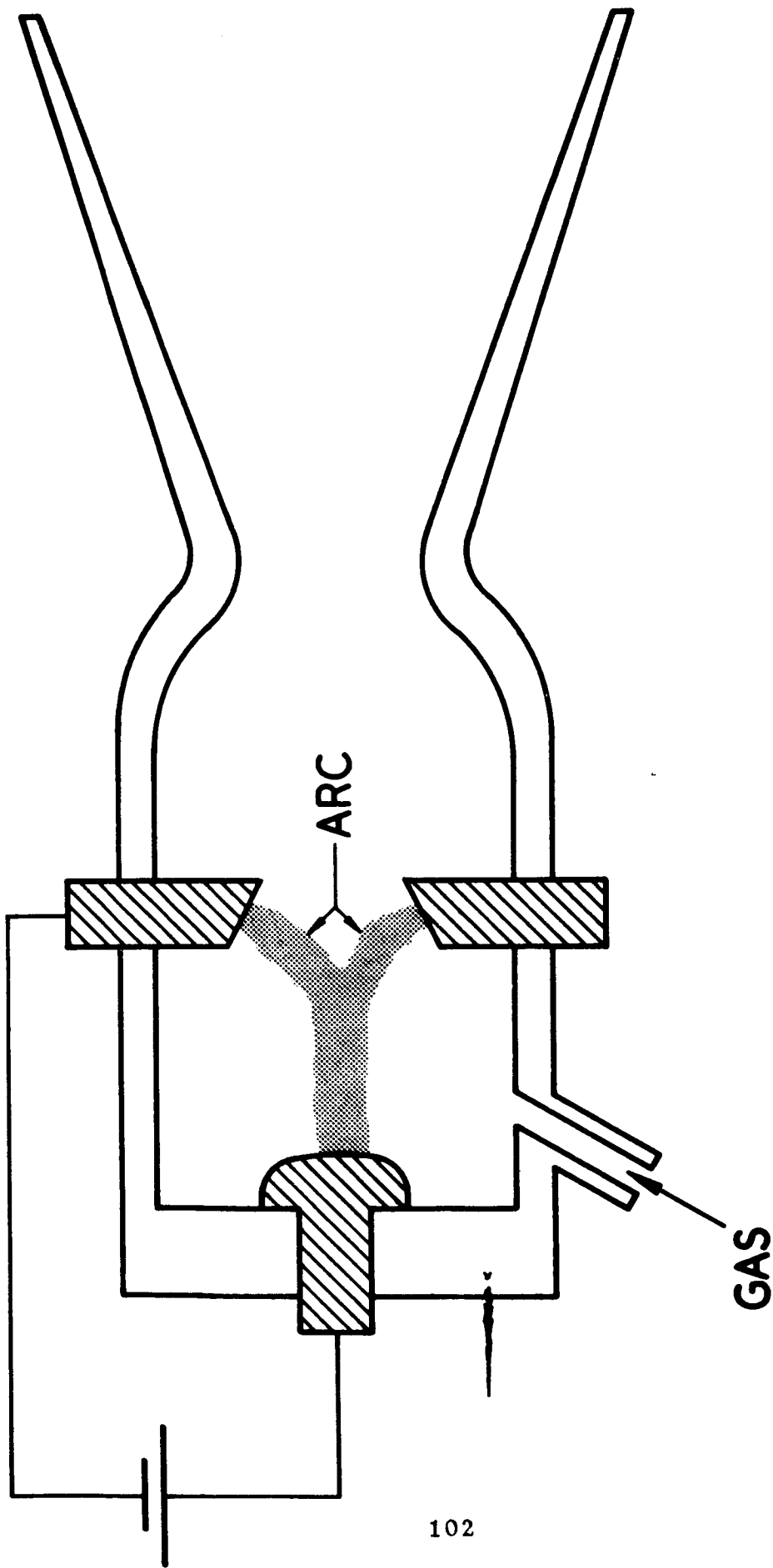


FIG. 25 - Schematic of arc-heated rocket motor

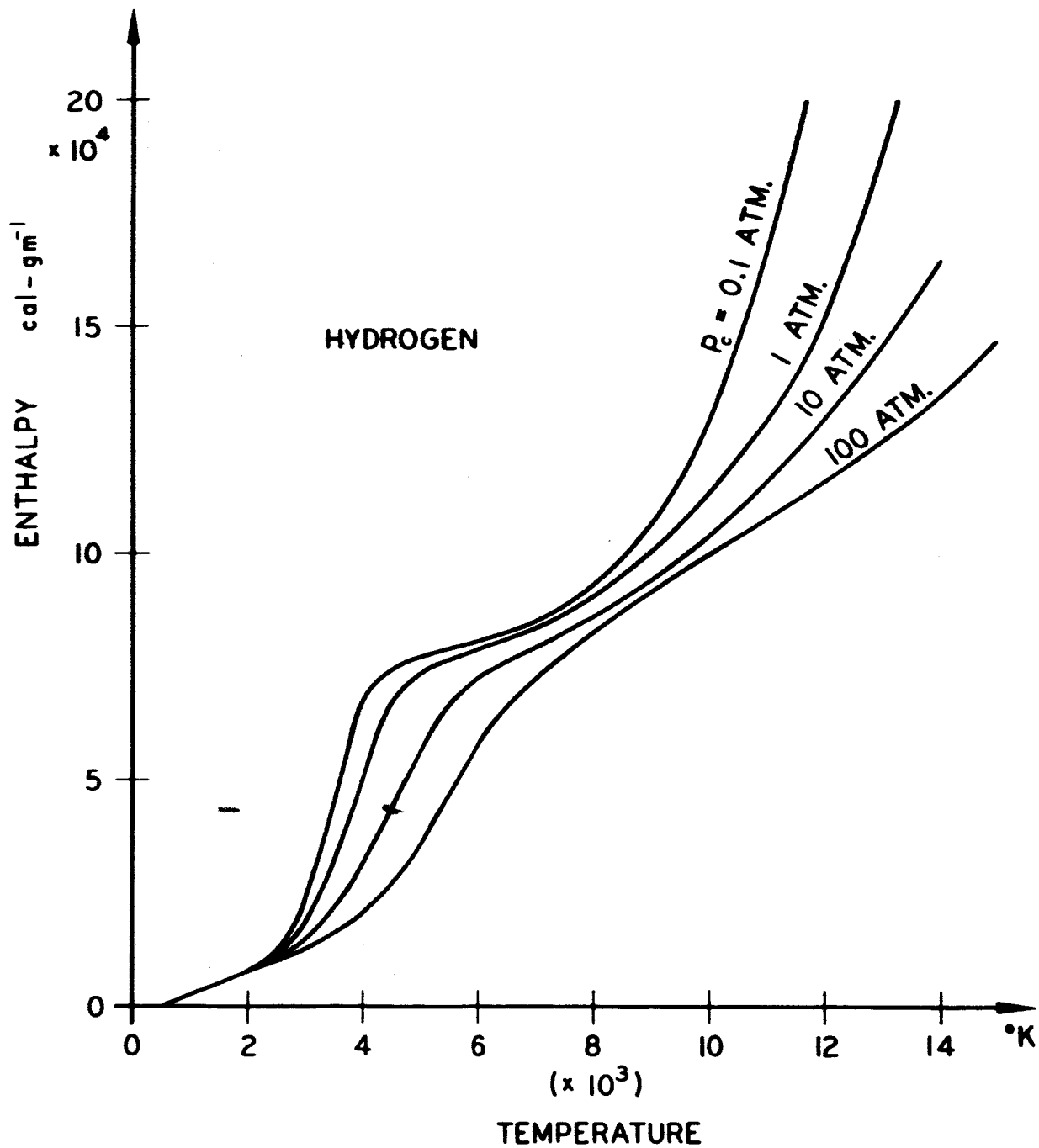


FIG. 26 - Enthalpy of hydrogen as a function of temperature and chamber pressure

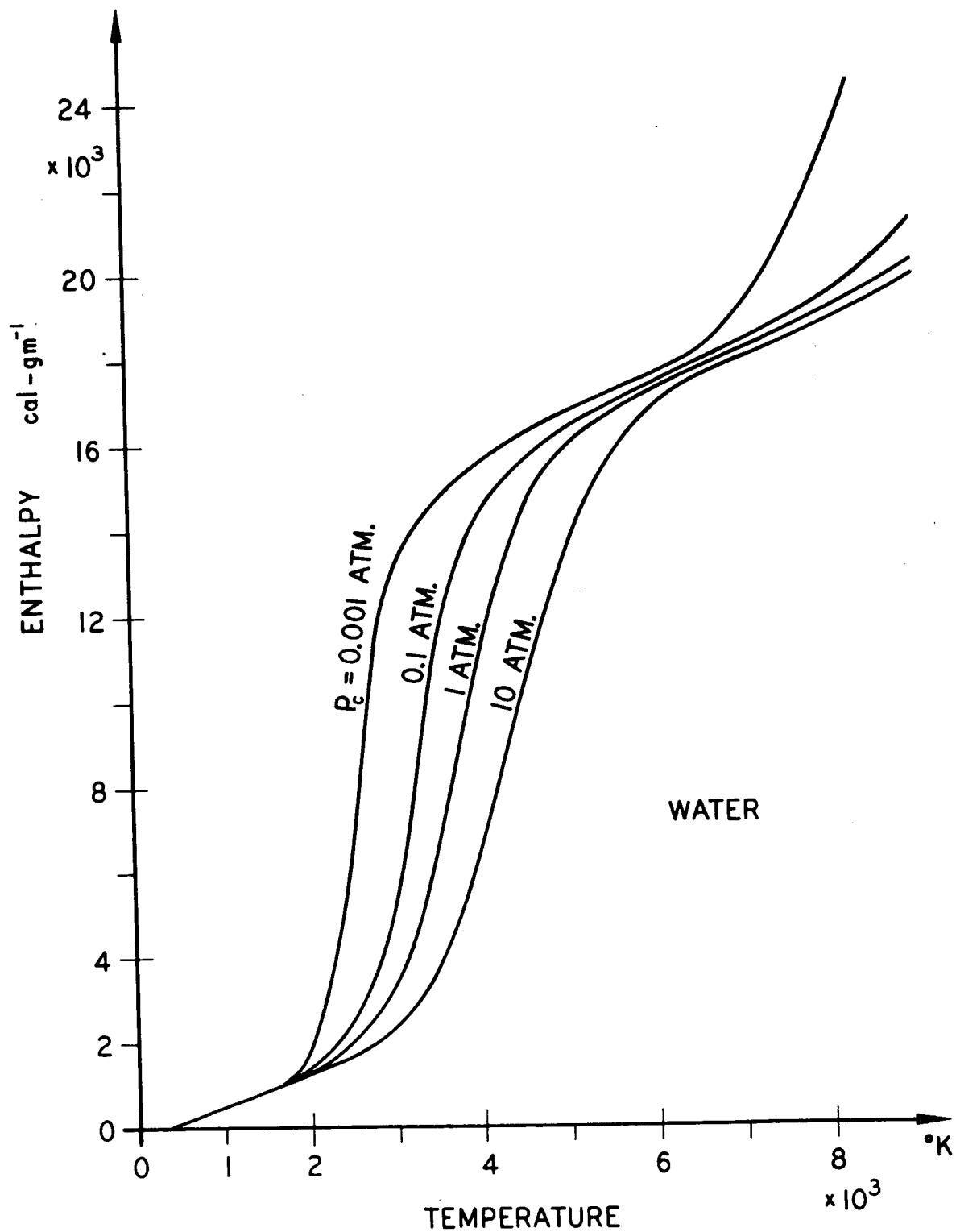


FIG. 27 - Enthalpy of water as a function of temperature and chamber pressure.

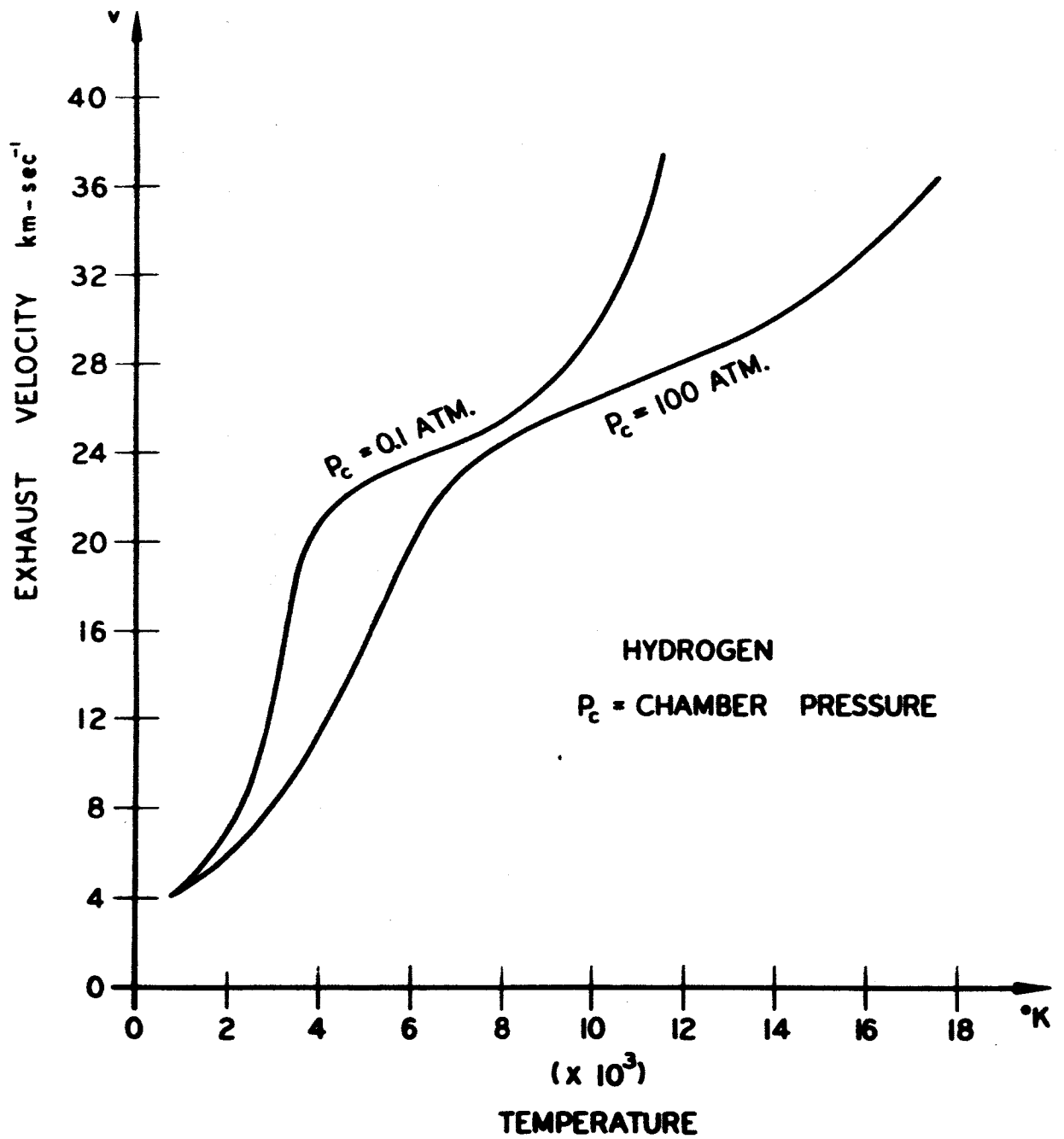


FIG. 28 - Exhaust velocity of hydrogen as a function of temperature and chamber pressure

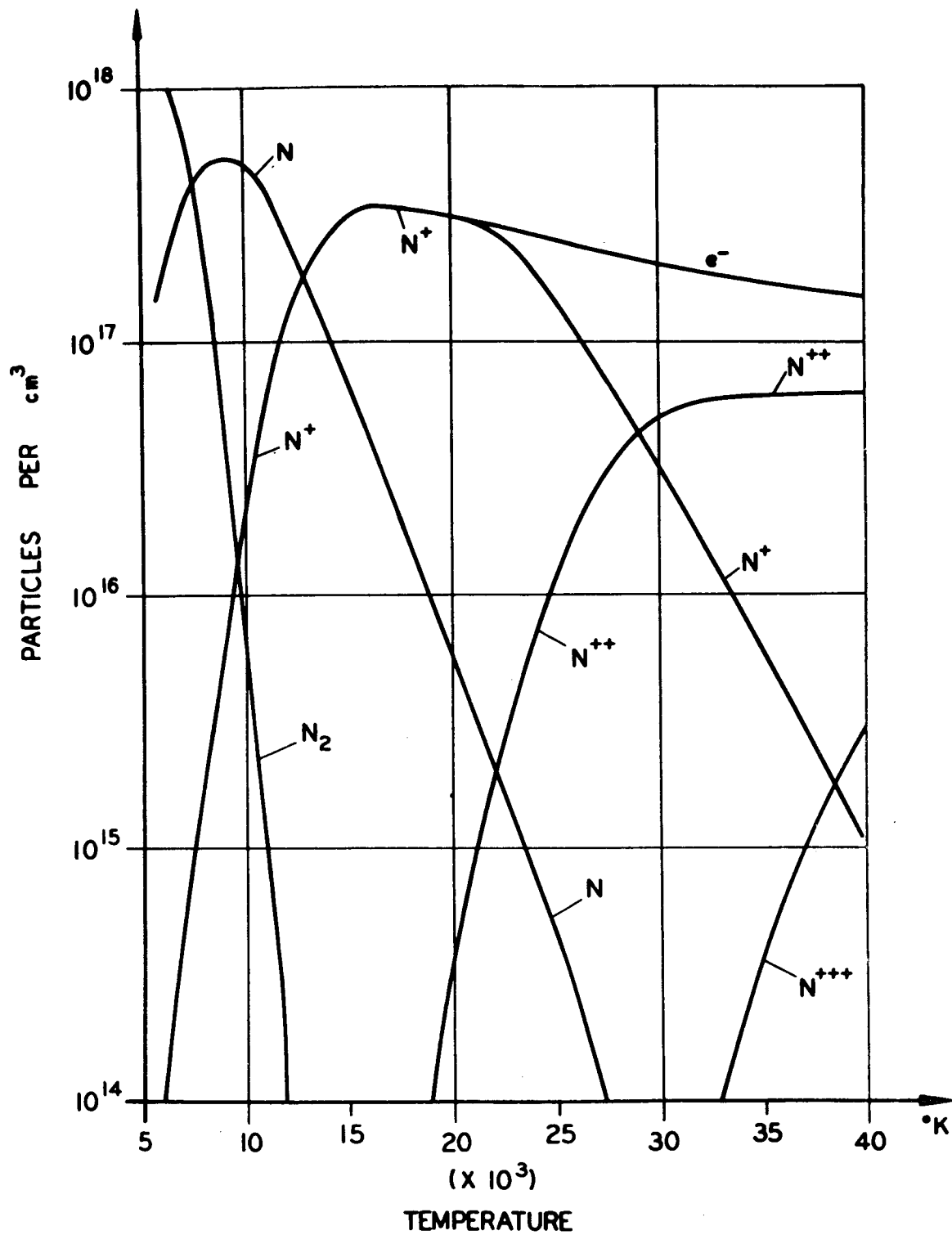


FIG. 29 - Dissociation and ionization of nitrogen as a function of temperature

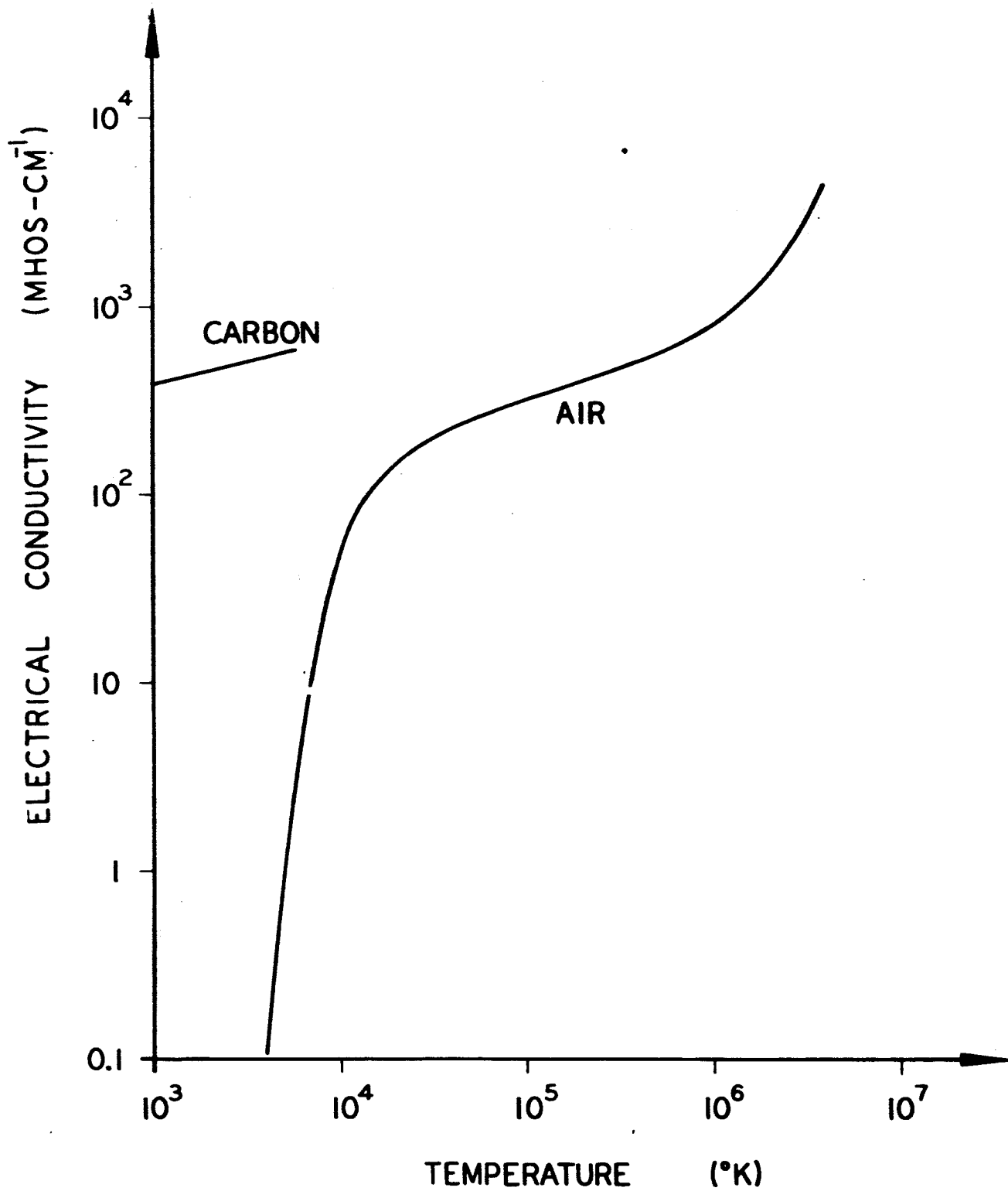


FIG. 30 - Electric conductivity of air as a function of temperature

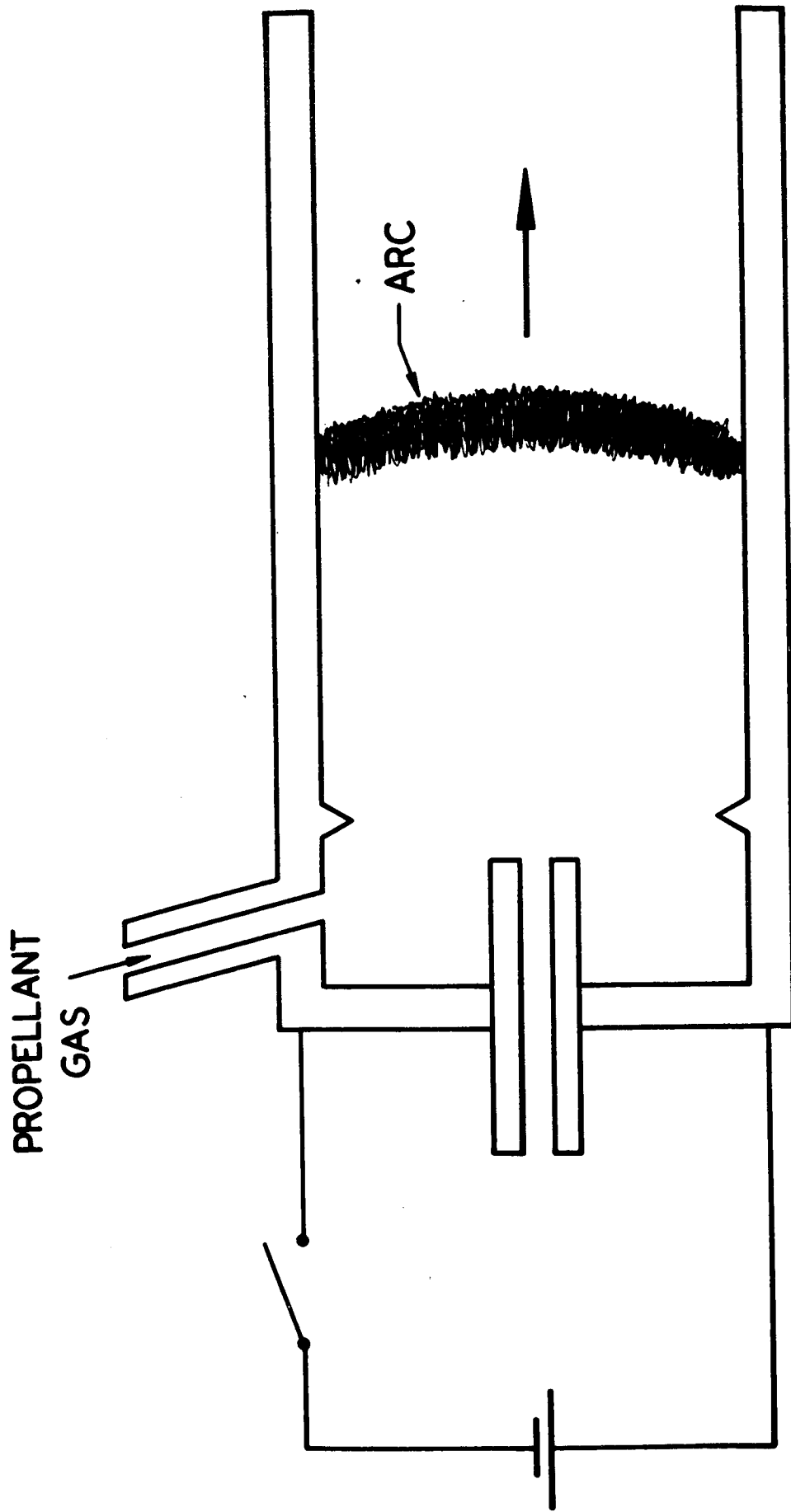


FIG. 31 - Rail-type plasma accelerator

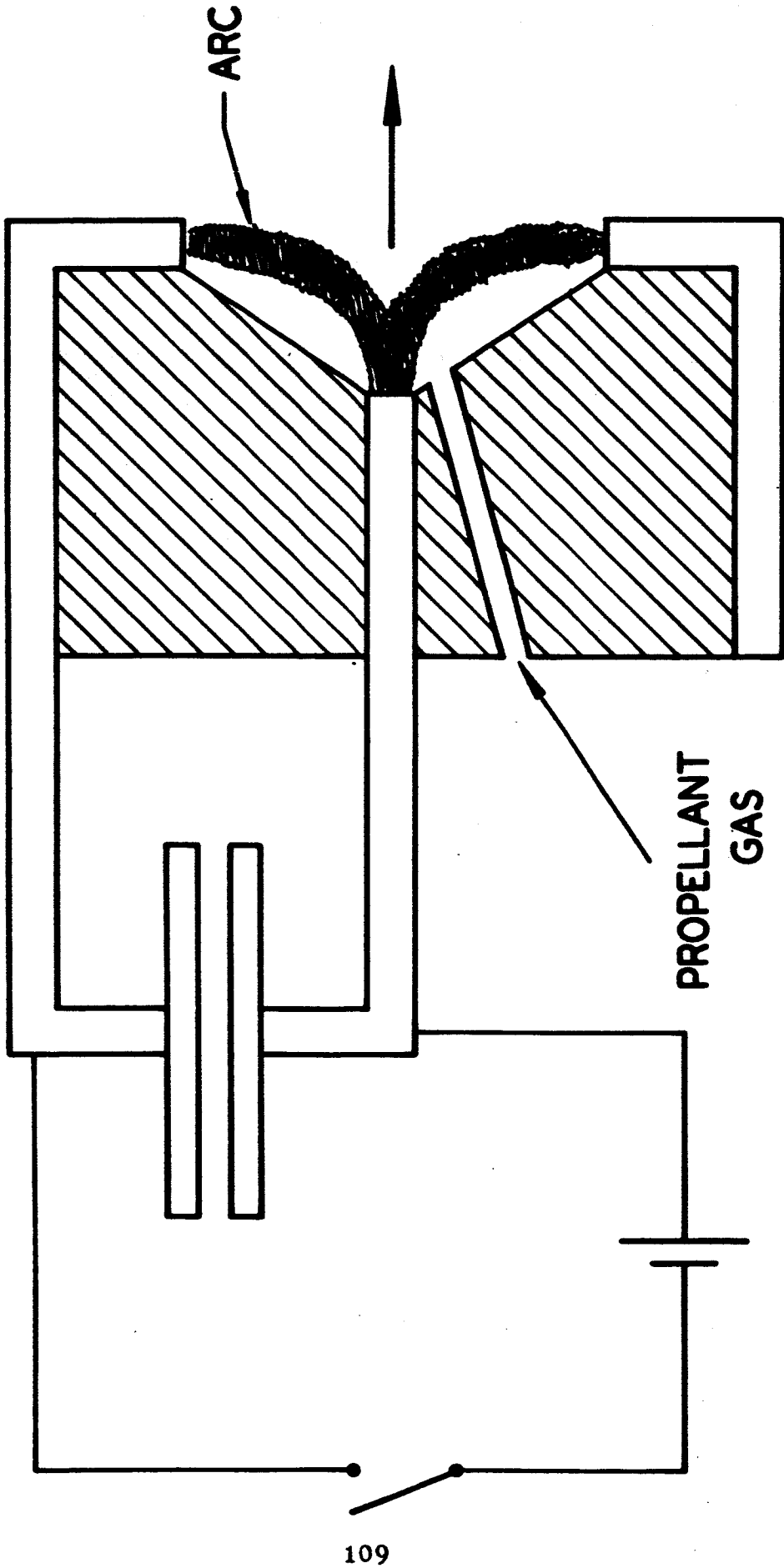


FIG. 32 - Button-type plasma accelerator

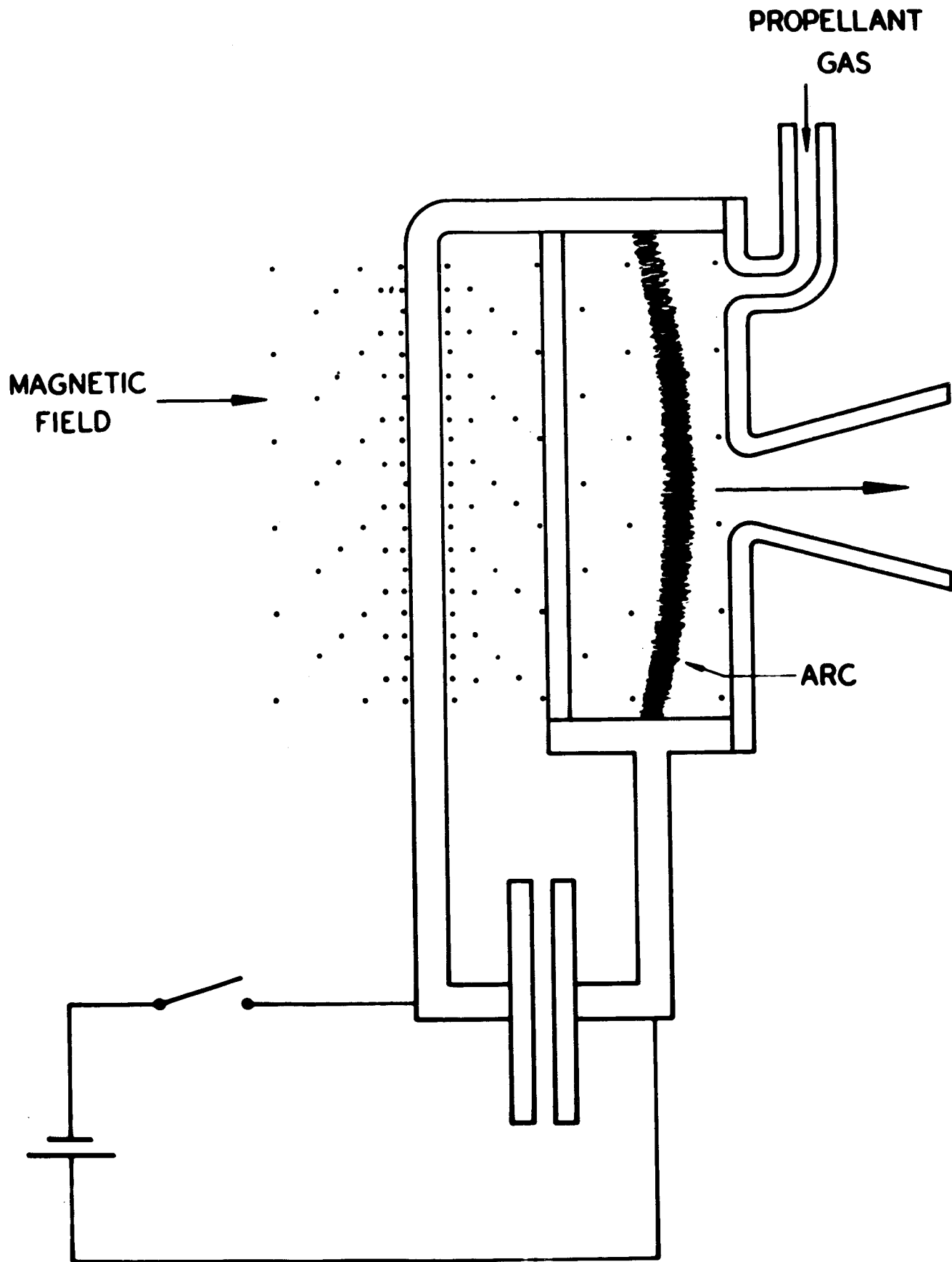


FIG. 33 - Back-strap type plasma accelerator

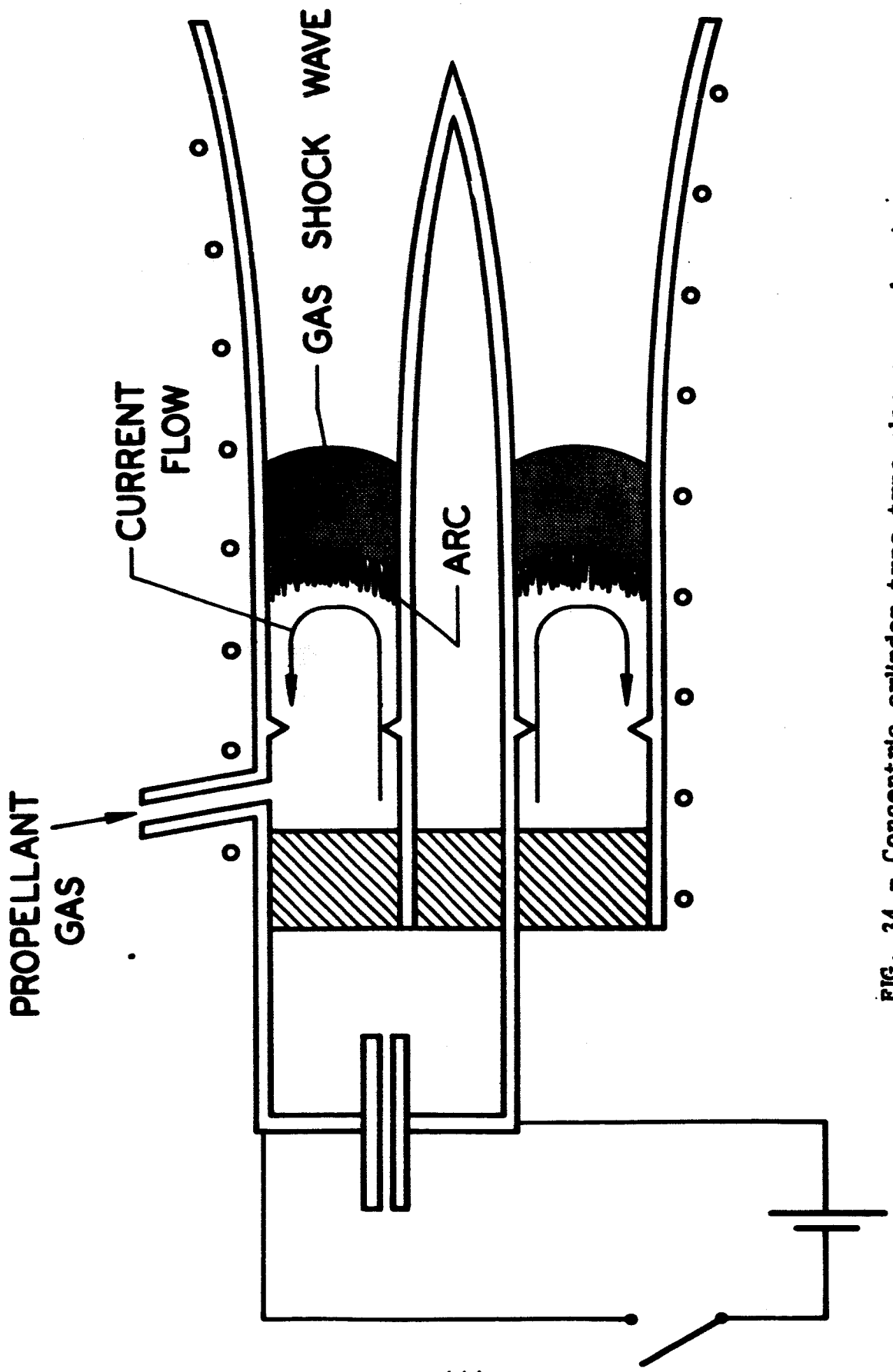
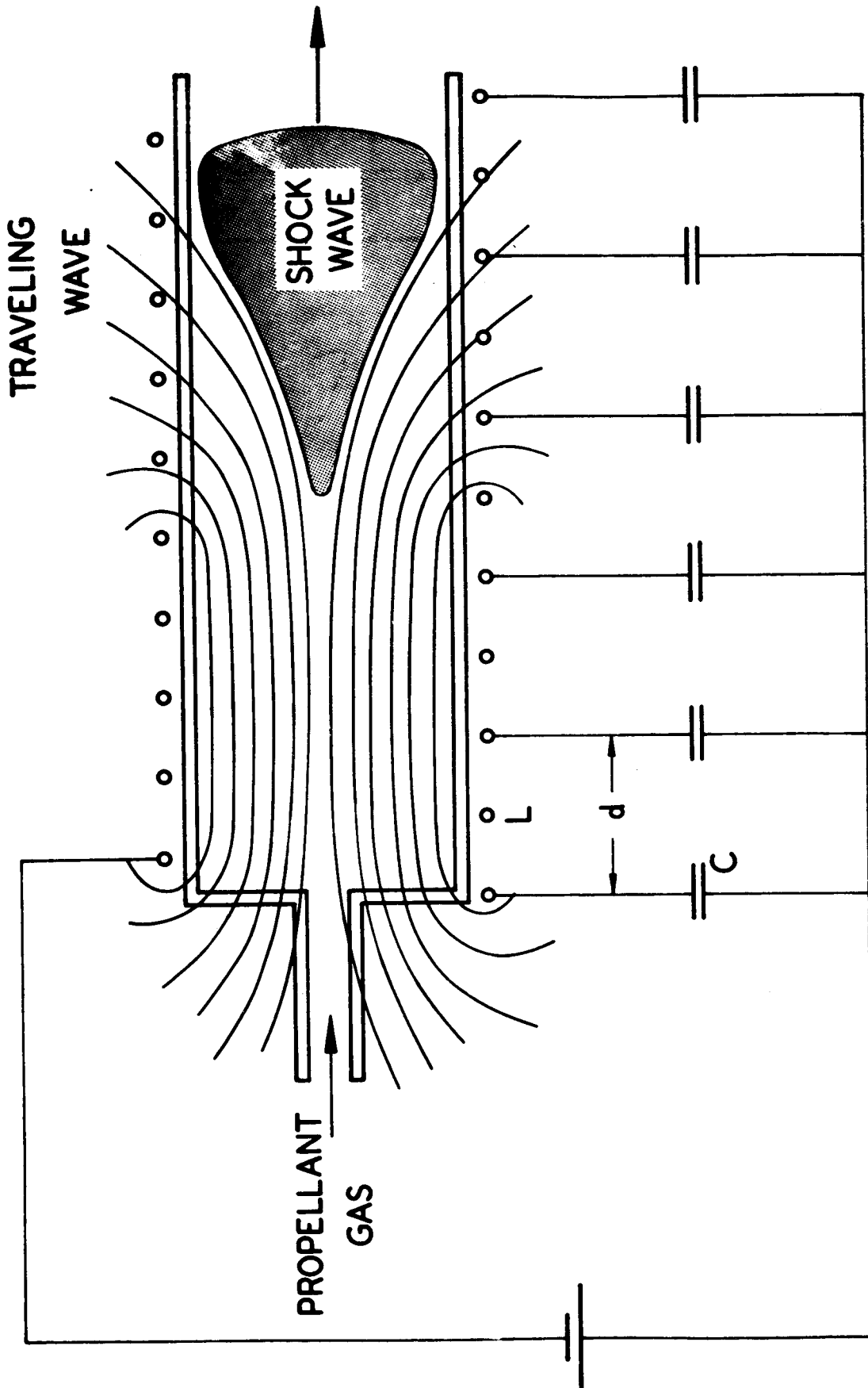


FIG. 34 - Concentric cylinder-type plasma accelerator



VELOCITY OF TRAVELING WAVE: d/\sqrt{LC}

FIG. 35 - Traveling wave-type plasma accelerator